Final Report

1 June 2010 – 31 December 2012

Project Title:

A Super-Regional Testbed to Improve Models of Environmental Processes for the US Atlantic and Gulf of Mexico Coasts: Shelf Hypoxia in the Northern Gulf of Mexico

Project Lead (PI) name, affiliation, email address

John M. Harding, Northern Gulf Institute, jharding@ngi.msstate.edu

Co-PI(s) name(s), affiliation, email address

Katja Fennel, Dalhousie University, katja.fennel@dal.edu
Rob Hetland, Texas A&M University, hetland@tamu.edu
Jerry Wiggert, University of Southern Mississippi, jerry.wiggert@usm.edu

Co-I(s) name(s), affiliation, email address

Martinho Marta Almeida, mart@ tamu.edu
Pat Fitzpatrick, Mississippi State University, fitz@ngi.msstate.edu
Courtney Harris, Virginia Institute of Marine Science, ckharris@vims.edu
Jiatang Hu, Dalhousie University, jiatang.hu@ dal.edu
Matt Howard, Texas A&M University, mkhoward@ tamu.edu
Dong Shan Ko, Naval Research Laboratory, ko@nrlssc.navy.mil
Yee Lau, Mississippi State University, lau@gri.msstate.edu
Arnaud Laurent, Dalhousie University, arnaud.laurent@dal.ca
Bruce Lipphardt, University of Delaware, brucel@udel.edu
Steve Morey, Florida State University, morey@coaps.fsu.edu
Jiangtao Xu, NOAA Coast Survey Development Laboratory, jiangtao.xu@noaa.gov

Project objectives and goals

The long-term goal of the shelf hypoxia project is the evaluation, and transition to operations, of a coupled, biogeochemical/physical model capable of forecasting the real-time evolution of shelf ecosystem processes in the northern Gulf of Mexico.

The objectives of year 1 efforts were to:

(1) Expose the CI team to the cyberinfrastructure challenges of a case study to aid in their design and development of the super-regional testbed intended to enhance academic/operational collaboration and transitions,
(2) Address the hypothesis that regional boundary conditions impact the initiation and evolution of synoptic scale shelf hypoxia events in the northern Gulf of Mexico,
(3) Provide a preliminary comparison of NOAA and EPA research approaches to synoptic scale shelf hypoxia prediction in the northern Gulf of Mexico,
(4) Transition a *regional* circulation prediction system for the Gulf of Mexico and Caribbean as a baseline operational capability applicable to future planned shelf hypoxia prediction capabilities as well as relevant to real-time Coast Guard search and rescue operations, harmful algal bloom tracking, oil spill response applications, and other marine-related needs in the region.

(5) Transition an initial distribution capability for retrospective results of real-time operational ocean predictions for the Gulf of Mexico and elsewhere for future science and operational applications

Description of research conducted during the reporting period and milestones accomplished and/or completed

SHELF HYPOXIA APPROACH & MILESTONES		Proposal Milestones								
3.5	***Assess Hydrodynamic Skill***	July to Sep	Oct to Dec	Jan to Mar	Apr to Jun	Jul to Sep	Oct to Dec	**% Complete**	**Task Lead - Hetland**	**Finish Date**
3.5.1	Compile/organize/store all physical data							100%	Hetland	31-May-11
3.5.2	Provide hindcast outputs (NOAA GOM POM, IASNFS, GoM HYCOM)							100%	Hetland/ Harding/ Ko/ Patchen	31-Mar-11
3.5.3	Couple H/ROMS to hindcast outputs							100%	Hetland/ Morey	31-Mar-11
3.5.4	Run Hindcast models (H/ROMS uncoupled, H/ROMS coupled to Hind cast outputs, nGOM FVCOM coupled to NGOM POM.)							100%	Hetland	30-Jun-11
3.5.5	Evaluate/Develop skill assessment tools (physical)							100%	Hetland/ Lipphardt	30-Jun-11
3.5.6	Evaluate/compare coupled runs (physical)							100%	Hetland	30-Sep-11
3.5.7	Final Analyses/ Summary Report							100%	Hetland	31-Dec-11
3.6	***Assess Ecosystem Model Skill***	July to Sep	Oct to Dec	Jan to Mar	Apr to Jun	Jul to Sep	Oct to Dec	**% Complete**	**Task Lead - Fennel**	**Finish Date**
3.6.1	Compile/organize/store all biogeochemical data							100%	Fennel	30-Apr-11
3.6.2	Evaluate/Develop skill assessment tools (biogeochemical)							100%	Fennel/ Lipphardt	30-Jun-11
3.6.3	Run uncoupled and coupled hindcast physical models with hypoxia code included							100%	Fennel	31-Jul-11
3.6.4	Evaluate/compare coupled runs (biogeochemical)							100%	Fennel	30-Sep-11
3.6.5	Run EPA hypoxia code coupled to IASNFS NCOM							100%	Ko	30-Jun-11
3.6.6	Evaluate/compare Hindcast H/ROMS coupled to IASNFS NCOM (biochemical)							100%	Fennel/ Ko/CI Team	31-Oct-11
3.6.7	Final Analyses/ Summary Report							100%	Fennel	31-Dec-11
3.7	***Evaluate transition NAVO AMSEAS NCOM***	July to Sep	Oct to Dec	Jan to Mar	Apr to Jun	Jul to Sep	Oct to Dec	**% Complete**	**Task Lead - Wiggert**	**Finish Date**
3.7.1	Identify real-time evaluation data (physical ocean & atmos.)							100%	Wiggert	31 Apr 11
3.7.2	Accumulate real-time evaluation data (physical ocean & atmos)							100%	Wiggert/ Bub	30-Jun-11
3.7.3	Provide 3 hrly, 3 km, Real-Time Forecast NAVO AMSEAS NCOM output on NGI/NCDDC EDAC OceanNOMADS							100%	Harding/ Bub/ Cross	Continuing
3.7.4	Provide NAVO OPTEST Evaluation Tools							100%	Wiggert/ Bub	31-Mar-11
3.7.5	Evaluate/develop additional real time & post-time skill assessment tools							100%	Wiggert/ Lipphardt/ Fitzpatrick	31-Aug-11
3.7.6	Evaluate NAVO AMSEAS							100%	Wiggert	31-Dec-11
3.7.7	Evaluate NAVO AMSEAS atmospheric forcing							100%	Fitzpatrick	31-Jul-11
3.7.8	Transition NAVO/AMSEAS from pre-operational to operational							100%	Wiggert/ Bub	30-Sep-11
3.7.9	Transition NGI Developmental OceanNOMADS to Operational NCDDC Ocean NOMADS							100%	Harding/Cross	30-Jun-11
3.7.10	Final Analyses/ Summary Report							100%	Wiggert/Harding	31-Dec-11
3.8	***Overall SURA Shelf Hypoxia Project***	July to Sep	Oct to Dec	Jan to Mar	Apr to Jun	Jul to Sep	Oct to Dec	**% Complete**	**Task Lead - Harding**	**Finish Date**
3.8.1	Consolidated Summary Report							100%	Harding/ Hetland/ Fennel/ Wiggert	31-Dec-11

Description of significant research results, protocols developed, and research transitions

1. *Established direct collaboration between academic hypoxia researchers and NOAA CSDL operational Gulf of Mexico hypoxia model developers.* [Contacts: Rich Patchen (NOAA CSDL), Katja Fennel (Dalhousie) & John Harding (NGI); See Appendix A for details]

2. *Created consolidated, error-checked, multi-year hypoxia data set and provided to SURA CI team and to NODC for future availability via NOAA Hypoxia Watch Data Portal.* [Contacts: Scott Cross (NOAA NCDDC), Katja Fennel (Dalhousie) & John Harding (NGI); See Appendix B for details]

3. *Nested vs unnested physical simulations of the northern Gulf shelf show impact on horizontal salinity distributions resulting from the nesting. A strong spike in signal-to-noise ratio in summer likely results from strong, small-scale eddies formed on the edge of the Mississippi/ Atchafalaya river plume front.* [Contacts: Rob Hetland (TAMU); See Appendix C for details]

4. *While the nested physical simulations show improvements in salinity distributions compared to the unnested simulations, initial analyses of the shelf biogeochemical model nested within different physical Gulf models does not show definitive improvement in response to the physical boundary condition treatment. Given that the hypoxic layer is confined to the bottom few meters, the results from these comparisons do suggest that subsequent research needs to focus on the model representation of the bottom boundary layer (e.g. vertical resolution, diffusivity etc.) and the biogeochemical interaction between the bottom waters and the underlying sediment (especially sediment oxygen consumption).* [Contacts: Katja Fennel (Dalhousie) & Rob Hetland (TAMU); See Appendix D for details]

5. *Specific Improvements to Models: Linking Sediment Transport and Biogeochemical Models within ROMS.* [Courtney Harris (VIMS) & Katja Fennel (Dalhousie); See Appendix E for details.]

6. *Analysis of ROMS near bottom trajectories during June-July 2007 showed residence times > 90 days in some hypoxic areas and hypoxic water masses originating offshore, near the shelf break.* [Contact: Bruce Lipphardt (U. Delaware); See Appendix F for details].

7. *ROMS simulations with realistic boundary conditions and instantaneous remineralization provide a more realistic inshore position of hypoxic area relative to EPA GEMS with comparable representation of hypoxic area size. The EPA GEMS hypoxic area and phytoplankton biomass are consistently too far offshore for each of the four years. ROMS with climatological boundary conditions and instantaneous remineralization gets the inshore location correct but appears to under-represent the size of hypoxic area relative to EPA GEMS. Future hypoxic zone area and phytoplankton biomass comparisons of ROMS, using the Hetland and DiMarco sediment oxygen consumption formulation, with EPA GEMS would be of interest as these ROMS simulations better represented the size of the hypoxic area even with climatological boundary conditions but, as with the EPA GEMS, tended to be too far offshore relative to the instantaneous remineralization cases.* [Contacts: Katja Fennel (Dalhousie) & Dong Shan Ko (NRL); See Appendix G for details]

8. *Supported transition of U.S. Navy operational Gulf of Mexico regional ocean nowcast/forecast capability.* [Contacts: Jerry Wiggert (USM), Frank Bub (Naval Oceanographic Office), Pat Fitzpatrick(NGI) & John Harding (NGI); See Appendix H for details]

9. *Provided insight relevant to NOAA CSDL operational Gulf of Mexico coastal nowcast/forecast system developers.* [Contacts: Rich Patchen (NOAA CSDL), Jerry Wiggert (USM) & John Harding (NGI); See Appendix I for details]

10. *Restructured NCDDC/NGI developmental EDAC facilitated transition of top NOAA NODC FY 11 external milestone for retrospective OceanNOMADS capability as Navy "White Front Door" for operational ocean nowcast/forecast products.* [Contacts: Scott Cross (NOAA NCDDC) & John Harding (NGI); See Appendix J for details]

11. *Provided collaborative linkage between the SURA Super-Regional Testbed's Shelf and Estuarine Hypoxia teams through Wiggert's Role as a principal architect in development of the ChesROMS Biogeochemical Model.* [Contacts: Jerry Wiggert (USM), Raleigh Hood (UMCES); See Appendix K for details]

Collaborator / partner name, affiliation, email address, description of relationship

Frank Bub, Naval Oceanographic Office, frank.bub@navy.mil ; Provide AMSEAS forecast fields. Provide advice on transition process to overall testbed project. Provide Navy model evaluation results, tools and advice. Serve as shelf hypoxia project advisor.

Scott Cross, NOAA National Coastal Data Development Center, scott.cross@noaa.gov; Provide guidance on NOAA OceanNOMADS plans. Serve as shelf hypoxia project advisor.

John Lehrter, EPA Gulf Ecology Division Laboratory, lehrter.john@epa.gov; Provide multi-year hypoxia cruise data. Serve as shelf hypoxia project advisor.

Alan Lewitus, NOAA Center for Sponsored Coastal Ocean Science Research. Alan.lewitus@noaa.gov; Serve as shelf hypoxia project advisor.

Chris Mooers, Portland State University, cmooers@cecs.pdx.edu; Serve as shelf hypoxia project advisor.

Rich Patchen, NOAA Coast Survey Development Laboratory, rich.patchen@noaa.gov; Serve as shelf hypoxia project advisor.

Publications

Brown, C. W., R. R. Hood, W. Long, D. L. Ramers, C. Wazniak, **J. Wiggert**, J. Xu, R. Murtugudde, M. D. Wilson, J. Jacobs and R. Wood, Ecological Forecasting In Chesapeake Bay Using A Hybrid Mechanisic-Empirical Modeling Approach, J. Mar. Sys., ***in prep***.

Fennel, K., Hetland, R., Feng, Y., DiMarco, S., 2011. A coupled physical-biological model of the Northern Gulf of Mexico shelf: Model description, validation and analysis of phytoplankton variability, Biogeosciences 8, 1881-1899, doi:10.5194/bg-8-1881-2011

Fennel, K., Hu, J., Laurent, A., Hetland, R., Marta-Almeida, M., Lehrter, J., Model predictions of hypoxic area on the Texas-Louisiana Shelf are highly sensitive to sediment oxygen consumption parameterizations and stratification. In preparation.

Harding, J., S. Cross, F.Bub, and M. Ji. OceanNOMADS: Real-time and retrospective access to operational U.S. ocean prediction products. Draft in preparation for *EOS*.

Marta-Almeida, M., R. D. Hetland, X. Zhang. Evaluation of model nesting performance on the Texas-Louisiana continental shelf. Draft in preparation for *Ocean Modeling*.

Wiggert, J. D., R. R. Hood, W. Long, J. Xu, L. W. J. Lanerolle, M. B. Prasad, and C. W. Brown, Assessment of Biophysical Variability in a Coupled Physical-Biogeochemical Model Developed to Enable Water Quality and Ecological Forecasts of Chesapeake Bay, J. Mar. Sys., *in prep*.

Xu, J., W. Long, **J. D. Wiggert**, L. W. J. Lannerolle, C. W. Brown, R. Murtugudde, and R. R. Hood, Climate Forcing and Salinity Variability in the Chesapeake Bay, USA. Estuaries and Coasts: DOI 10.1007/s12237-011-9423-5, 2011.

Zhang, X., **M. Marta-Almeida, R. D. Hetland**. An operational nowcast/forecast system for the Texas-Louisiana continental shelf. Draft in preparation for *Journal of Operational Oceanography*

Presentations

Brown, C. W., R. R. Hood, W. Long, D. L. Ramers, C. Wazniak, **J. Wiggert**, J. Xu, R. Murtugudde, M. D. Wilson, J. Jacobs and R. Wood, Ecological Forecasting In Chesapeake Bay Using A Hybrid Mechanisic-Empirical Modeling Approach, Meeting: 2011 Advances in Marine Ecosystem Modelling Research, Plymouth, UK, 27-30 June 2011.

Brown, C. W., R. R. Hood, W. Long, D. L. Ramers, C. Wazniak, **J. Wiggert**, R. Murtugudde, M. B. Decker, D. Wilson, and J. Xu, Development of a Chesapeake Bay Ecological Prediction System, Meeting: 2011 Aquatic Sciences Meeting, ASLO, San Juan, Puerto Rico, 13-18 February 2011.

Brown, C. W., R. R. Hood, W. Long, D. L. Ramers, C. Wazniak, **J. Wiggert**, R. Murtugudde, Mary Beth Decker, G. C. de Magny, D. Wilson, and J. Xu, Development of a Chesapeake Bay Ecological Prediction System, Meeting: 2010 ICES Annual Science Conference, Nantes, France, 20-24 September 2010.

Cross, S., J. Harding, and A.R. Parsons, Retrospective access to operational U.S. ocean model products through the OceanNOMADS system. 2012 Ocean Sciences Meeting, Salt Lake City, Utah, February 20-24, 2012 (submitted)

Feng, Y., Jackson, G., DiMarco, S., **Hetland, R., Fennel, K.,** Friedrichs, M.A., Understanding hypoxic area variability in the Northern Gulf of Mexico from a three-dimensional coupled physical-biogeochemical model, 2012 Ocean Sciences Meeting, Salt Lake City, Utah, February 20-24, 2012 (submitted)

Fennel, K., Hu, J., Hetland, R., DiMarco, S., Simulating hypoxia on the Texas-Louisiana shelf in the northern Gulf of Mexico, CERF 21th Biennial Conference, Daytona Beach, Florida, November 6-10, 2011 (oral presentation)

Harding, J., OceanNOMADS: Transition of a NOAA ocean prediction archival capability**,** Presented at the Marine Technology Society TechSurge 2011: Oceans in Action, Biloxi, MS, 22-23 August 2011. (Invited)

Harding, J., Super-Regional Testbed for Improving Forecasts of Environmental Processes for the U.S. Atlantic and Gulf of Mexico Coasts: Shelf Hypoxia Progress/ Plans, Presented at the 2nd Annual Gulf of Mexico Research Coordination Workshop, Bay St. Louis, MS, 31 March – 1 April 2011.

Harding, J., C. Friedrichs, and R. Luettich, The Role of the SURA Testbed in the Improvement of U.S. Coastal and Estuarine Prediction, Presented at Coastal Zone 2011, Chicago, ILL, 17-21 July 2011.

Harding, J., K. Fennel, R. Hetland, and **J. Wiggert**, An overview of shelf hypoxia efforts in the SURA Super-Regional Modeling Testbed, To be presented at 10th Symposium on the Coastal Environment at the the 92nd Annual Meeting of the American Meteorology Society, New Orleans, LA, 22-26 January 2012.

Harding, J., K. Fennel, R. Hetland, and **J. Wiggert**, The SURA Super-Regional Modeling Testbed: an overview of the shelf hypoxia team's activities, Presented at the 2011

Northern Gulf Institute Annual Conference: An Earth Systems Approach to Northern Gulf Science and Management, Mobile, AL, 17-19 May 2011.

Harding, J., S. Cross, F.Bub, and M. Ji, OceanNOMADS: Real-time and retrospective access to operational U.S. ocean prediction products, To be presented at the American Geophysical Union 2011 Fall Meeting, San Francisco, CA, 5-9 December 2011. (Invited)

Harris, C.K., J.J. Birchler, J.P. Rinehimer, C.R. Sherwood, and L. Sanford. Sediment transport models: putting sediment into biology, and biology into sediment. Chesapeake Bay Modeling Forum, VIMS, Gloucester Point, VA. May, 2011.

Harris, C., Coupling Sediment Transport and Biological Processes within a Numerical Ocean Model, Gordon Research Conference on Coastal Ocean Modeling, 26 June 2011, South Hadley, MA

Harris, C.K., J.J. Birchler, J.P. Rinehimer, C.R. Sherwood, and L. Sanford. Sediment transport models: putting sediment into biology, and biology into sediment. Poster presented at the Chesapeake Hydrodynamic Workshop, Edgewater, MD, June 9 – 10, 2011.

Harris, C. K., Fennel, K., Hetland, R., Wilson, R., Coupling Sediment Transport to Biogeochemical Processes: Effects of Resuspension on Oxygen Consumption, 2012 Ocean Sciences Meeting, February 20-24, Salt Lake City, Utah (submitted)

Hetland, R. D. Physical mechanisms that control seasonal hypoxia on the Texas-Louisiana continental shelf. Poster presented at the Gordon Research Conference on Coastal Ocean Modeling, Mt. Holyoke, NH, June 26 – July 1, 2011.

Hood, R. R., C. W. Brown, **J. D. Wiggert**, W. Long, J. Xu, R. Wood, J. Jacobs, M. B. K. Prasad, and L. W. J. Lanerolle, CBEFS: The Chesapeake Bay Ecological Forecasting System, Meeting: 2011 Aquatic Sciences Meeting, ASLO, San Juan, Puerto Rico, 13-18 February 2011.

Long, W., R. Hood, C. Friedrichs, M. Friedrichs, K. Sellner, **J. Wiggert**, J. Xu, and L. Lanerolle, The Community Operational Chesapeake Bay Regional Ocean Modeling System (ChesROMS) and Its Skill Assessment, Meeting: 92nd Annual Meeting of the American Meteorology Society, New Orleans, LA, 22-26 January 2012.

Marta-Almeida, M., R. D. Hetland, X. Zhang. Evaluation of model nesting performance on the Texas-Louisiana continental shelf. Poster presented at the Gordon Research Conference on Coastal Ocean Modeling, Mt. Holyoke, NH, June 26 – July 1, 2011.

Wiggert, J.D., J.M. Harding, F.L.Bub, P.J. Fitzpatrick, and K.C. Woodard, Evaluation of the AMSEAS Gulf of Mexico/Caribbean regional forecast system: A SURA Super-Regional Modeling Testbed Activity. 2012 Ocean Sciences Meeting, Salt Lake City, Utah, February 20-24, 2012 (submitted).

Wiggert, J. D., R. R. Hood, W. Long, J. Xu, C. W. Brown, B. K. Mathukumalli, and L. W. J. Lanerolle, Assessment of the Biogeochemical Fields from a Coupled Physical-Biogeochemical Model used in Providing Water Quality and Ecological Forecasts of the Chesapeake Bay, Meeting: 2011 Advances in Marine Ecosystem Modelling Research, Plymouth, UK, 27-30 June 2011.

Wiggert, J. D., W. Long, J. Xu, R. R. Hood, B. K. Mathukumalli, L. W. J. Lanerolle, and C. W. Brown, Assessment of a Coupled Physical-Biogeochemical Model Developed for Water Quality and Ecological Forecast use in Chesapeake Bay, Meeting: 2011 Aquatic Sciences Meeting, ASLO, San Juan, Puerto Rico, 13-18 February 2011.

Appendix A:

Summary Accomplishment(s): Established direct collaboration between academic hypoxia researchers and NOAA CSDL operational Gulf of Mexico hypoxia model developers.

NOAA CSDL transition plan for real-time hypoxia forecasts for Gulf of Mexico include transition of hydrodynamic only FVCOM coastal model as part of Northern Gulf Operational Forecast System (NGOFS) with transition in early 2012 (see nGOM domain in Figure A1). Jiangtao Xu of CSDL is developing the hypoxia forecast component scheduled for a future transition to operations. She is investigating Katja Fennel's hypoxia formulation in both ROMS and FVCOM. The SURA shelf hypoxia testbed has allowed funded, direct interaction of Jiangtao and Katja. [Contacts: Rich Patchen (NOAA CSDL), Katja Fennel (Dalhousie) & John Harding (NGI)]

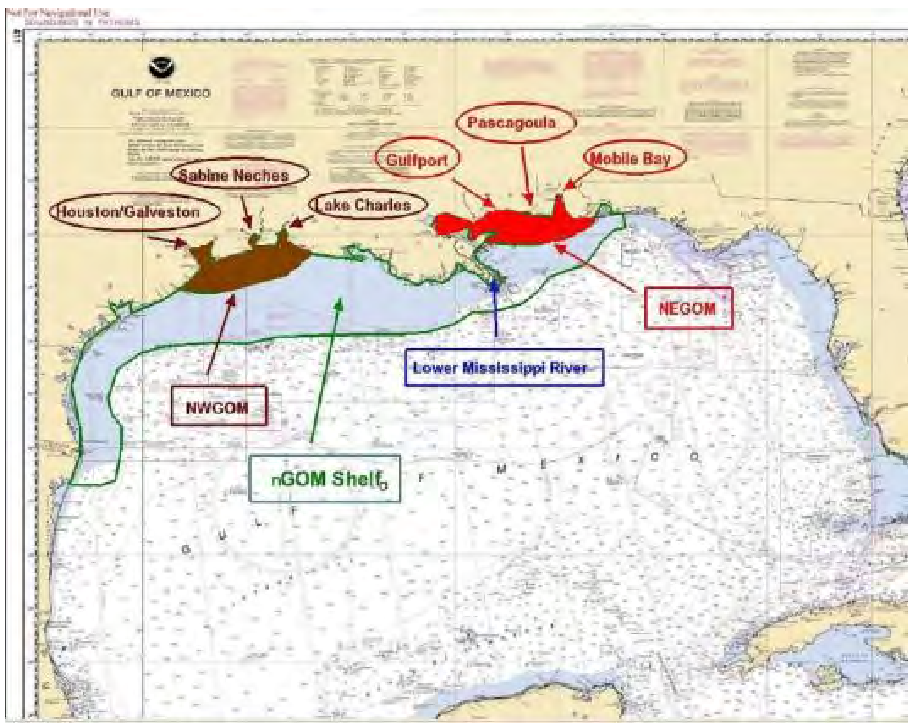

Figure A1: NOAA CSDL planned coastal physical model implementations (nGOM shelf domain above currently planned for 2nd Qtr FY 12 initial NGOFS coastal ocean forecast operational capability)

Appendix B:

Summary Accomplishment(s): Created consolidated, error-checked, multi-year hypoxia data set and provided to SURA CI team and to NODC for future availability via NOAA Hypoxia Watch Data Portal.

Data compilation effort for the SURA shelf hypoxia testbed has created a consolidated multi-year data set planned for inclusion in the NOAA NCCDC Hypoxia Watch portal maintained for the national Hypoxia Task Force (Figure B1). This new compilation includes 2008-2009 NOAA NCCOSC-funded research surveys, NOAA NMFS fisheries SEAMAP survey data, as well as EPA surveys conducted by the EPA research lab in Gulf Breeze, FL. Copies of this data set have been provided to NODC (see http://www.nodc.noaa.gov/cgibin/OAS/prd/accession/details/73142) as well as to the SURA Cyber Infrastructure Team for conversion to NetCDF and storage on the SURA testbed portal. This data set is also available on the NCDDC /NGI developmental server at http://northerngulfinstitute.org/edac [Contacts: Scott Cross (NOAA NCDDC), Katja Fennel (Dalhousie) & John Harding (NGI)]

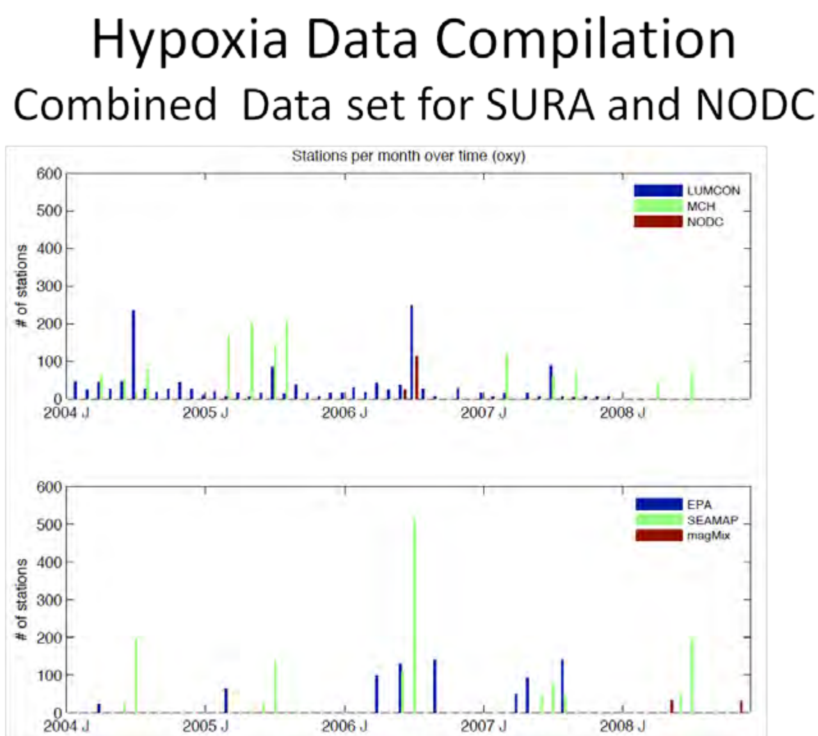

Figure B1: Number of stations by data source and time

Appendix C:

Summary Accomplishment(s): Nested vs unnested physical simulations of the northern Gulf shelf show impact on horizontal salinity distributions resulting from the nesting. A strong spike in signal-to-noise ratio in summer likely results from strong, small-scale eddies formed on the edge of the Mississippi/ Atchafalaya river plume front. [Contacts: Rob Hetland (TAMU)]

Introduction

Texas A&M University currently runs the community Regional Ocean Modeling System (ROMS) circulation model (~2 km grid resolution) on the northwest Gulf of Mexico shelf (Hetland & DiMarco, 2008). Using an embedded biochemical formulation (Fennel et al, 2006) this model is used to investigate hypoxia in the northern Gulf of Mexico. This coupled code is currently used to perform hindcast experiments to understand the development and evolution of the dead zone on the Texas and Louisiana shelf. The physical code presently uses climatological boundary conditions. Using 2004-2009 hindcasts, this task attempted to provide insight into the physical impact of using climatological boundary conditions relative to more realistic boundary conditions provided by three different Gulf basin models. The three full Gulf simulations used as boundary conditions were the NOAA Coast Survey Development Laboratory NGOM(Patchen, NOAA CSDL, personal communication), the Naval Research Laboratory (NRL) Inter American Seas (IASNFS) Navy Coastal Ocean Model (NCOM; Ko et al,, 2003), and the NRL Gulf Of Mexico Hybrid Coordinate Community Ocean Model (HYCOM ; Prasad & Hogan, 2007). The biogeochemical comparisons are detailed in Appendices D, F, & G

Hydrodynamic Model Nesting Procedure

The multi-model nesting technique applied to the ROMS northern Gulf of Mexico model is adapted from the method used by Barth et al. (2008) in their nested ROMS simulation of the eastern Gulf of Mexico. Near the nested model's open lateral boundaries, each of the prognostic variables (baroclinic and barotropic velocity, temperature, salinity, and free surface displacement) is incrementally relaxed toward the respective variables of the outer model, which may be any three-dimensional primitive equation hydrodynamic model, typically with different vertical and horizontal grid resolution, interpolated to the nested model grid.

For a prognostic variable *R*, Newtonian relaxation is performed at each time step as

$$\frac{\partial R}{\partial t} = \cdots + \frac{dt}{\tau}(R - R_{outer})$$

where τ is a relaxation timescale, *dt* is the model time step, and R_{outer} is the corresponding variable from the outer model interpolated to the nested model grid. For the nesting application used here, τ is set so that the relaxation coefficient $C_r = dt / \tau$ decays away from the boundary over a distance comparable to the internal deformation radius.

This method has the advantages of essentially assimilating the three-dimensional structure of currents and transient features (such as eddies) that migrate into the nested model domain, providing for a smooth transition from the outer model to the nested model, and preventing reflection of high-frequency energy from the boundaries.

Comparisons

The salinity fields of a coastal ROMS simulation of the northern Gulf of Mexico were compared running stand-alone (climatological boundary conditions) and nested within three separate Gulf of Mexico physical models (HYCOM, IASNFS, NGOM) from 2004 through 2008. Animations available at http://pong.tamu.edu/~mma/sura/anims_models.php show differences in the various models when all run independently due primarily to different wind forcing and riverine input in each of the simulations (e.g., Figure C1; Note that these plots and associated Python code were provided to the CI team as example of useful output for ocean modelers) Comparing the unnested ROMS for the various years (from the above address) with the nested results shown at http://pong.tamu.edu/~mma/sura/anims_nested.php, illustrates the qualitative impact of the nesting.

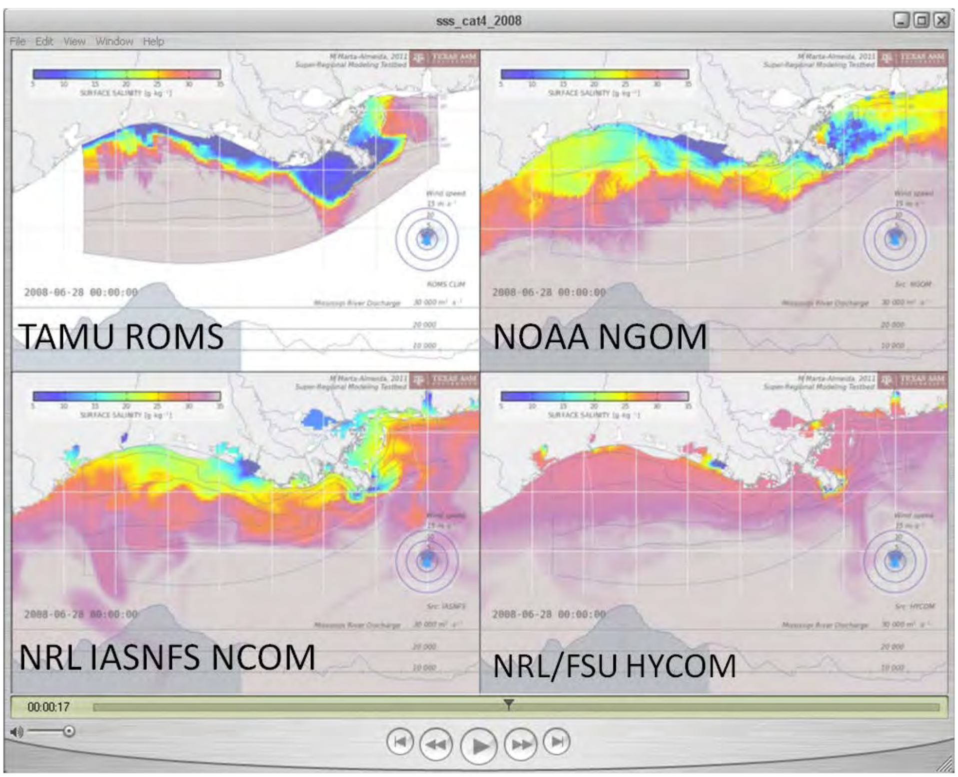

Figure C1: Salinity maps for coastal ROMS, NOAA GOM, NRL IASNFS and NRL/FSU HCOM Gulf independent simulations showing differences likely due to different wind forcing and salinity inflow.

Comparing fresh water flux through each boundary (Figure C2) further illustrates the differences between the ROMS simulations with climatological boundary forcing and those nested within the larger domain models. With the exception of the eastern boundary case, the largest differences are typically between the climatological boundary conditions and the various model-derived boundary conditions.

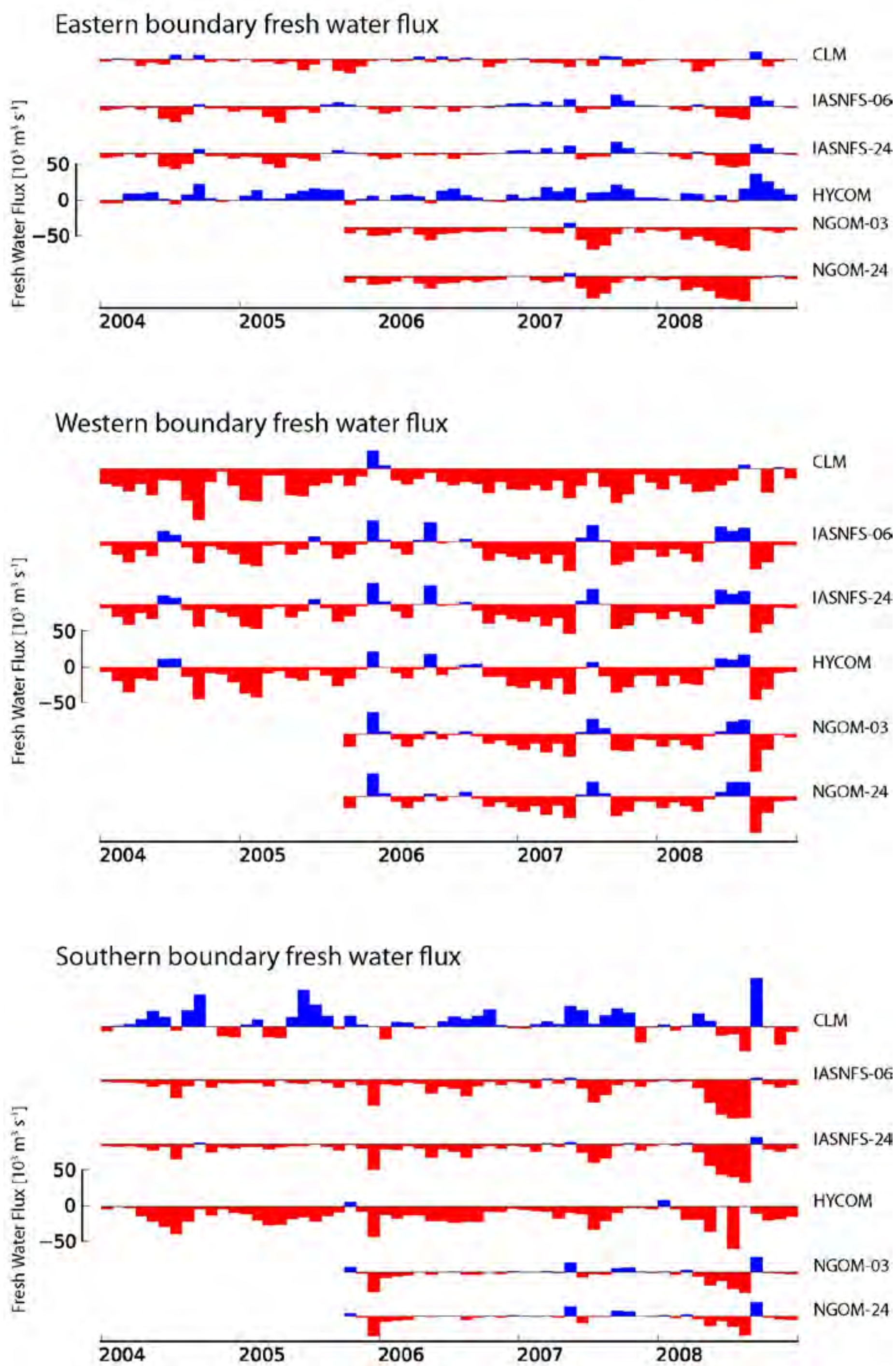

Figure C2: This figure shows monthly averages of fresh water flux through each boundary along a transect just within the nudging region for the various boundary conditions used for the nested model. Red bars indicate months with net fresh water flux leaving the domain, blue bars represent fresh water entering the domain.

Calculating skill scores, defined as 1-sum(observations - model) ^{2} / sum(observations-climatology) ^{2}, for the four cases compared to salinity data obtained with all MCH program profiles for multiple years, from surface to 50 m depth, the skill of the nested runs was all above 0.5 while the skill for the unnested case was 0.38. Differences in the nested runs stimulated a numerical experiment to investigate the sensitivity to slight changes of wind forcing and riverine input. A comparison of the model skill based on a number of historical hydrographic surveys (Table C1), shows that nesting the shelf model in various Gulf scale models improves the skill relative to the shelf model with climatological boundary conditions as well as the skill of the parent models themselves in predicting shelf tracer distributions.

Obs.	date	days	n prof	ROMS CLIM	Original Models					ROMS Nested				
					HYCOM-24	IASNFS-24	IASNFS-06	NGOM-24	NGOM-03	HYCOM-24	IASNFS-24	IASNFS-06	NGOM-24	NGOM-03
MCH	02 Apr 04	5	58	0.32	0.07	0.31	0.33			0.30	0.60	0.52		
	26 Jun 04	5	60	0.27	0.10	0.29	0.28			0.63	0.67	0.71		
	21 Aug 04	5	63	0.39	-0.05	0.24	0.19			0.38	0.67	0.70		
	23 Mar 05	6	104	0.45	0.21	0.44	0.53			0.49	0.45	0.48		
	20 May 05	6	100	0.26	0.09	-0.01	0.16			0.52	0.44	0.39		
	08 Jul 05	5	142	0.67	0.45	0.36	0.54			0.60	0.70	0.69		
	18 Aug 05	6	231	0.65	0.12	0.76	0.77			0.71	0.75	0.72		
	23 Mar 07	6	225	0.59	0.21	-0.46	-0.44	0.65	0.61	0.58	0.70	0.70	0.56	0.54
	17 Jul 07	3	110	0.50	-0.21	0.18	0.29	0.37	0.37	0.51	0.53	0.60	0.58	0.56
	06 Sep 07	4	139	*-3.80*	*-0.48*	*-0.48*	*-0.65*	*-2.73*	*-2.70*	*-0.38*	*-1.93*	*-2.51*	*-1.88*	*-0.96*
	16 Apr 08	2	43	0.50	0.29	0.33	0.20	0.69	0.71	0.49	0.51	0.47	0.59	0.54
	17 Jul 08	3	71	0.60	-0.11	0.50	0.52	0.54	0.50	0.67	0.61	0.60	0.71	0.68
	all dates	56	1346	0.42	0.12	0.13	0.17	0.48	0.45	0.54	0.56	0.55	0.51	0.52
SEAMAP	14 May 04	61	41	0.11	0.03	0.16	0.16			0.43	0.47	0.54		
	15 Jun 05	45	22	-1.30	-0.23	-0.02	0.11			-0.06	0.16	0.22		
	14 Jun 06	32	265	-0.29	-0.56	-2.74	-2.44	0.61	0.60	-0.20	-0.83	-0.96	0.56	0.61
	07 Jun 07	57	48	-0.05	-0.39	-0.02	0.16	0.08	0.08	0.19	0.08	0.21	0.31	0.25
	11 Jun 08	35	229	-0.34	-0.21	0.37	0.44	0.40	0.42	0.40	0.33	0.32	0.34	0.43
	all dates	230	605	-0.04	-0.35	-0.87	-0.73	0.47	0.48	0.16	-0.12	-0.16	0.43	0.49

Table C1: Skill metrics for a series of hydrographic cruises are shown for each model configuration. Positive skill values that are within 20% of the maximum skill are shown in red. It is clear that the nested model generally performs the best, given the high percentage of red values within the nested model portion of the table. It should be noted that nesting improves the shelf model, as compared to using climatological boundary conditions, but it does not seem to matter which model is used as the parent model.

Using the 2008 IASNFS nested run, the river discharge and wind speed amplitude were increased and decreased by 5%. If the simulation responded in a linear way to the forcing, the differences between the two simulations should be about 5% compared to the mean variability in the base case. This is similar to a signal-to-noise ratio, where the standard deviation of the differences is the noise, normalized by the standard deviation of the variability in the base model case, which is the signal. We therefore calculated signal to noise ratio [std(difference) / std(base case simulation)], using all MCH salinity data for all 2008 and for summer 2008 for each of the multiple forcing modifications and for the ensemble mean. Figure C3 shows a strong spike in the signal-to-noise ratio during summer. There are strong, small-scale eddies that are 50 km or smaller that form on the edge of the Mississippi/Atchafalaya river plume front. These eddies shift positions with only minor changes in the forcing or boundary condition information. Because these eddies are small, and difficult to sample, our hypothesis is that this results in a substantial noise floor for the simulation. For the Louisiana shelf in summer, the signal-to-noise ratio is about 1:1, meaning that the eddy variability is on par with the natural variability in the mean state. Note that the effect of each perturbation is very similar indicating that it is not really the nature of the perturbation that matters, but just that there is some perturbation that causes a difference in the models.

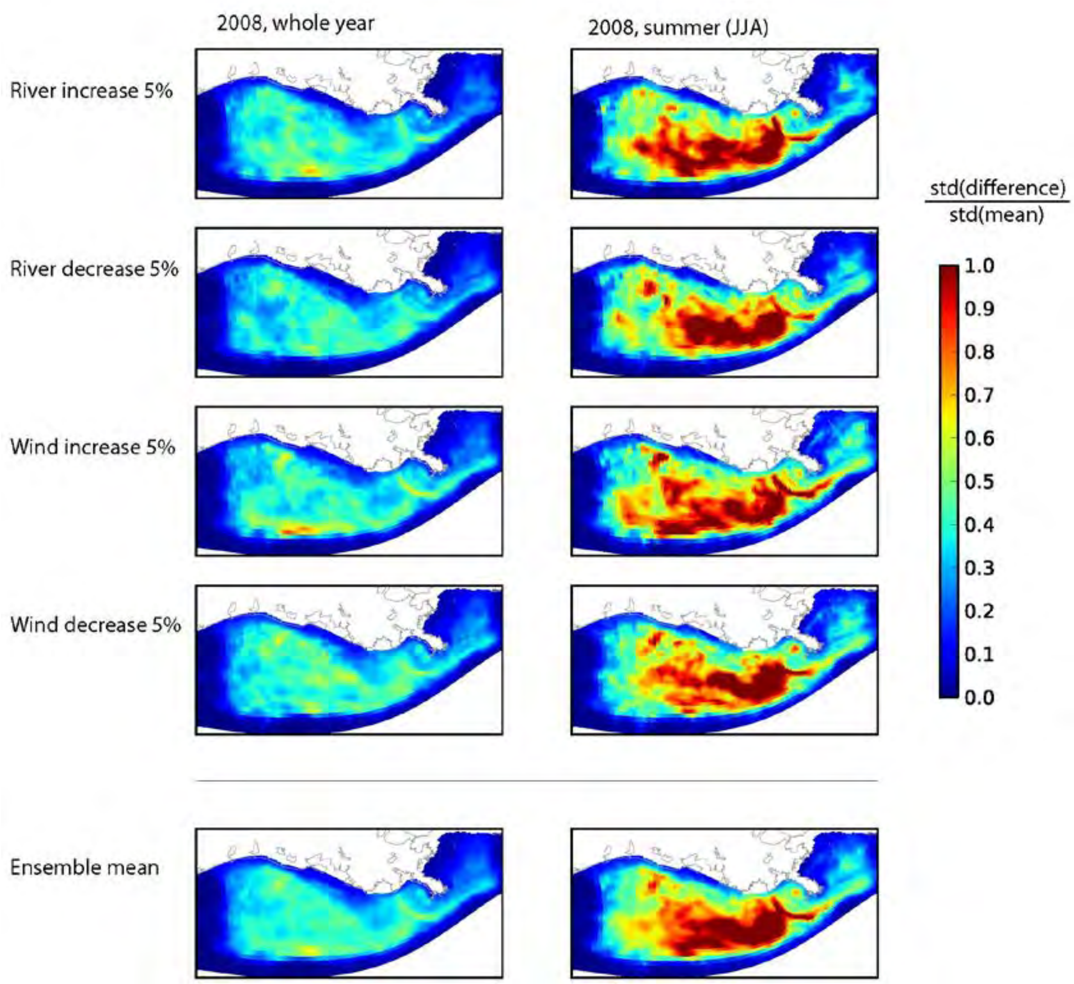

Figure C3: Signal to noise ratio [std(difference) / std(base case simulation)] using all MCH salinity data for all 2008 and the summer 2008 for each of the multiple forcing modifications and the ensemble mean. Note that the effect of each perturbation is very similar, indicating that it is not really the nature of the perturbation that matters, but just that there is some perturbation that causes a difference in the models.

The nesting technique used for the previous studies was incorporated into a prototype operational ocean prediction system for the Texas-Louisiana shelf. The developmental real-time model results may be found at http://pong.tamu.edu/~mma/oof/. This developmental model was used as the basis of a prediction for the hypoxic area in 2011, based on a simplified parameterization of benthic respiration first described by Hetland and DiMarco (2008). Figure C4 shows the predicted area of the sea-floor affected by hypoxic conditions in mid-July. The area was normalized by choosing a critical oxygen value such that the hypoxic area matches that measured by an earlier cruise. The model was able to predict the area of hypoxia to a reasonably close degree (about 19,000 km^2 predicted by the model in mid-July, vs. 17,520 km^2 observed, and the predicted values from a statistical model in June of between 22,253 and 26,515 km^2).

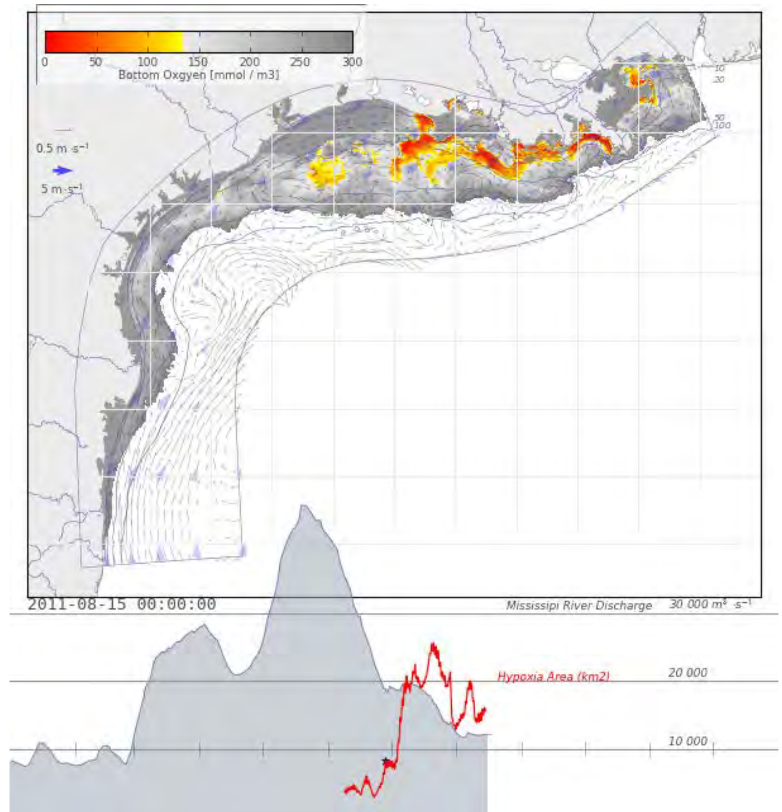

Figure C4: The predicted area affected by hypoxia in mid-August, based on our prototype operational hydrodynamic model (Zhang *et al*., manuscript in preparation), with a simple parameterization of benthic respiration based on Hetland and DiMarco (2008).

References

Barth, A., A. Alvera-Azcárate, and R.H. Weisberg (2008). Assimilation of High-Frequency Radar Currents in a Nested Model of the West Florida Shelf, *Jour. Geophys. Res*., 113, C08033, doi:101029/2007JC004585.

Fennel, K., Wilkin, J., Levin, J., Moisan, J., O'Reilly, J., and Haidvogel, D., 2006. Nitrogen cycling in the Middle Atlantic Bight: results from a three-dimensional model and implications for the North Atlantic nitrogen budget, Global Biogeochem. Cy., 20, GB3007, doi:10.1029/2005GB002456

Hetland, R.D., DiMarco, S.F., 2008. How does the character of oxygen demand control the structure of hypoxia on the Texas–Louisiana continental shelf? *J. Mar. Syst*. 70, 49–62.

Ko, D.S., Preller, R., Martin, P., 2003. An Experimental Real-Time Intra America Seas Ocean Nowcast/Forecast System for Coastal Prediction. Proceedings, 5th Conference on Coastal Atmosphere and Oceanic Prediction and Processes, American Meteorological Society, Seattle, WA, August 6-12, 2003. *ams.confex.com/ams/pdfpapers/64664.pdf*

Appendix D:

Summary Accomplishment(s): While the nested physical simulations show improvements in salinity distributions compared to the unnested simulations, initial analyses of the shelf biogeochemical model nested within different physical Gulf models does not show definitive improvement in response to the physical boundary condition treatment. Given that the hypoxic layer is confined to the bottom few meters, the results from these comparisons do suggest that subsequent research needs to focus on the model representation of the bottom boundary layer (e.g. vertical resolution, diffusivity etc.) and the biogeochemical interaction between the bottom waters and the underlying sediment (especially sediment oxygen consumption). [Contact(s): Katja Fennel (Dalhousie University)]

Topic: Sensitivity and skill assessment of a biogeochemical model on the Texas-Louisiana continental shelf.

1. Description of model simulations

The shelf hypoxia model, based on ROMS, uses the biological component of Fennel et al. (2006, 2008, 2011) coupled with a description of the dynamics of dissolved oxygen (see Figure D1). The model was run with climatological boundary conditions (unnested simulations) and nested within three operational physical Gulf models (HYCOM, IASNFS, and NGOM) from 2004 through 2009.

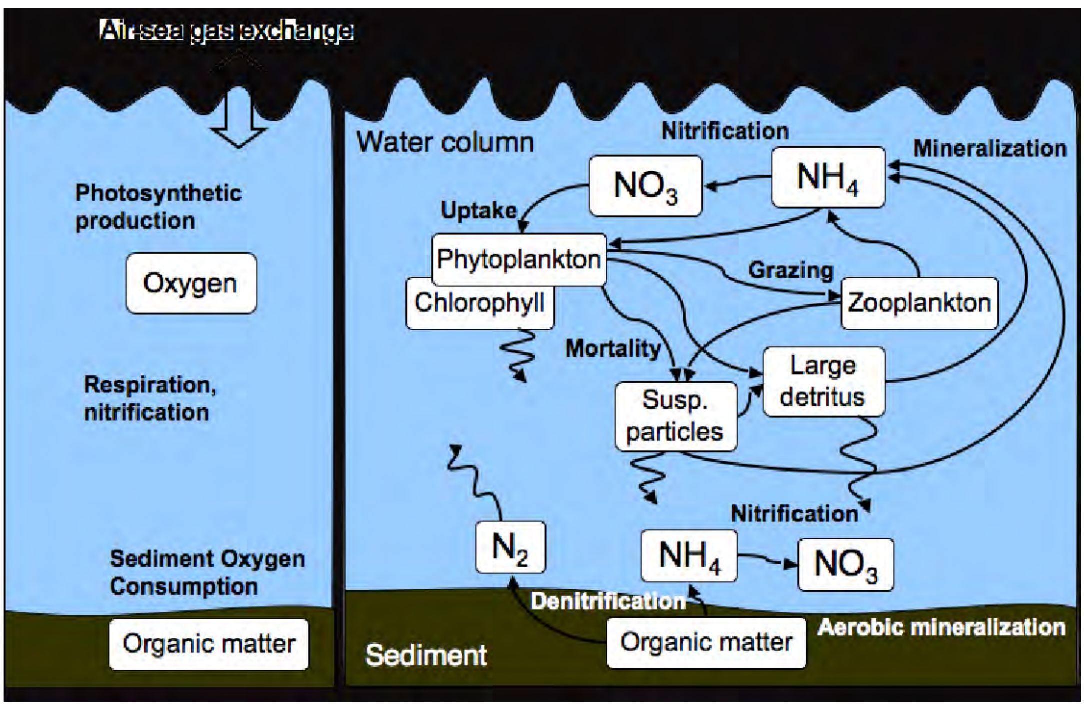

Figure D1: Biological model schematic.

1.1 Unnested simulations

The shelf hypoxia model with climatological boundary conditions used wind forcing from one station (BURL measurements), and has 20 vertical layers. In order to assess the model's sensitivity to the bottom boundary condition, three different treatments at the sediment-water interface (i.e. different parameterizations of sediment oxygen demand) were tested, including one with instantaneous remineralization (Fennel et al. 2011), one following Hetland and DiMarco (2008), and one following Murrell and Lehrter (2010).

1.2 Nested simulations

The models that are nested within HYCOM, IASNFS and NGOM were run with instantaneous remineralization and have a higher vertical resolution with 30 vertical layers. These three nested models were run with two different wind forcings, the BURL measurements and the NARR reanalysis, resulting in a total of six model simulations. These six simulations are subsequently referred to as “HYCOM, BURL forcing”, “HYCOM, NARR forcing”, “IASNFS, BURL forcing”, “IASNFS, NARR forcing”, “NGOM, BURL forcing”, and “NGOM, NARR forcing”. Note that the simulations nested within HYCOM and IASNFS were performed with a time step of 60s and started from January 01, 2004, while the simulations nested within NGOM were performed with a time step of 20s and started from October 05, 2005.

2. Model Evaluation through comparison with satellite chlorophyll data

2.1 Model-satellite maps

Figure D2 shows a comparison of simulated surface chlorophyll and SeaWiFS climatology in June.

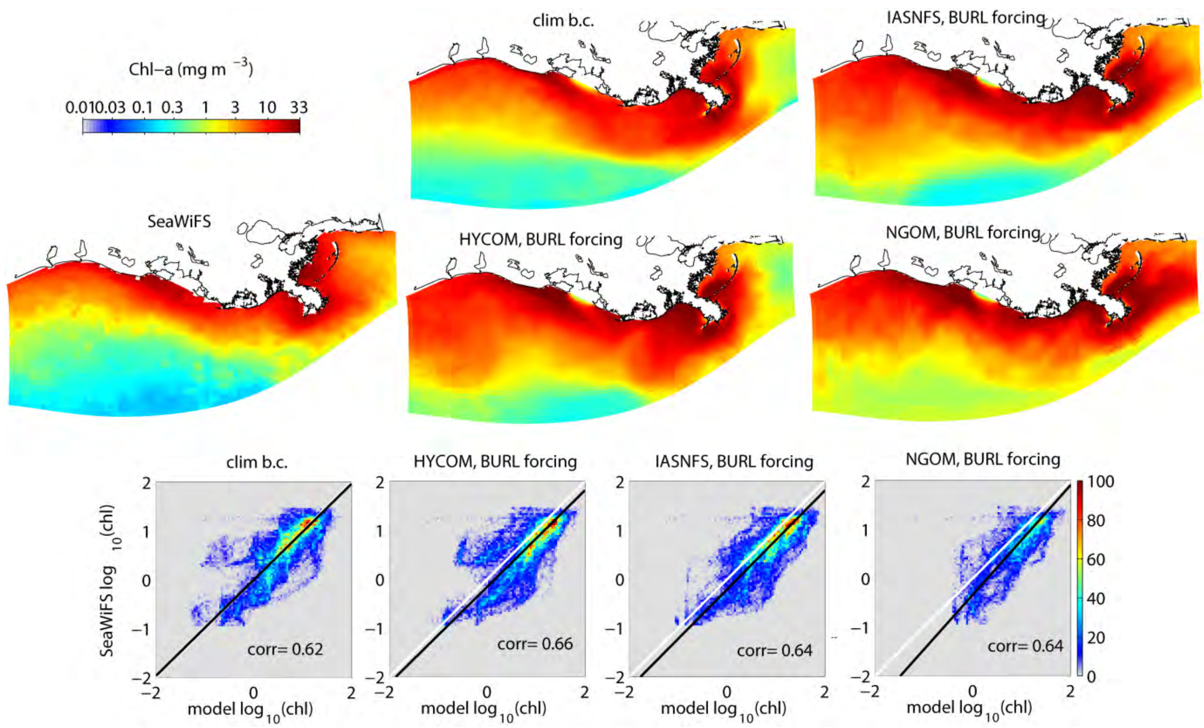

Figure D2: June climatology of surface chlorophyll for the years 2004 to 2008 for the SeaWiFS satellite observations and the model simulations (including one with climatological boundary conditions and three nested simulations with BURL wind forcing). 2-dimensional histogram of SeaWiFS over model chlorophyll and correlation are shown in the bottom row. The 1-to-1 line is shown in white. Color indicates the number of simulated and observed chlorophyll pairs per bin (see color scale at the bottom right).

2.2 Target and Taylor diagrams for comparison with satellite data

Figures D3 and D4 show the Target (Jolliff et al., 2009) and Taylor diagrams (Taylor, 2001) for surface chlorophyll, respectively, comparing the model simulations to the satellite data. The Target and Taylor diagrams are based on computations of the total root mean square difference (RMSD) between model results (*M*) and observations (*O*). The total RMSD is composed of two components, the bias quantifying the mean deviations between model and data, and the unbiased root mean square difference ($\mathrm{RMSD_u}$) representing the difference in variability. The bias is calculated as:

$$\mathrm{Bias} = \frac{1}{n}\sum_{k=1}^{n}\left[M(k) - O(k)\right],$$

where k is the spatial index, and n denotes the number of model/data pairs. The $\mathrm{RMSD_u}$ is computed as:

$$\mathrm{RMSD_u} = \sqrt{\frac{1}{n}\sum_{k=1}^{n}\left[\left(M(k) - \overline{M}\right) - \left(O(k) - \overline{O}\right)\right]^2},$$

where the overline denotes a mean value. Note that the target diagram (Jolliff et al., 2009) exploits the fact that RMSD squared is equal to the sum of $\mathrm{RMSD_u}$ squared and the bias squared. Additionally, model skill (Hetland and DiMarco, 2011) is defined as:

$$\mathrm{skill} = 1 - \sum_{k=1}^{n}\left[M(k) - O(k)\right]^2 \Big/ \sum_{k=1}^{n}\left[O(k) - C(k)\right]^2,$$

where C represents climatological values. A skill of zero suggests that the model error variance has the same magnitude as the variance in the observations relative to the climatology. A positive skill indicates that the model is a better predictor of the observations than the climatology.

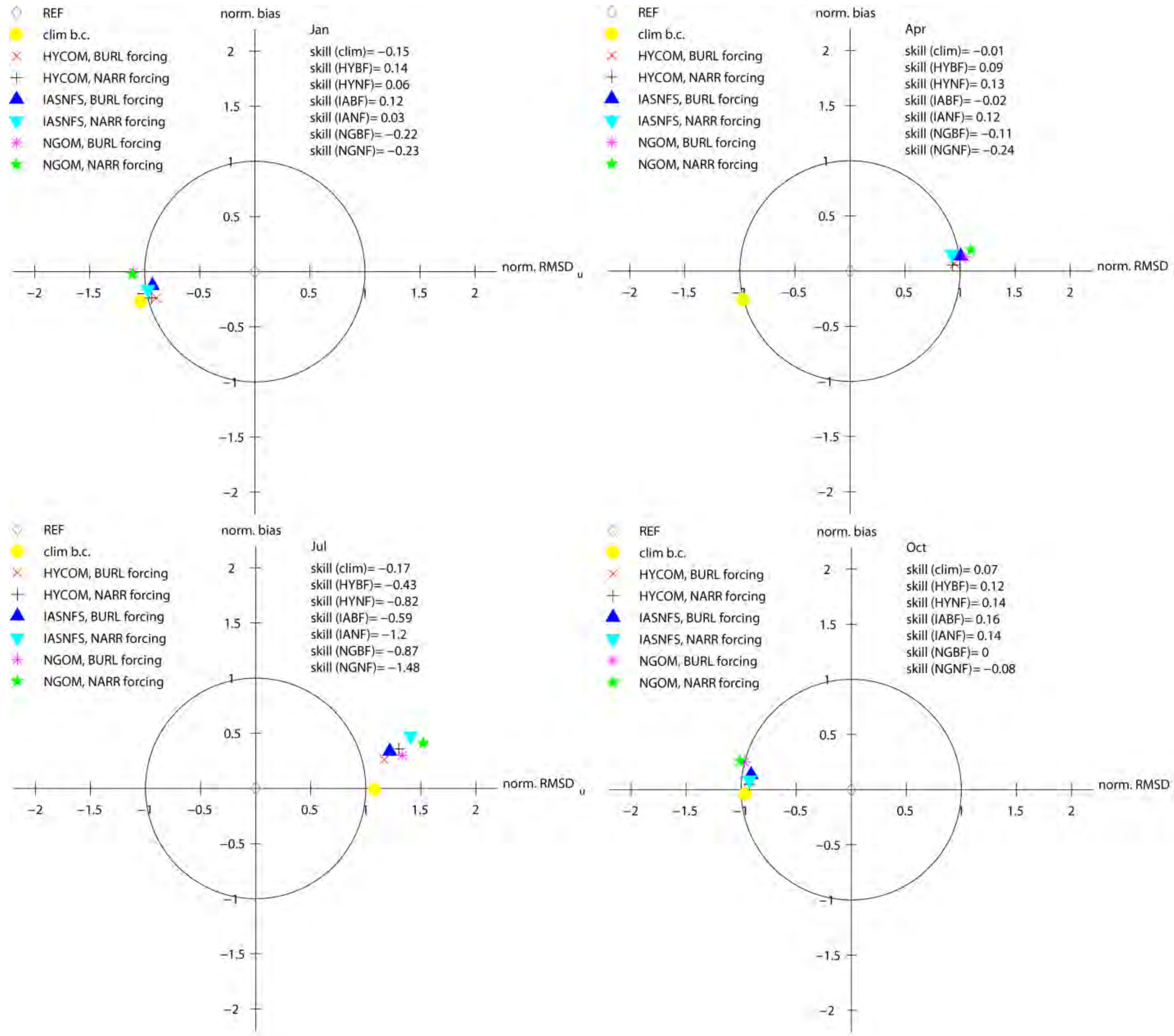

Figure D3: Target diagrams comparing monthly means of surface chlorophyll from the model and SeaWiFS satellite data in January (left, top), April (right, top), July (left, bottom), and October (right, bottom).

The distance from the origin is equal to the total RMSD. On the Target diagrams, the $RMSD_u$ is given the sign of the difference between the standard deviation of the model and observations. A positive $RMSD_u$ means that the model overestimates the observed variability, while a negative $RMSD_u$ means that the model underestimates the observed one. Note that the statistics shown are normalized to $\sqrt{\frac{1}{n}\sum_{k=1}^{n}\left[\left(O(k)-C(k)\right)\right]^2}$ so that the model skill defined in Eq. (3) is indicated on the Target diagrams as well: 1-skill is equal to the normalized RMSD squared; in this manner, the RMSE = 1 circle denotes a skill of zero, while symbols falling within and out of this circle indicate positive and negative skills, respectively.

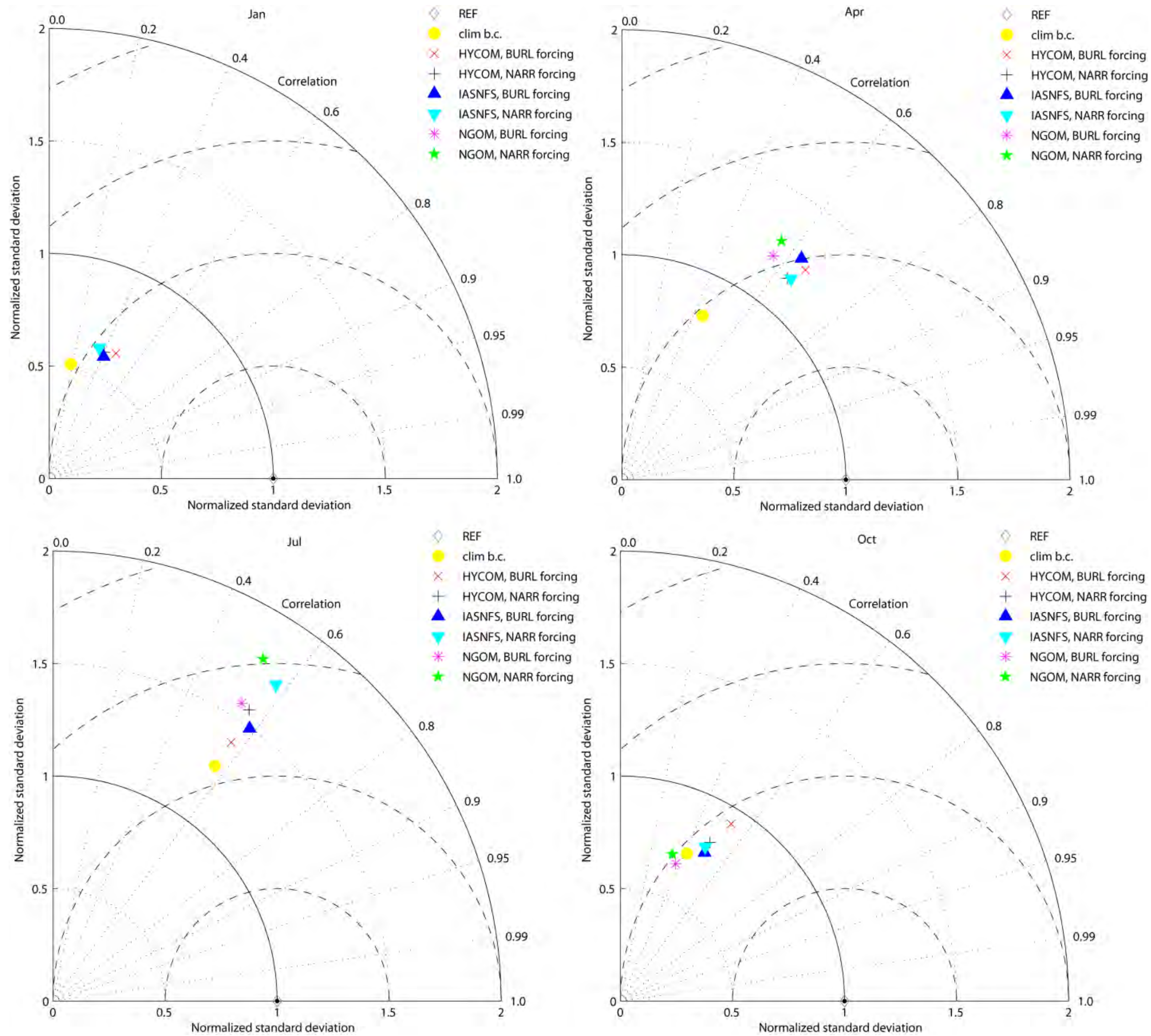

Figure D4: Taylor diagrams comparing monthly means of surface chlorophyll from the model and SeaWiFS satellite data in January (left, top), April (right, top), July (left, bottom), and October (right, bottom). The radial distances from the origin are proportional to the ratio standard deviations; the azimuthal positions indicate the correlation coefficient; and the distance between the “test” points and the “reference” points indicates the $RMSD_u$.

3. Model Evaluation through comparison with *in situ* observations

3.1 Bias histogram

Figure D5 shows the histograms of model bias in oxygen for the unnested simulations with three different SOD parameterizations and for the six nested simulations. Figure D6 shows the biases for *in situ* chlorophyll, primary production, ammonium, and nitrate.

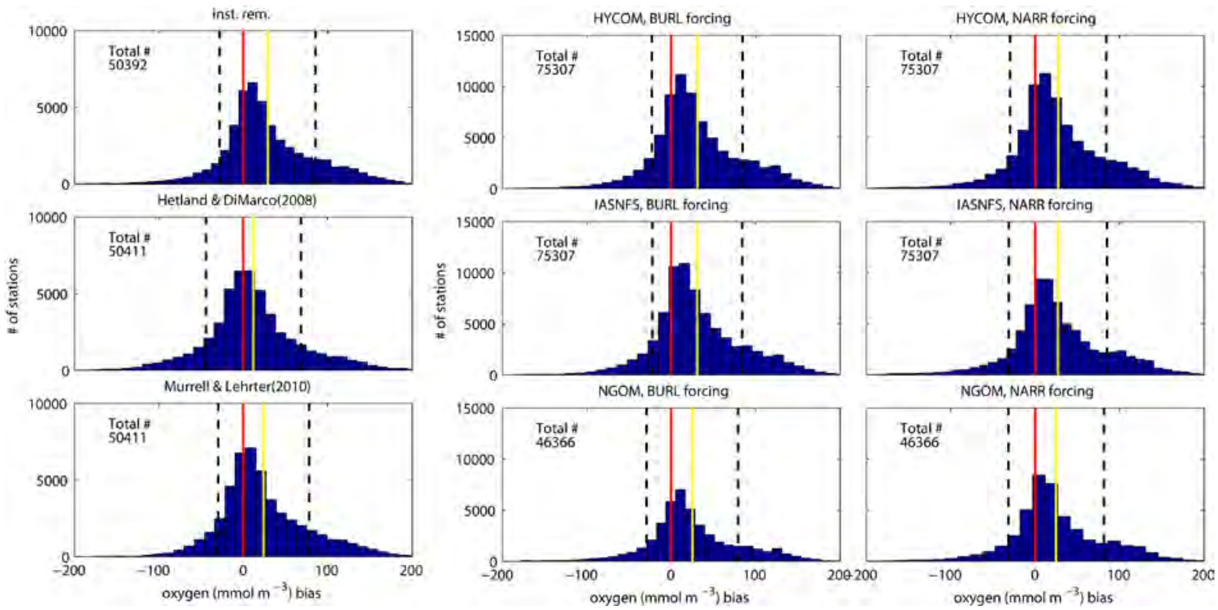

Figure D5: Histograms of model bias (model minus observations) in oxygen for 2004-2008 for three different SOD parameterizations (unnested simulations, left) and nested simulations with BURL wind forcing (middle) and with NARR wind forcing (right). The red line denotes a bias of zero, the yellow line indicates the mean bias, and the dashed line indicates one standard deviation from the mean.

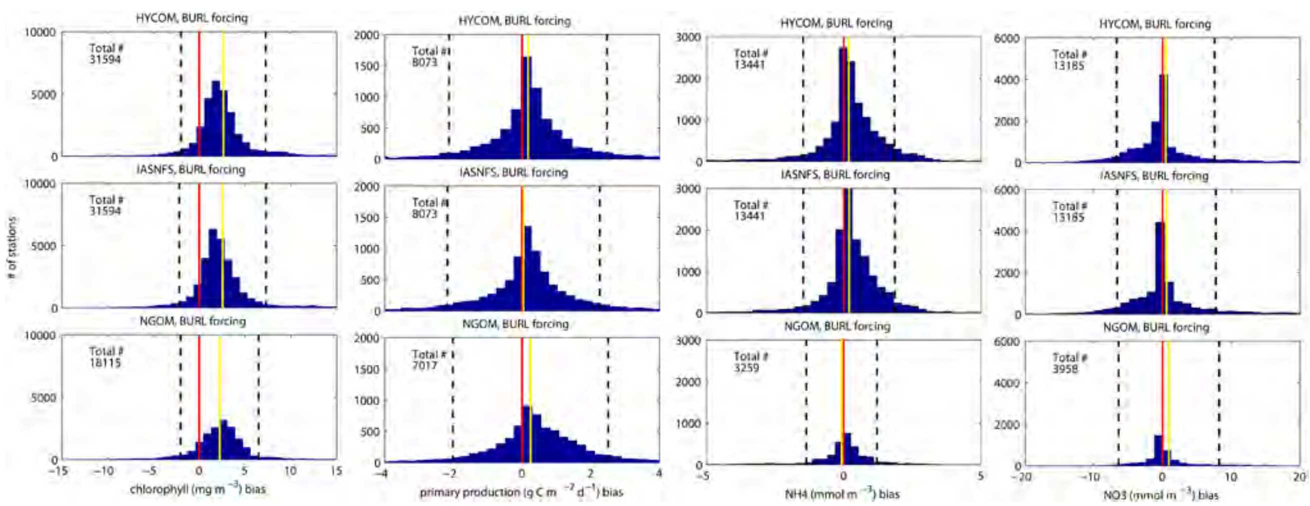

Figure D6: Histograms of model bias in chlorophyll, primary production, ammonium, and nitrate (columns) for 2004-2008 for three nested simulations with BURL wind forcing (rows).

When comparing the different parameterizations of sediment oxygen demand (left column in Fig. D5) it is obvious that the one by Hetland and DiMarco produces the lowest bias. In the comparisons against *in situ* chlorophyll, primary production, nitrate and ammonium (Fig. D6) biases are very small for the latter three properties, but noticable for chlorophyll. It should be pointed out that the bias in chlorophyll is much reduced when the model is compared to satellite chlorophyll, and that there is a bias between *in situ* and SeaWiFS chlorophyll.

3.2 2-dimensional histogram

Figures D7 and D8 show 2-dimensional histograms comparing oxygen from the model and observations in 2006 and 2007, respectively. It is apparent that the different treatments of the open boundaries have only small effects on the oxygen histograms, while the influence of different treatments of sediment oxygen demand is noticeable. The histogram for the simulation with Hetland and DiMarco's sediment oxygen parameterization, i.e. the simulation with smallest oxygen bias (see above), shows a bimodal pattern for oxygen concentrations below 200 mmol/m^3 with the model over- and underestimating the observed concentrations. This is an indication that the model is simulating oxygen drawdown at a reasonable magnitude but has difficulty predicting the spatial locations of this drawdown accurately.

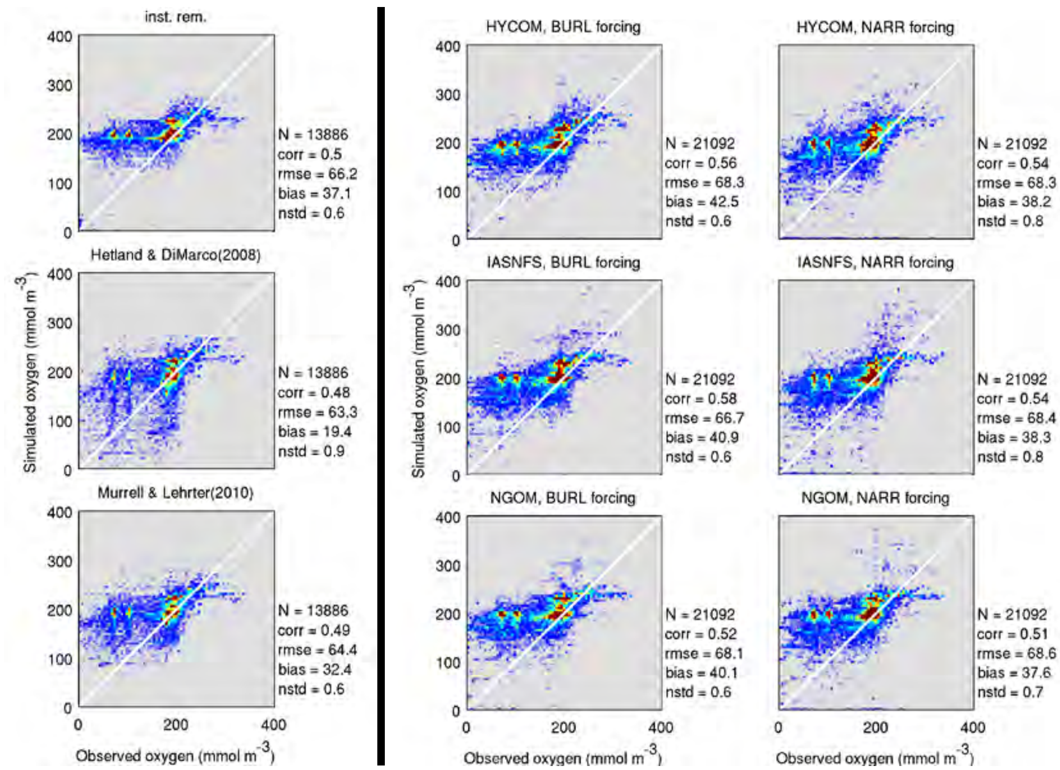

Figure D7: 2-dimensional histograms of simulated versus observed oxygen in 2006 for climatological boundaries and three different SOD parameterizations (left) and nested simulations with BURL wind forcing (middle) and with NARR wind forcing (right). The 1-to-1 line is shown in white. Number of model/data pairs (N), model bias, RMSD, correlation coefficients, and ratio of standard deviations are shown as well.

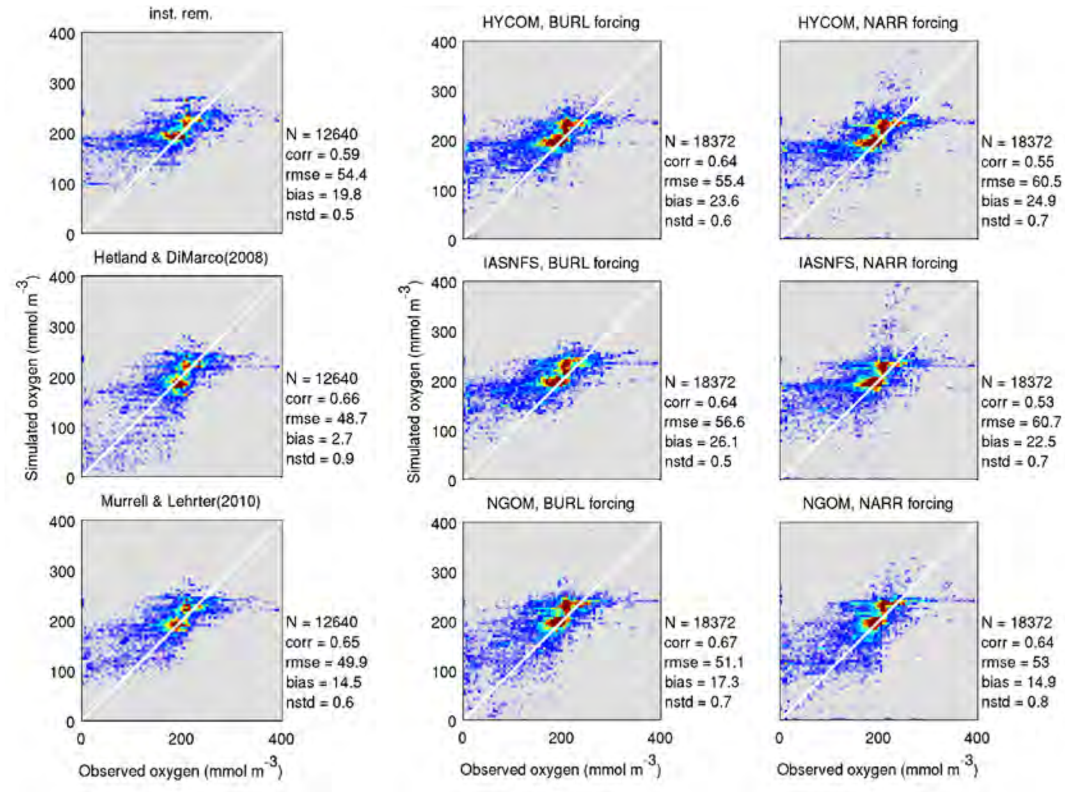

Figure D8: Same as Fig. D7 but for the year 2007.

3.3 Hypoxic area

Figure D9 compares the hypoxic area estimated from the model and observations in July 2004. Figure D10 shows the daily hypoxic area predicted by the model in conjunction with estimates from the observations. The comparisons in Fig. D9 show that the spatial details of the simulated hypoxic zone vary for different boundary treatments, but that the location is captured reasonable well with instantaneous remineralization. The total size of the hypoxic zone, however, tends to be underestimated with instantaneous remineralization and is captured more accurately with the parameterization of Hetland and DiMarco (Fig. D10). The latter, however, predicts the hypoxic zone to be located further offshore then observed (bottom, left panel of Fig. D9).

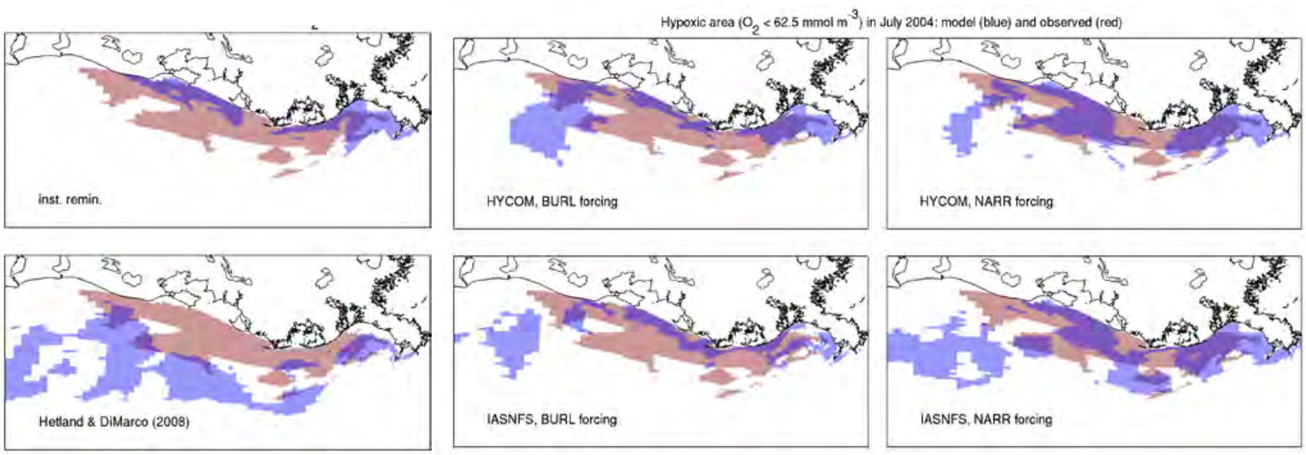

Figure D9: Hypoxic area estimated from the model (blue) and observations (red) in July 2004: two different SOD parameterizations (left) and nested simulations with BURL wind forcing (middle) and with NARR wind forcing (right).

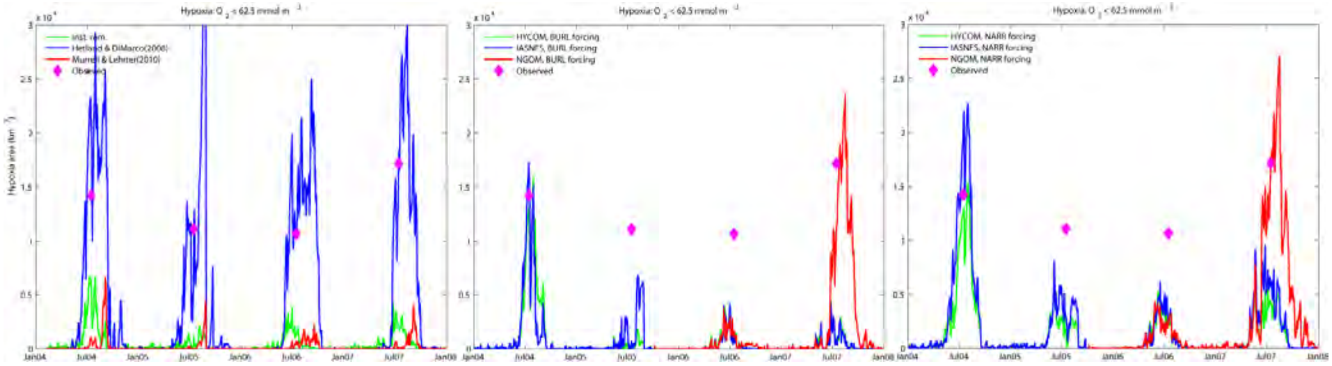

Figure D10: Daily hypoxic area predicted by the model (denoted by lines) and estimates from the observations (diamonds): three different SOD parameterizations (left) and nested simulations with BURL wind forcing (middle) and with NARR wind forcing (right).

Figures D9 & D10 suggest qualitatively that the simulations with realistic boundaries provide improved representation of the hypoxic area compared to the climatological boundary conditions when all use instantaneous remineralization.

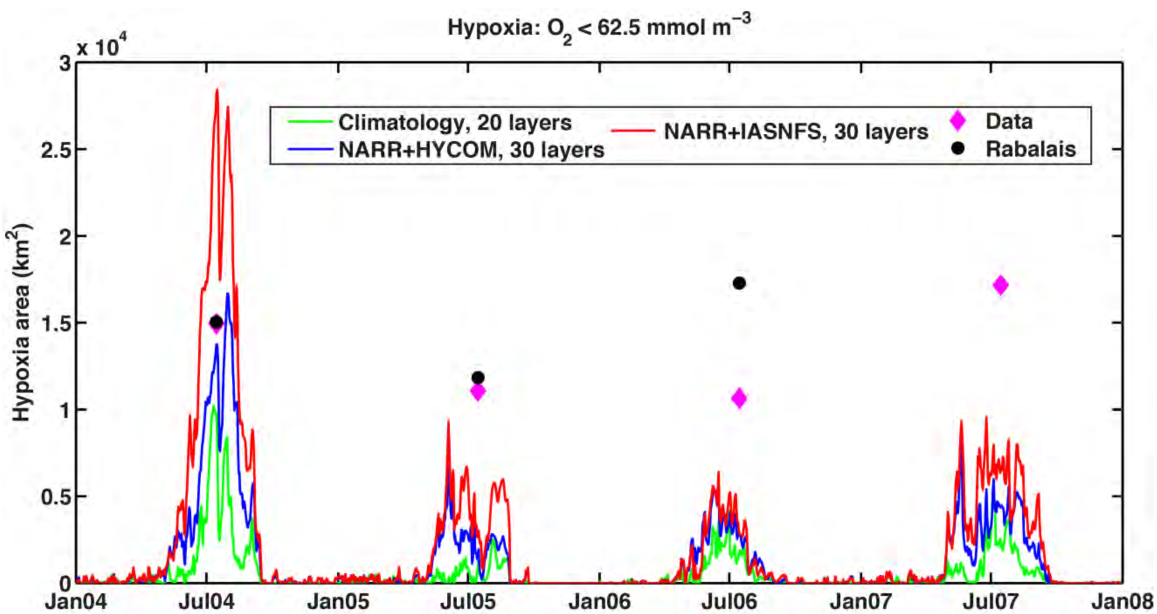

Figure D11: Daily hypoxic area (km^2) simulated with ROMS using instantaneous remineralization for climatological boundary conditions and lower vertical resolution (green line), and HYCOM-NARR (blue line) and IASNFS-NARR (red line) forcing and higher vertical resolution.

In Figure D11 an attempt is made to further illustrate the possible effect of changes in vertical resolution. The models with higher vertical resolution consistently predict larger hypoxic areas. The strong stratification and confinement of the hypoxic to the bottom boundary layer shown in the two representative profiles in Figure D12 illustrates why this might be so. However, since atmospheric forcing and horizontal boundary conditions have changes as well no conclusive inference can be drawn. This stratification also suggests that the treatment of vertical diffusivity needs closer examination in all these approaches.

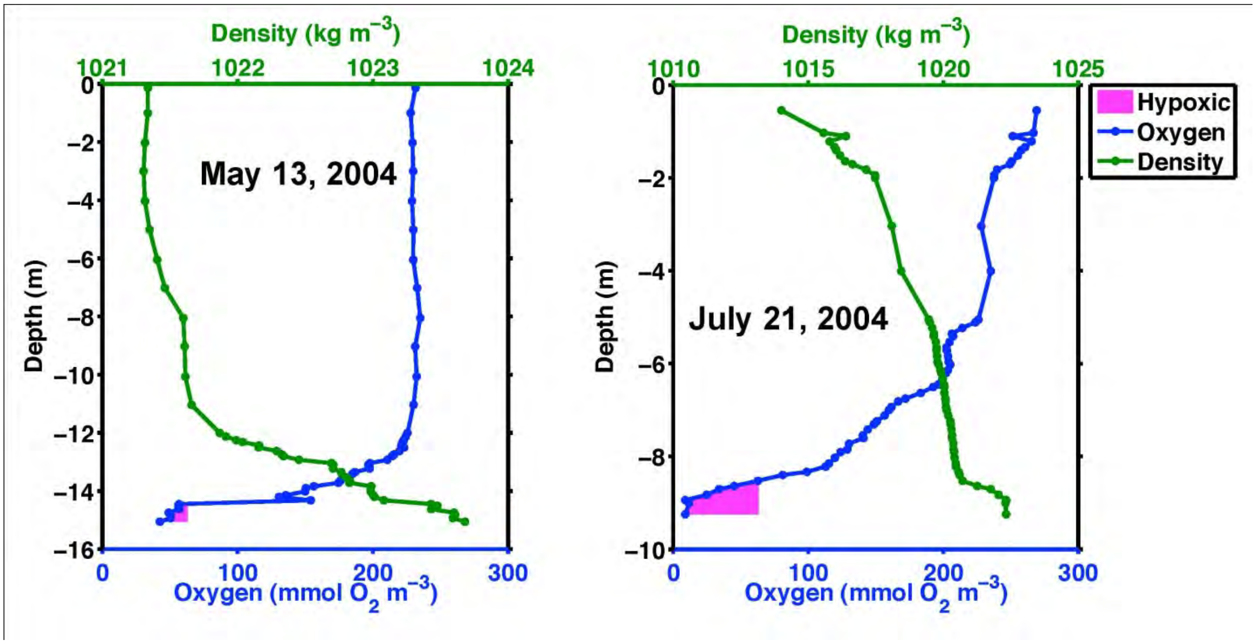

Figure D12: Two representative profiles of dissolved oxygen and density in the hypoxic zone from the LUMCON data set. Hypoxic water, indicated in magenta, coincides with the bottom boundary layer.

3.4 Target and Taylor diagrams for comparison with *in situ* data

3.4.1 Bottom oxygen

Figures D13 and D14 show the Target and Taylor diagrams, respectively, for bottom oxygen comparing the model simulations to the *in situ* observations. There are interannual differences in the fidelity of simulated oxygen distribution in summer with best results for 2006, where all boundary treatments give similar results. In 2008 the different boundary treatments result in the greatest spread, with NGOM BURL having the smallest bias and unbiased RMSE and climatological simulation having the largest bias and unbiased RMSE. A more detailed comparative analysis of the differences between simulations in that particular year may reveal clues as to why some simulations perform better with respect to dissolved oxygen.

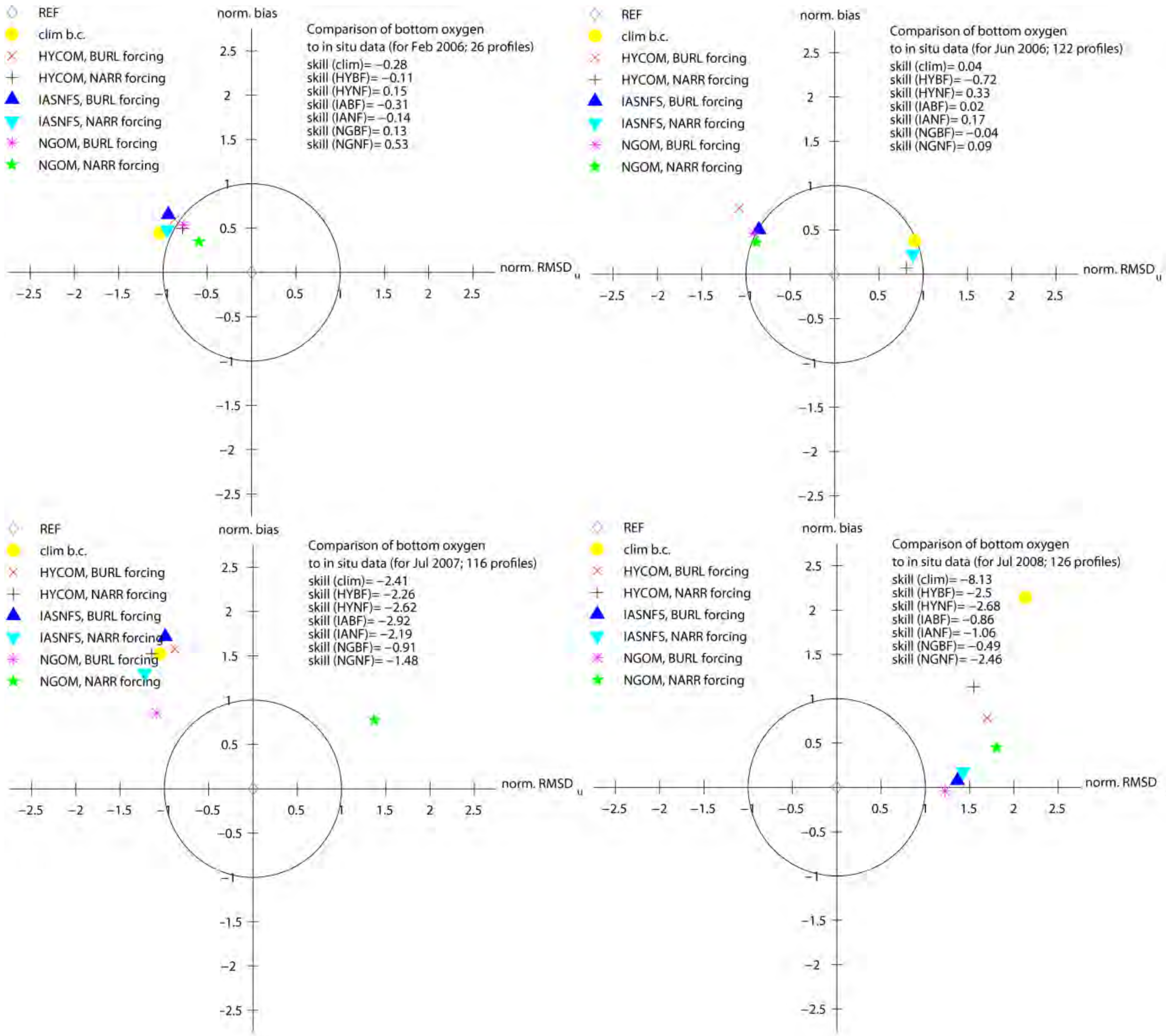

Figure D13: Target diagrams comparing bottom oxygen from the model and *in situ* data in February 2006 (left, top), June 2006 (right, top), July 2007(left, bottom), and July 2008 (right, bottom).

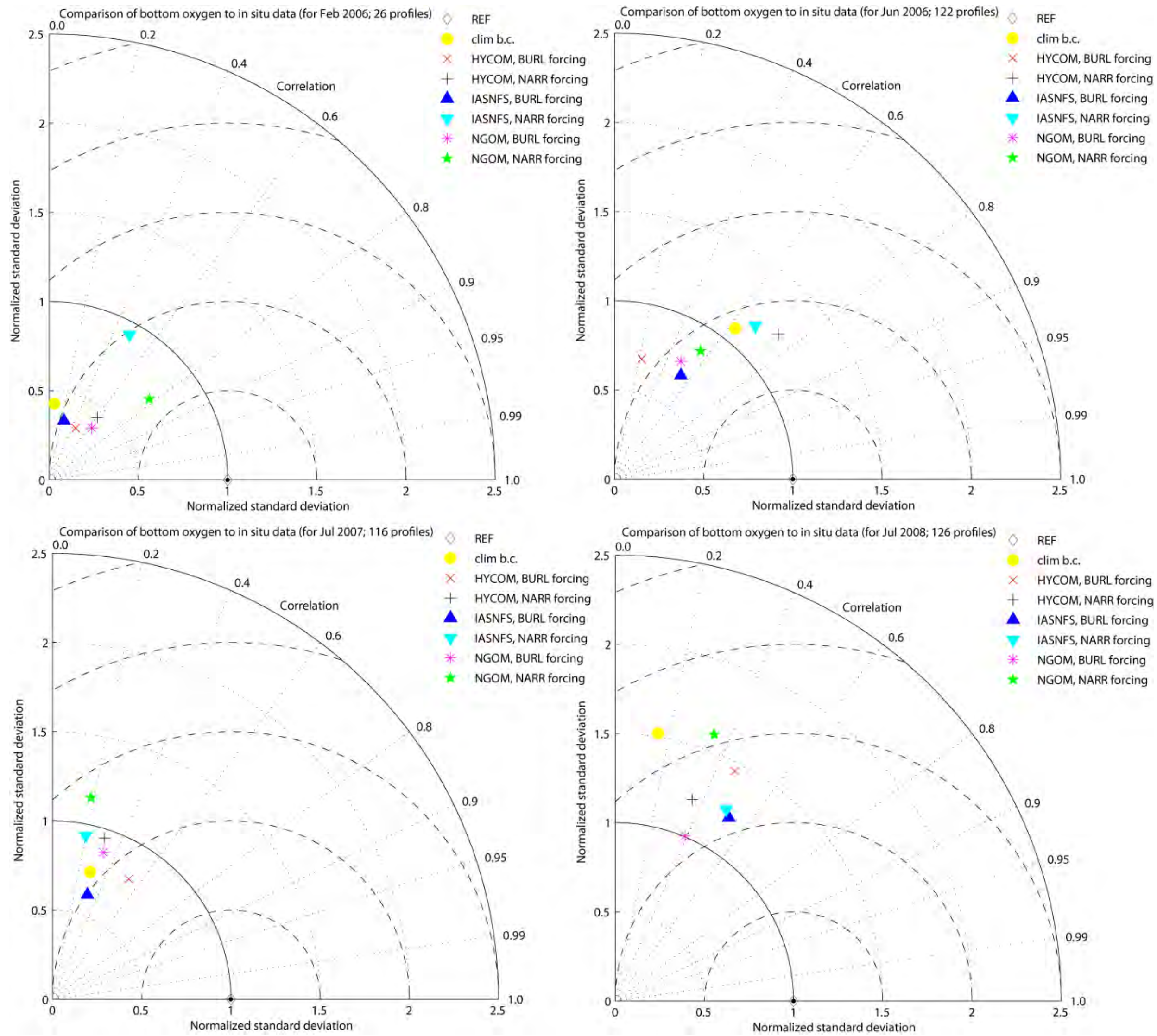

Figure D14: Taylor diagrams comparing bottom oxygen from the model and *in situ* data in February 2006 (left, top), June 2006 (right, top), July 2007(left, bottom), and July 2008 (right, bottom).

3.4.2 Surface chlorophyll, ammonium and nitrate and vertically-integrated primary production

Figures D15 and D16 show the Target and Taylor diagrams for *in situ* chlorophyll, ammonium, nitrate, and primary production, respectively, comparing the model simulations to the *in situ* observations in June 2006. The primary production and nitrate observations are reasonably well represented in all treatments, but not the agreement in *in situ* chlorophyll. This is consistent with findings discussed above and the fact that satellite and *in situ* chlorophyll are biased against each other.

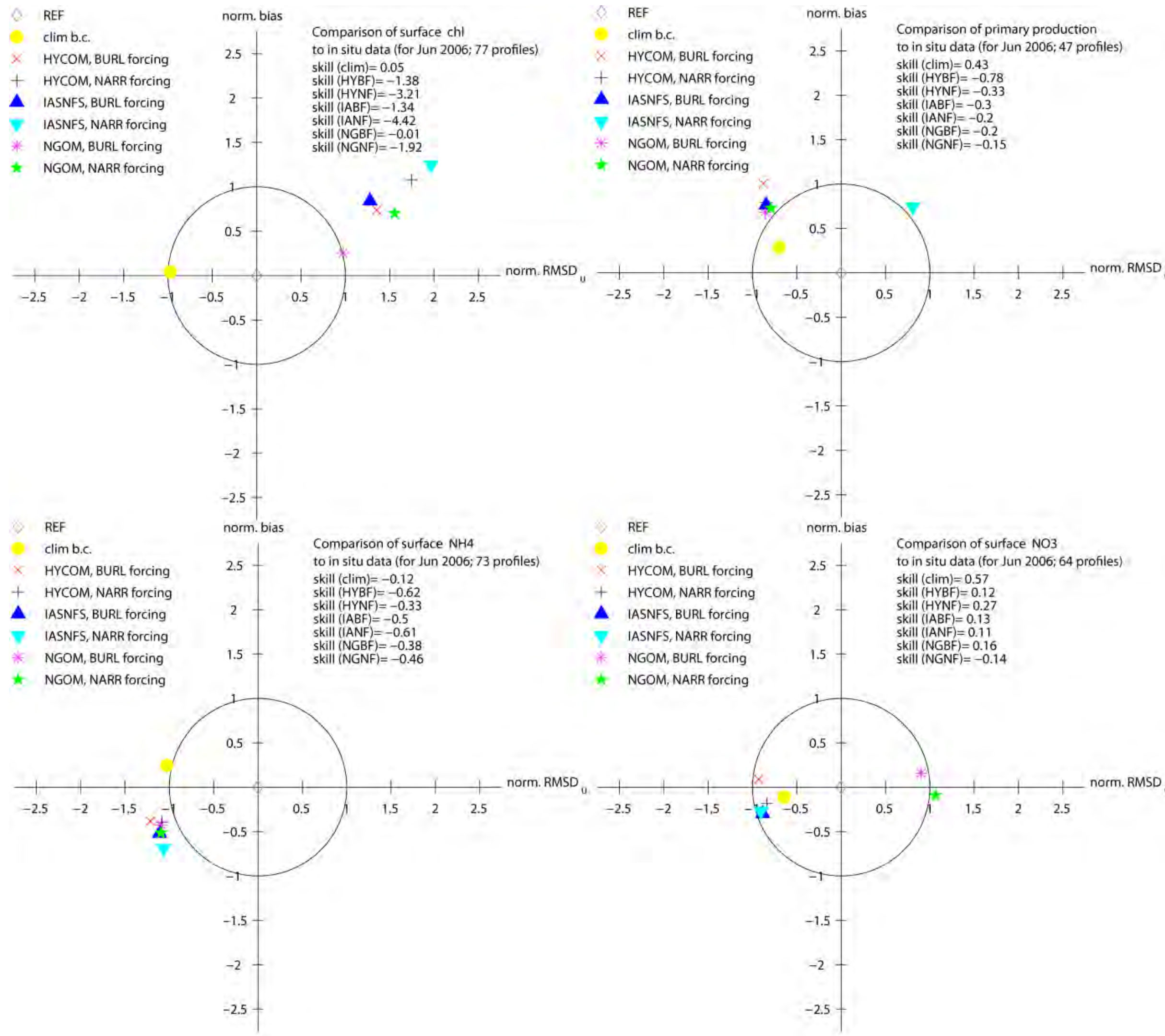

Figure D15: Target diagrams comparing chlorophyll (left, top), primary production (right, top), ammonium (left, bottom), and nitrate (right, bottom) from the model and *in situ* data in June 2006.

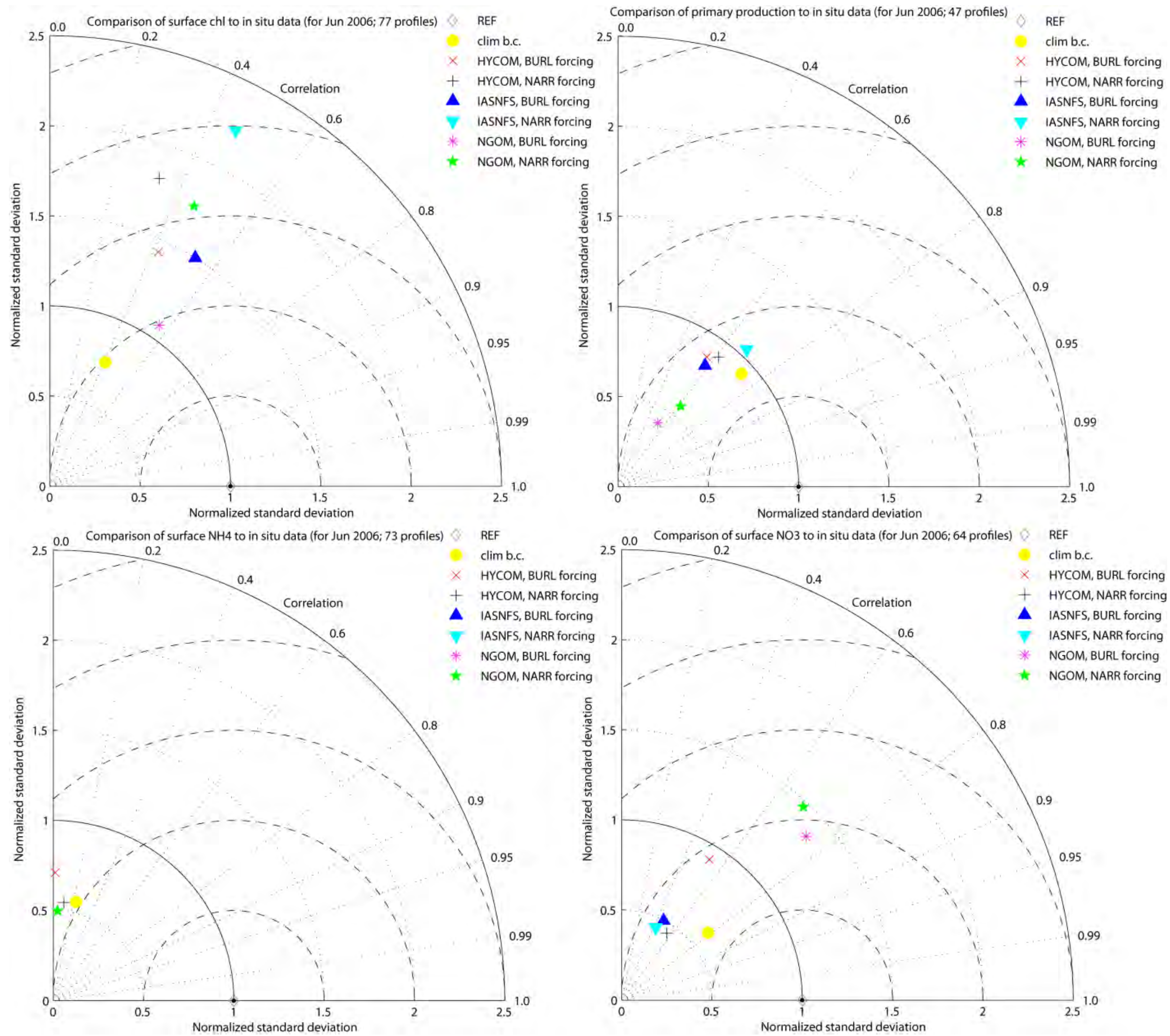

Figure D16: Taylor diagrams comparing chlorophyll (left, top), primary production (right, top), ammonium (left, bottom), and nitrate (right, bottom) from the model and *in situ* data in June

Summary

Initial analyses of the shelf biogeochemical model, nested within different physical Gulf models, suggests no definitive improvement in the biogeochemical variables in response to the physical boundary condition treatment (in contrast to the salinity response in Appendix C).

On the TX-LA shelf, hypoxic conditions are mostly confined to the bottom boundary layer, thus sufficient model resolution of the bottom boundary layer and accurate calculation of SOD is crucial for simulation of hypoxic conditions.

ROMS with instantaneous remineralization formulation for sediment oxygen consumption was successful in predicting hypoxic conditions in 2004, but not in 2005, 2006 and 2007. In 2005 no model was successful. In 2006 and 2007, the parameterization of Hetland and DiMarco was more successful. The true oxygen consumption likely lies in between these formulations which represent approaches on opposite ends of the spectrum of possibilities in that the first essentially removes any memory effect of the sediment focusing sole on instantaneous supply of organic matter, while the latter ignore variations in organic matter supply to the sediment.

In summer, hypoxic conditions near the freshwater sources are persistent and simulated well by considering organic matter supply (i.e. the instantaneous remineralization treatment), but not in the western part of the hypoxic zone.

In the western part of the hypoxic conditions are dynamic/ephemeral and strongly determined by local stratification (bottom water AOU and stratification are highly correlated).

References

Fennel , K., Wilkin, J., Levin, J., Moisan, J., O'Reilly, J., Haidvogel, D., (2006) Nitrogen cycling in the Mid Atlantic Bight and implications for the North Atlantic nitrogen budget: Results from a three-dimensional model. Global Biogeochemical Cycles 20, GB3007, doi:10.1029/2005GB002456.

Fennel, K., Wilkin, J., Previdi, M., Najjar, R. (2008) Denitrification effects on air-sea CO2 flux in the coastal ocean: Simulations for the Northwest North Atlantic. Geophysical Research Letters 35, L24608, doi:10.1029/2008GL036147

Fennel, K., Hetland, R., Feng, Y., DiMarco, S., (2011) A coupled physical-biological model of the Northern Gulf of Mexico shelf: Model description, validation and analysis of phytoplankton variability, *Biogeosciences* **8**, 1881-1899, doi:10.5194/bg-8-1881-2011

Hetland, R. and DiMarco, S. (2008) How does the character of oxygen demand control the structure of hypoxia on the Texas-Louisiana continental shelf?, J. Marine Syst., 70, 49–62, 2008.

Joliff J, Kindle JC, Shulman I, Penta B, Friedrichs MAM, Helber R, et al. (2009) Summary diagrams for coupled hydrodynamic-ecosystem model skill assessment. J. Mar. Syst. 76:64–82

Murrell, M.C., Lehrter, J.C., (2011) Sediment and lower water column oxygen consumption in the seasonally hypoxic region of the Louisiana continental shelf, Estuaries and Coasts, 34, 912-924

Taylor, K. E. (2001), Summarizing multiple aspects of model performance in a single diagram, J. Geophys. Res., 106(D7), 7183 – 7192.

Appendix E:

Summary Accomplishment(s): Substantial Progress Made Linking Sediment Transport and Biogeochemical Models within ROMS. [Courtney Harris (VIMS) & Katja Fennel (Dalhousie)]

Substantial progress has been made recently toward linking the sediment transport model (Warner et al. 2008) with the biogeochemical model (Fennel et al. 2006) within the Regional Ocean Modeling System (ROMS). The two modules now interact through tracers that represent oxygen in the water column and within the sediment bed's porewater, and through organic matter envisioned as particulate organic matter (POM) both suspended in the water column, and on the sediment bed (Figure E1). The POM travels within the sediment as suspension, and on the sea bed can be buried, resuspended, and redeposited. POM interacts with the large detritus of the biogeochemical model in that it can be either a source or sink for the organic matter of the detritus through an assumed equilibrium, reversible sorption process. Additionally, POM is reactive and influences oxygen levels both within the water column, as well as consuming oxygen as it is remineralized on the seabed (Figure E1). The model can accommodate many classes of POM, each of which requires parameters to specify its hydrodynamic properties (settling velocity and critical shear stress), and remineralization rate on the bed and in the water column.

Another advancement within ROMS, needed for reasonable geochemical profiles within the sediment bed, was the implementation of a diffusive mixing on the sediment bed, meant to represent bioturbation of the bed. To summarize, full linking of the sediment transport model required several model improvements: (1) implementation of biodiffusion on the sediment bed for porewater and particulate matter; (2) development of a module to handle reactive tracers on the sediment bed; (3) linkage of the POM to detritus via sorption within the water column.

Two boundary conditions for porewater concentrations of oxygen have been implemented that serve as end members. The first assumes no diffusion of oxygen occurs across the sediment-water interface, so that oxygen is only added to / subtracted from the seabed via deposition or erosion of oxic sediment. The second assumes unlimited diffusion of oxygen across the sediment-water interface by setting porewater oxygen concentration equal to the overlying water column at all timesteps.

A one-dimensional test case has been developed that includes biodiffusion of porewater and particulate tracers within the sediment bed, sorptive exchange between POM and detrital classes, and reaction terms for POM and porewater oxygen. The water column is 20-m deep, and a ~12-cm thick sediment bed is uses. This estimates runs for a one-year cycle and uses seasonally varying air temperature. Initially, the water column contains POM that immediately settles to the seabed under quiescent conditions. For the first several months of the year, several wind events cause resuspension of the sediment bed, as temperature increases cause an increase in detrital concentrations in the water column (Figure E2). With every resuspension event, POM and sediment is suspended into the water column, and via sorption cause a sink for detrital matter. During the second part of the model run, conditions are quiescent, and the oxygen and detritus concentrations in the water column respond to seasonal temperature changes. Figure E3 shows snapshots of the sediment bed at the beginning of the model run, during a peak resuspension event, immediately after the final resuspension event, and at the end of the model run. Changes between day 8 and 166 are due to resuspension, which allows POM to sorb organic matter from the water column and transfer it to the seabed. Changes between days 116 and 350 are due to sediment bed reactions that consume seabed oxygen and organic matter, and biodiffusion that mixes the particulate and porewater tracers in the upper 3 – 6 cm of the seabed.

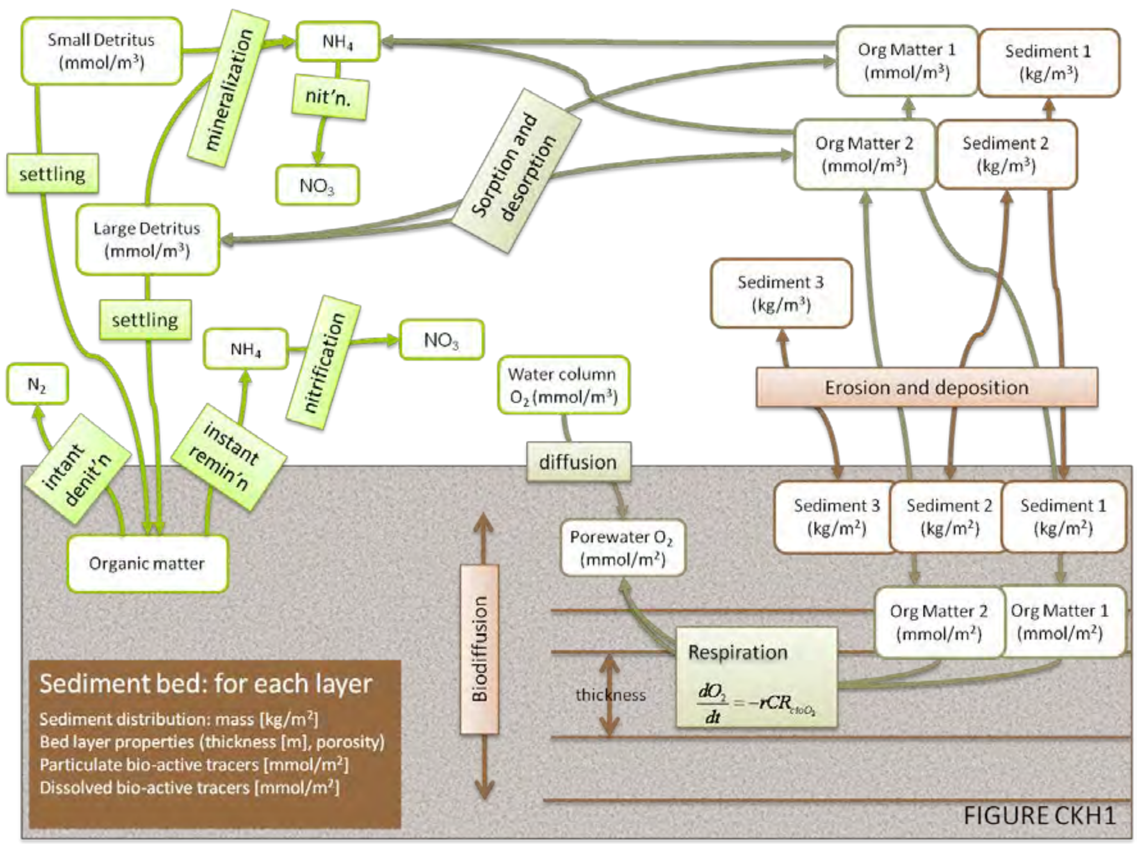

Figure E1: Schematic of coupled Sediment-Biological model within ROMS. Biological model components in green, sediment transport model in brown, and newly developed SedBio components in sage. Clear boxes represent tracers and arrows/shaded boxes represent processes.

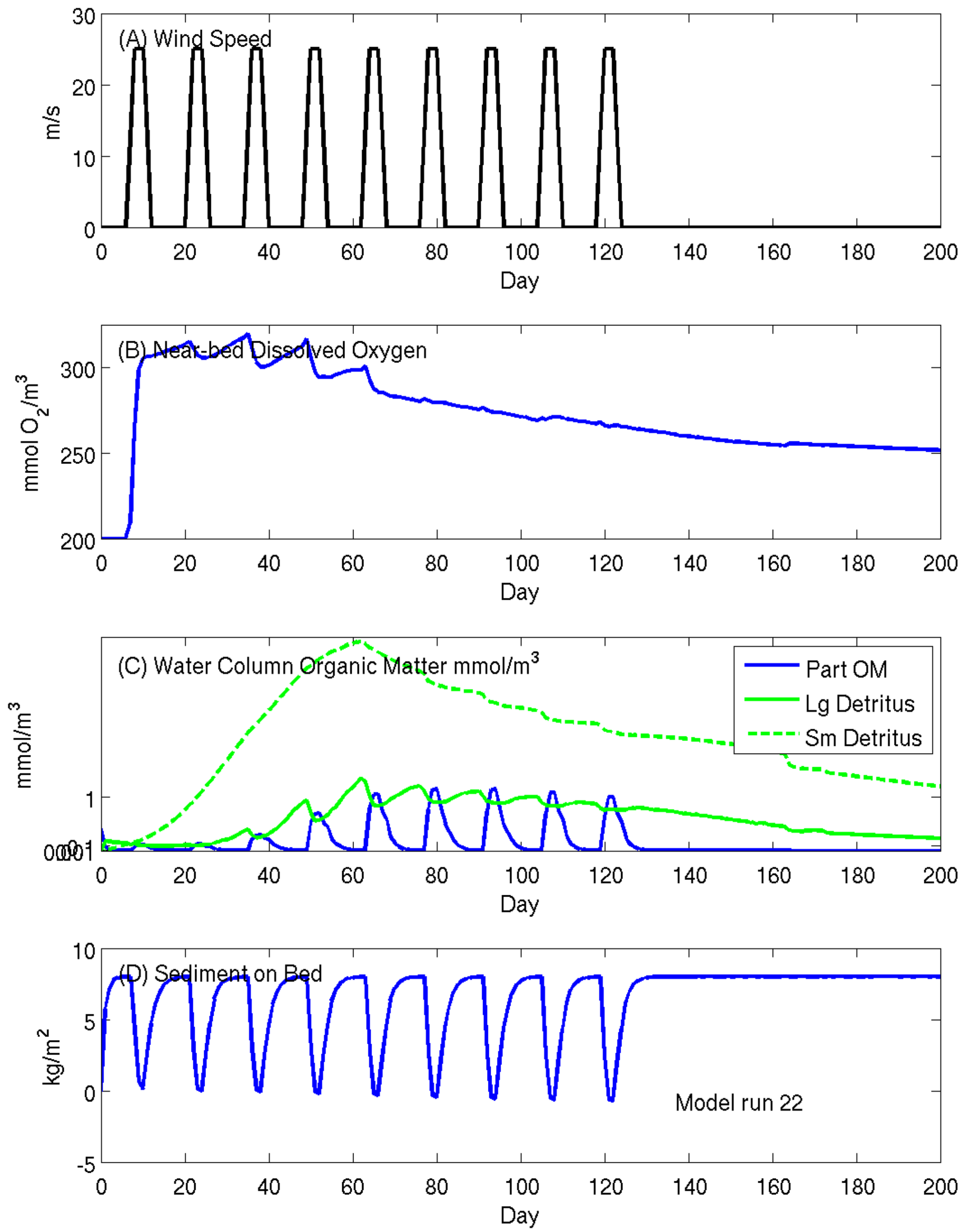

Figure E2: SEDBIO_TOY one-dimensional model run for 200 days. (A) Input wind speed (m/s); (B) Near-bed dissolved oxygen (mmol/m3); (C) Water column organic matter (mmol/m3); biological detritus in green and POM in blue; and (D) Sediment on bed (kg/m2) showing time series of erosion and deposition.

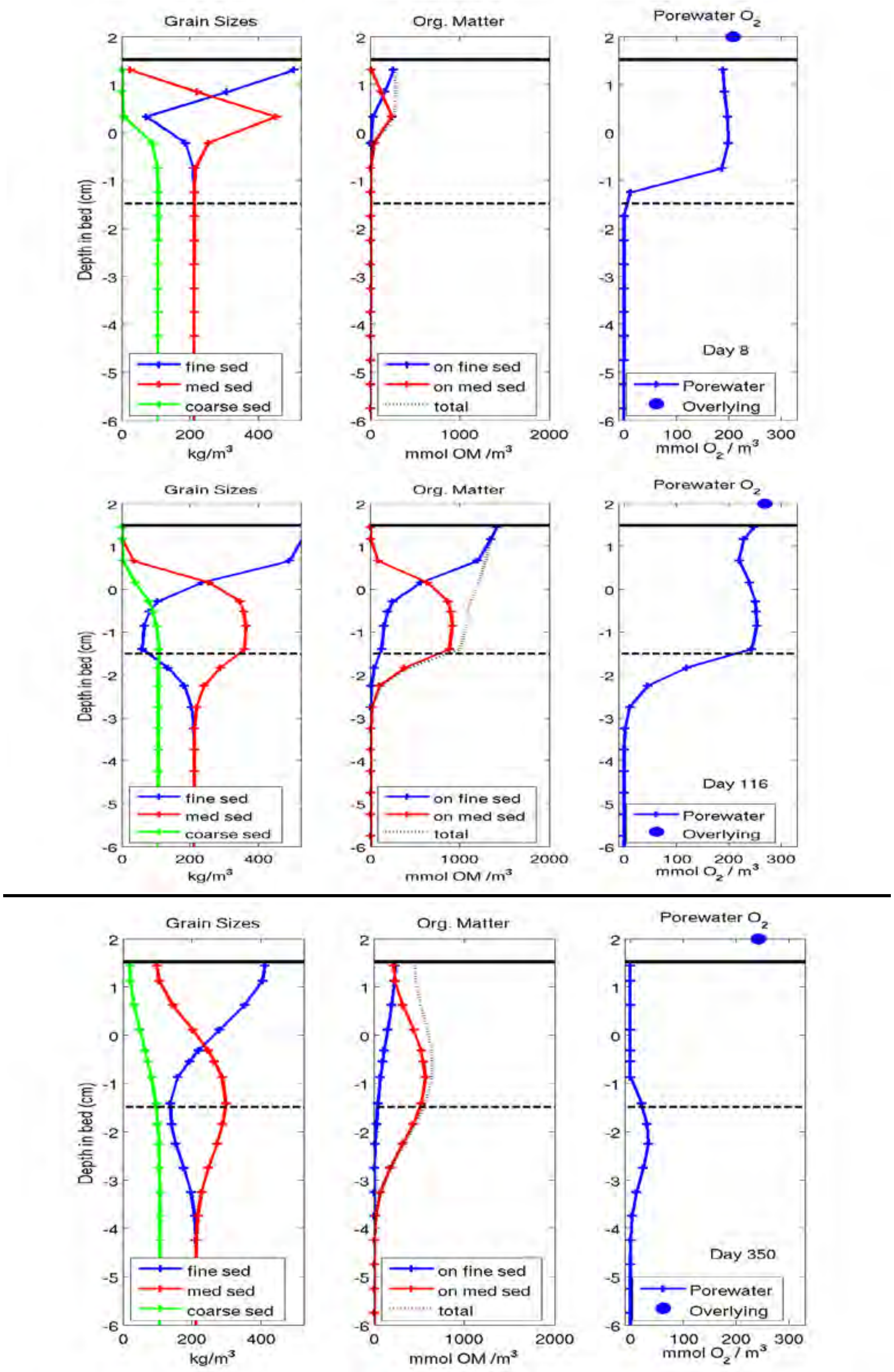

Figure E3: Profiles of the sediment bed showing (A) grain size variation in the bed (see legend); (B) POM concentration on the fine (blue) and coarser (red) fine-grained sediment; and (C) Porewater oxygen concentration. Vertical axis shows depth (cm) in the bed. Solid black line shows instantaneous sediment bed surface, and dashed line is 3 cm below, indicating the lower layer of the zone of strong bioturbation. Panels represent days 8 (top), 116 (middle), and 350 (bottom) in the model run.

References

Warner, J.C., C.R. Sherwood, R.P. Signell, C.K. Harris, and H. Arango. 2008. Development of a three-dimensional, regional, coupled wave-, current-, and sediment-transport model. Computers and Geosciences, 34: 1284 – 1306.

Fennel, K., Wilkin, J., Levin, J., Moisan, J., O'Reilly, J., and Haidvogel, D., 2006. Nitrogen cycling in the Middle Atlantic Bight: results from a three-dimensional model and implications for the North Atlantic nitrogen budget, Global Biogeochem. Cy., 20, GB3007, doi:10.1029/2005GB002456

Appendix F:

Summary Accomplishment(s): Analysis of ROMS near bottom trajectories during June-July 2007 showed residence times > 90 days in some hypoxic areas and hypoxic water masses originating offshore, near the shelf break.

Lagrangian analysis of near bottom velocities from the coupled biochemical-physical ROMS model showed surprisingly long residence times in three regions of interest on the shelf south of Louisiana. Figure F1 shows example residence time maps for three regions of interest for particles launched on July 1, 2007. Residence times > 90 days are found in all three regions. When hypoxic near-bottom water from July 1 was advected backward in time using ROMS velocities (Figure F2), this water was found to originate near the shelf break. [Contact: Bruce Lipphardt (U. Delaware)].

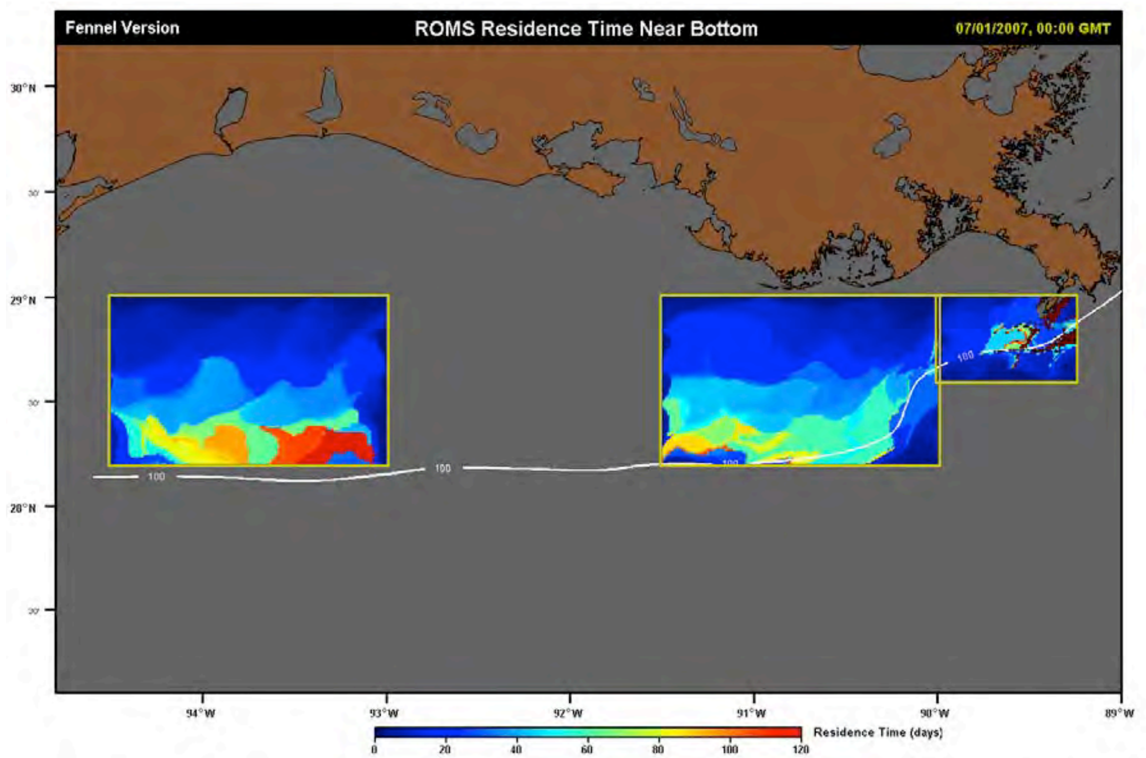

Figure F1: Maps of near-bottom residence times (in days) for particles launched in three regions of interest (gold boxes) at 0000 UT on July 1, 2007. Residence time is defined as the time it takes for particles launched on a regular grid to exit the region of interest.

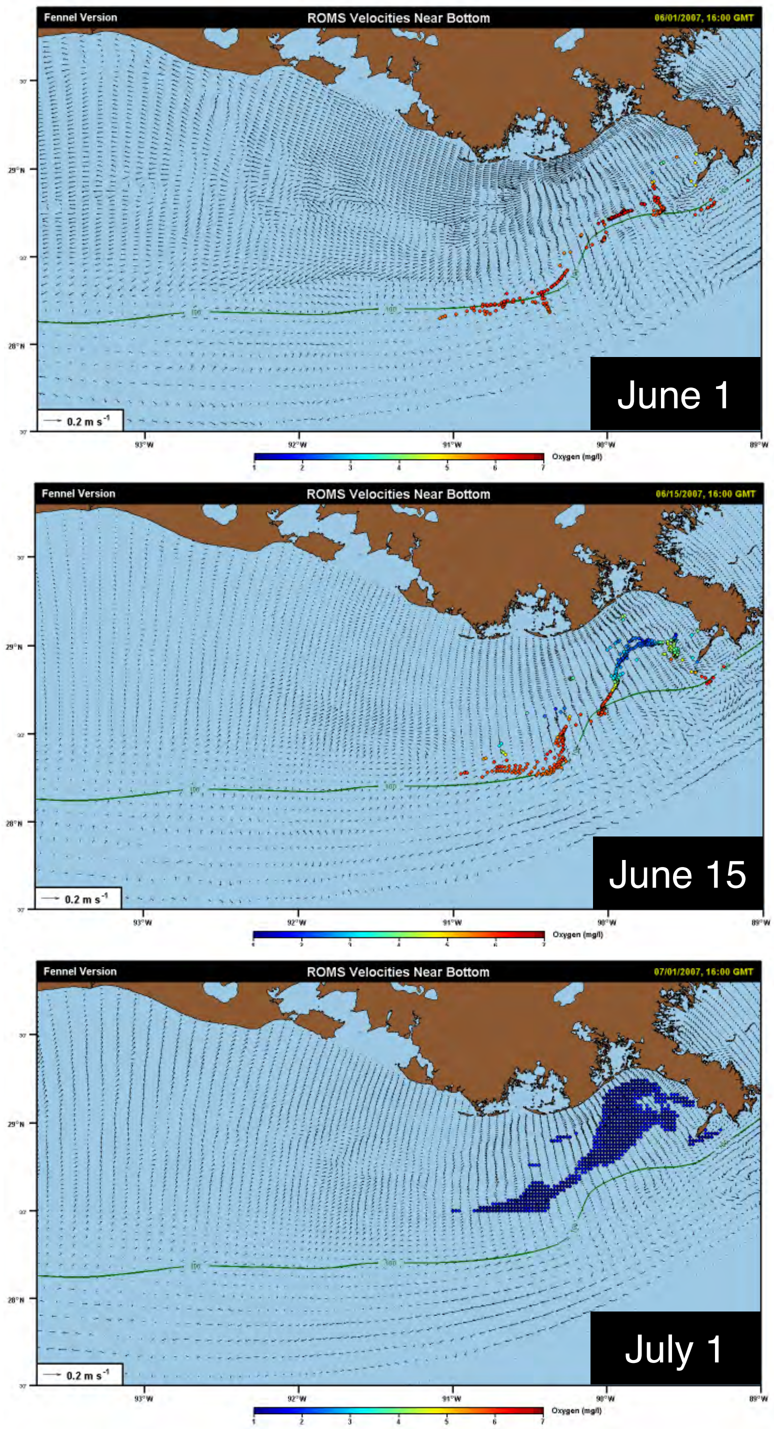

Figure F2: Snapshots of near-bottom particle positions on June 1, June 15, and July 1, 2007 for trajectories computed using velocities from the ROMS coupled biological-physical model. The particles are color coded to show their instantaneous dissolved oxygen concentration (in mg/l). The colorbars show the oxygen scale.

Appendix G:

Summary Accomplishment(s): *ROMS simulations with realistic boundary conditions and instantaneous remineralization provide a more realistic inshore position of hypoxic area relative to EPA GEMS with comparable representation of hypoxic area size. The EPA GEMS hypoxic area and phytoplankton biomass are consistently too far offshore for each of the four years. ROMS with climatological boundary conditions and instantaneous remineralization gets the inshore location correct but appears to under-represent the size of hypoxic area relative to EPA GEMS. Future hypoxic zone area and phytoplankton biomass comparisons of ROMS, using the Hetland and DiMarco sediment oxygen consumption formulation, with EPA GEMS would be of interest as these ROMS simulations better represented the size of the hypoxic area even with climatological boundary conditions but, as with the EPA GEMS, tended to be too far offshore relative to the instantaneous remineralization cases.*

Topic: Comparison of simulation results of ROMS and EPACOM-GEM3D models for the Texas-Louisiana continental shelf.

Description of model simulations

The simulations used for the comparison are made with ROMS using the Fennel et al. (2006, 2008, 2011) biological model (seven model runs) and the EPACOM-GEM3D coupled model (one model run) of the Texas-Louisiana continental shelf.

The EPACOM-GEM3D (hereafter GEM) model run used for the comparison is the version 3 of the model available at this location:
http://testbedapps.sura.org/thredds/dodsC/shelf_hypoxia/gem3d/agg.nc

The EAPCOM-GEM3D is a high resolution 3D hypoxia model which is an extension of a 1D model developed by the EPA for hypoxia simulation (Eldridge and Roelke, 2010) and integrated with a circulation model on 2-km horizontal grids and 20 vertical layers on the shelf that covers the Louisiana shelf. The circulation model (EPACOM) is forced with real-time wind, air pressure, heating/cooling, salinity flux and tides. The open boundary conditions are derived from a regional model that covers the Gulf of Mexico (IASNFS: Ko et al., 2003). The important river runoffs from 95 rivers and streams based on USGS and Army Corps of Engineers daily measurement are included in the model. The hypoxia model (GEM3D) consists of a plankton food web model that has 6 phytoplankton groups and 1 zooplankton group and a multi-element diagenetic model that traces oxygen, nitrogen, phosphate, carbon and various organic matters.

The multi-year model simulation has been conducted. For the version 3, it is initialized with NODC monthly DO, DIN and DIP climatology. The monthly climatology is also used for the open boundary conditions.

The ROMS model runs include simulations with climatological boundary conditions and boundary conditions from two different operational physical models for the Gulf (HYCOM and IASNFS). Simulations with climatological boundary conditions and three treatments of the biological bottom boundary condition at the sediment-water interface are used:

- Instantaneous remineralization of particulate matter (inst. remin.)
- Hetland & DiMarco (2008) sediment oxygen demand (SOD) parameterization

- Murrell & Lehrter (2010) SOD parameterization

Simulations with more realistic physical boundary conditions use two different wind forcings (BURL, NARR) and two types of boundary conditions (HYCOM, IASNFS) resulting in four model runs in total:

- HYCOM boundary conditions and BURL wind forcing
- IASNFS boundary conditions and BURL wind forcing
- HYCOM boundary conditions and NARR wind forcing
- IASNFS boundary conditions and NARR wind forcing

Simulations with boundary conditions from the NGOM model were not included in this comparison because the NGOM boundary conditions were not available for July 2004 and 2005. It should also be noted that horizontal boundary conditions for the biological variables use the same climatological values for all simulations.

Analysis

Bottom hypoxia

Bottom hypoxic conditions were calculated from bottom oxygen concentrations simulated with ROMS and GEM and observations made during the LUMCON hypoxia cruises in July. The critical value used for oxygen concentration is 62.5 mmol m^{-3}. If the simulated oxygen concentration is below this value during any day of the LUMCON cruises, the water in considered hypoxic.

Phytoplankton biomass

Phytoplankton biomass (mmol N m^{-3}) is available for the ROMS output but has been calculated for the GEM model. Phytoplankton concentration (cell m^{-3}) was transformed into phytoplankton biomass (mmol N m^{-3}) using the minimum (0.12×10^{-9}) and the maximum (0.959×10^{-9}) values of the nitrogen cell quota (mmol N $cell^{-1}$) from Eldridge & Roelke (2009). Note that chlorophyll concentrations are not available for the GEM model. Comparisons of simulated and observed chlorophyll were not attempted because these would have had to rely on further assumptions converting GEM output to chlorophyll.

Hypoxia comparisons

Below we compare spatial maps of hypoxic conditions predicted by the different models with the LUMCON observations and show time series of hypoxic area. Spatial maps of simulated and observed hypoxic areas are presented for the period 2004-2007 (Figures G1-G4). In 2004 all ROMS simulations capture the hypoxic conditions near the delta accurately. The ROMS models with HYCOM-NARR and IASNFS-NARR forcing also capture the hypoxic conditions near Atchafalaya Bay and further downstream. The EPA-GEM model produces a patch of hypoxic conditions that is too far offshore. In 2005 all models underestimate hypoxic conditions. The ROMS model with Hetland & DiMarco’s SOD parameterization is the only model that predicts a large hypoxic regions, however, it is located too far offshore. In 2006 the Hetland and DiMarco treatment is the only model among the ROMS variants that captures hypoxic conditions reasonably. The EPA-GEM model also predicts hypoxic conditions reasonably in this year. In

2007 the ROMS model with Hetland & DiMarco treatment produces the best prediction of hypoxia.

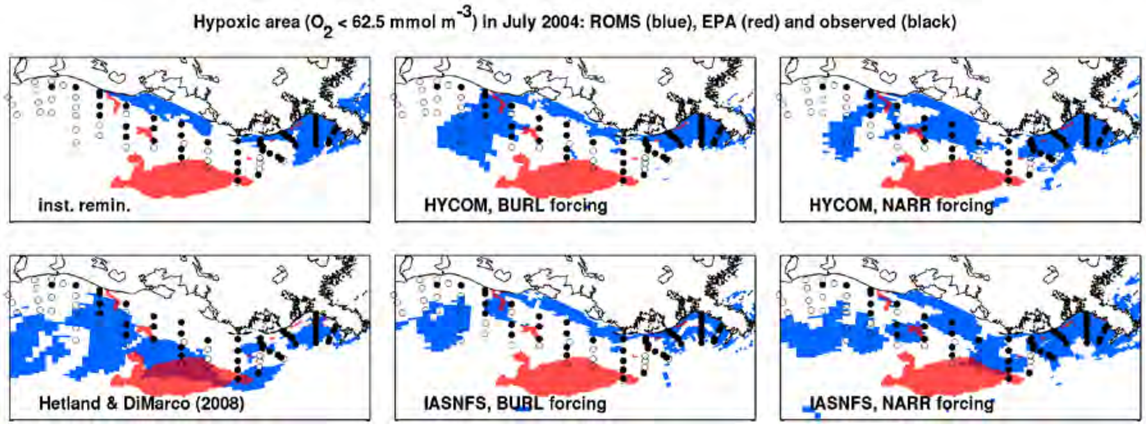

Figure G1: Comparison between the hypoxic area simulated with ROMS and EPACOM-GEM3D (EPA) and the observed hypoxic conditions during the LUMCON cruise in July 2004. Simulated hypoxic areas from ROMS and GEM are shown as blue and red areas, respectively. Observations are shows as circles; filled circles indicate hypoxic conditions. Each panel shows the same hypoxic area simulated with GEM (red) but different simulations of ROMS (blue), namely ROMS using instant remineralization (upper left) or the Hetland & DiMarco (2008) bottom boundary condition (lower left) with climatological boundary conditions. All other panels show ROMS with instant remineralization as bottom boundary condition but either HYCOM or IASNFS boundary forcing and BURL or NARR wind forcing (center and right panels).

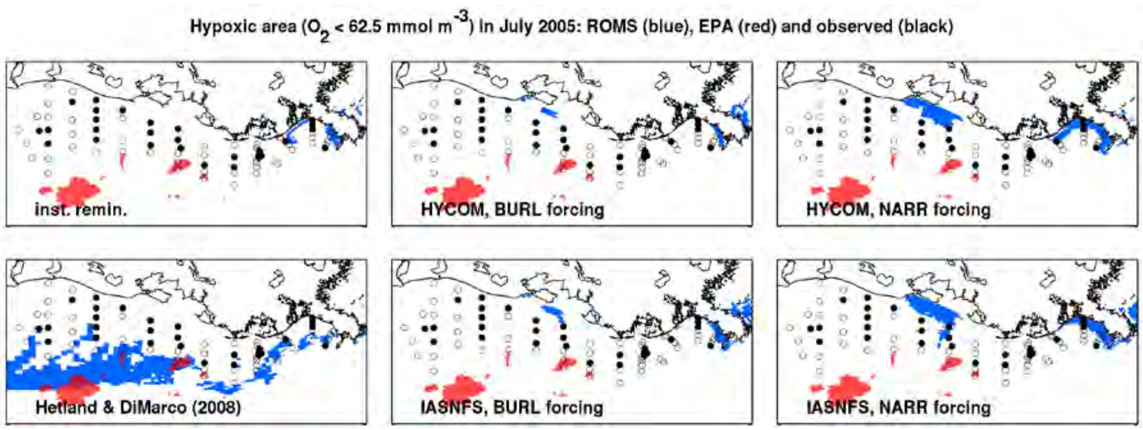

Figure G1: Like figure G1, but for July 2005.

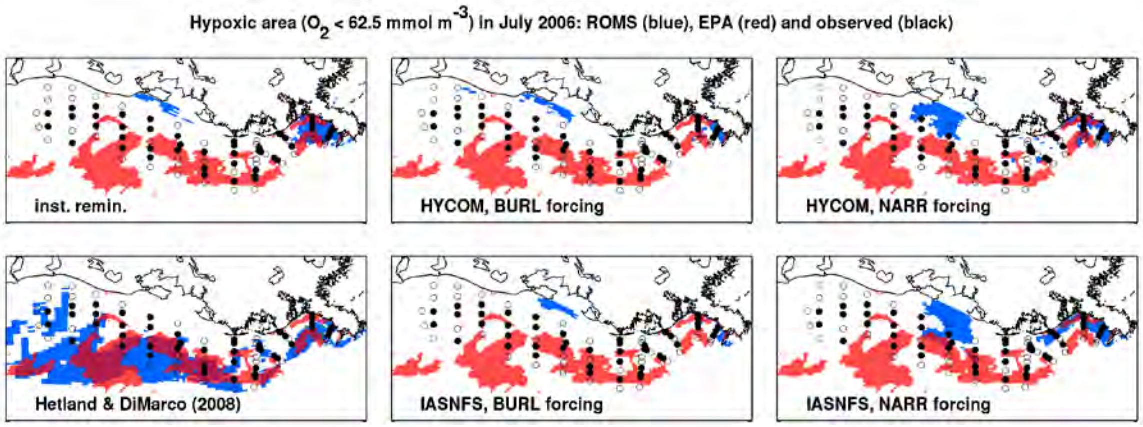

Figure G2: Like Figure G1, but for July 2006.

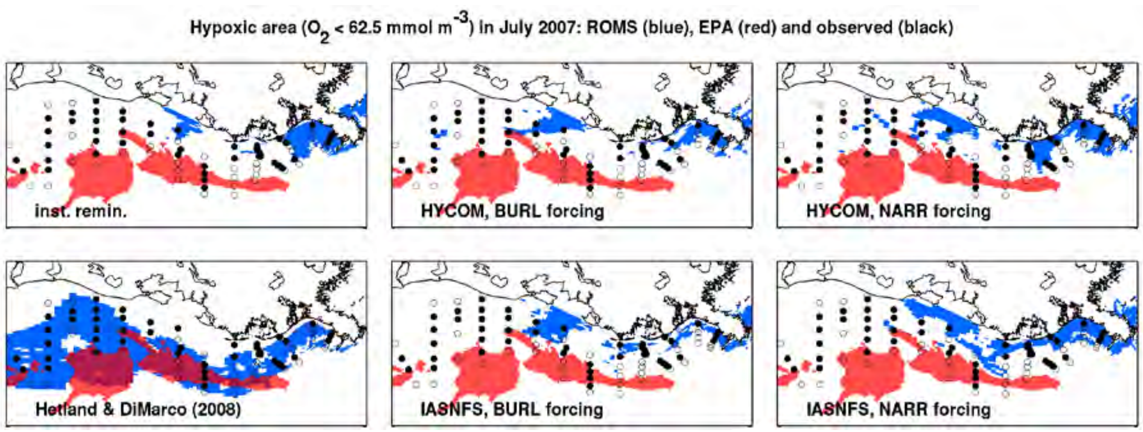

Figure G3: Like Figure G1, but for July 2007.

Time series of simulated and observed total hypoxic area for the period 2004-2007 are shown in Figure G5. The predicted hypoxic area is largest for the ROMS simulation with Hetland and DiMarco parameterization that tends to overestimate the observed hypoxic area. The other simulations (ROMS with climatological boundary and different treatments of sediment oxygen consumption and the EPA-GEM model with realistic boundaries) underestimate hypoxic area although the EPA-GEM appears to come closest, being consistent with the other nested results shown in Figure D10 (Appendix D). It should be noted that the ROMS model with climatological boundary conditions has a lower vertical resolution than the nested ROMS variants (20 vertical layers versus 30). It is possible that the refinement in vertical resolution increases the size of the predicted hypoxic area.

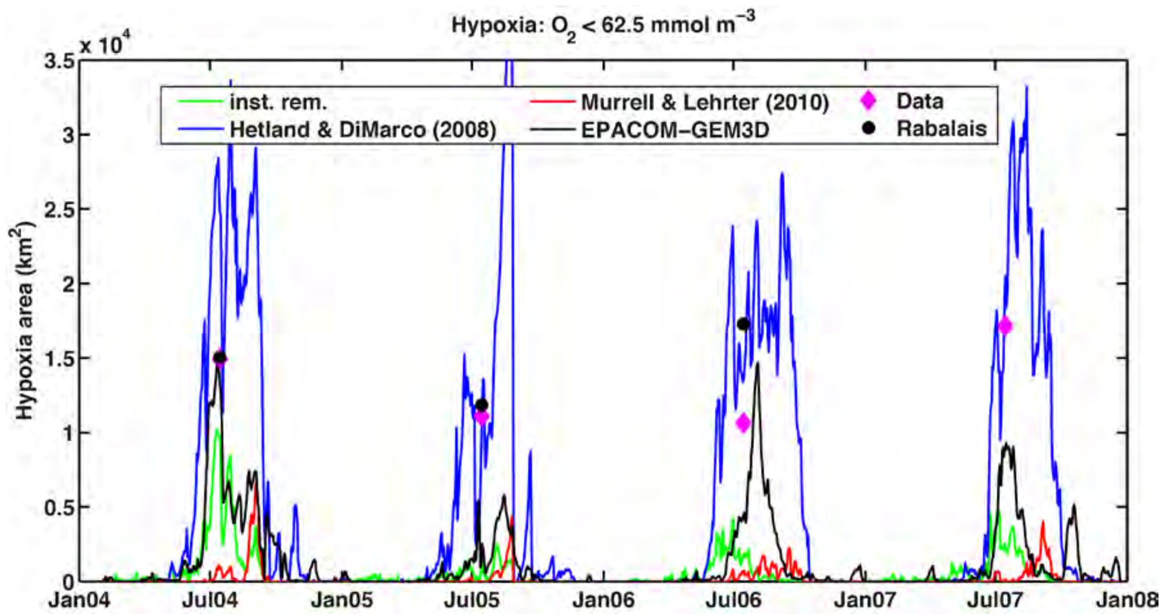

Figure G4: Daily hypoxic area (km^2) simulated with ROMS using instantaneous remineralization (green line), Hetland & DiMarco (2008) parameterization (blue) or Murrell & Lehrter (2010) parameterization (red line) all with climatological boundary conditions and simulated with the EPACOM-GEM3D model (black line). The mid-summer total hypoxic area during the LUMCON cruises (magenta diamonds) and reported by Rabalais (black dots) are presented as well.

July surface phytoplankton biomass comparisons

Below we show attempts to compare simulated phytoplankton concentrations for 2004-2007 (Figures G6-G9) between the EPA-GEM model and the ROMS model with instantaneous remineralization and climatological dynamic boundary conditions. The comparison is made difficult by the fact that both models use different units (the EPA-GEM model predicts phytoplankton in cell per volume, while ROMS used mol N per volume). Phytoplankton predicted by EPA-GEM was converted to mol N per volume using minimum and maximum conversion factors. It is obvious that the EPA-GEM model predicts higher phytoplankton biomass offshore, than the ROMS model (comparing GEM with min conversion factor on ROMS).

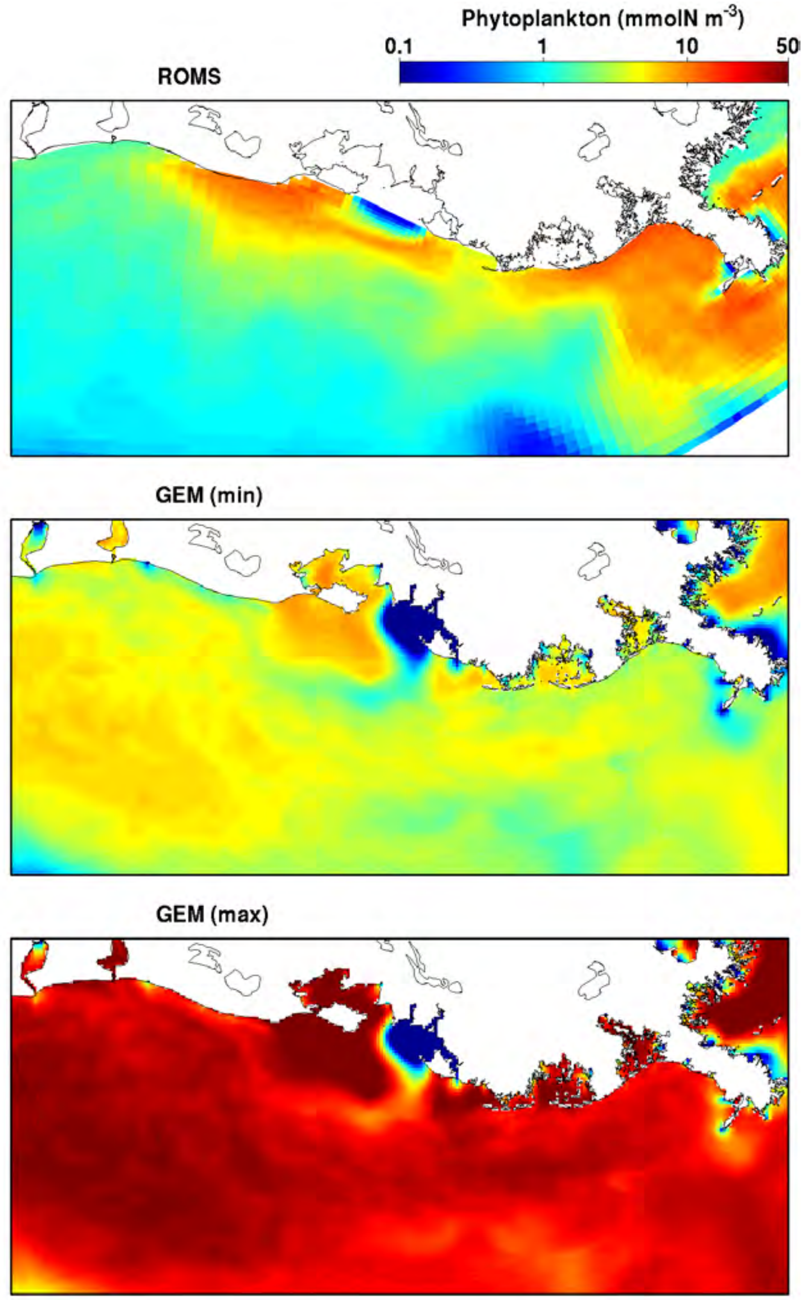

Figure G6: Average surface phytoplankton biomass during July 2004 simulated with ROMS using instant remineralization bottom boundary condition with a climatological forcing (top) and simulated with EPACOM-GEM3D and calculated using the minimum (center) and the maximum (bottom) values of the nitrogen cell quota from Eldridge & Roelke (2009).

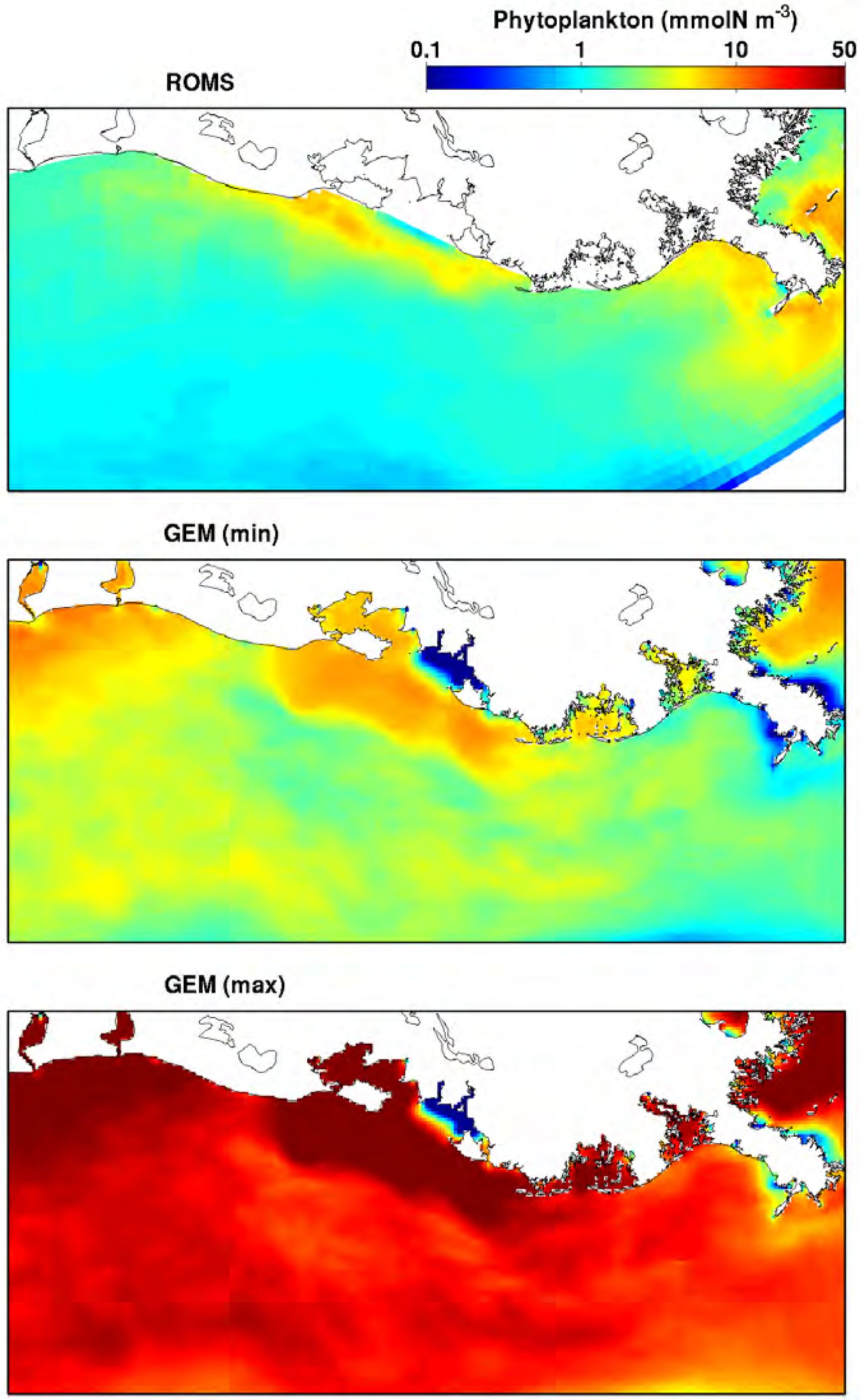

Figure G7: Like Figure G6 for July 2005.

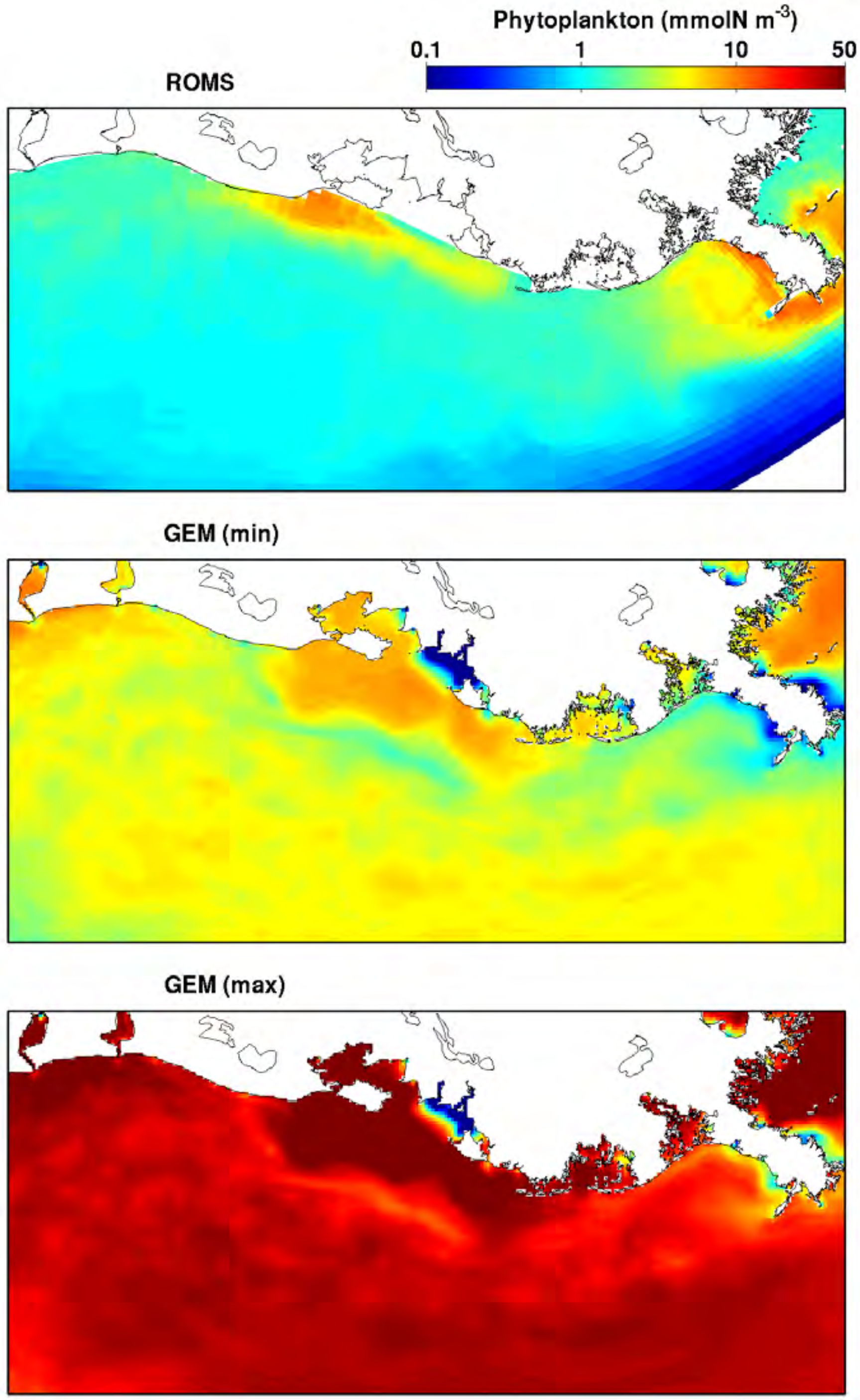

Figure G8: Like Figure G6 for July 2006.

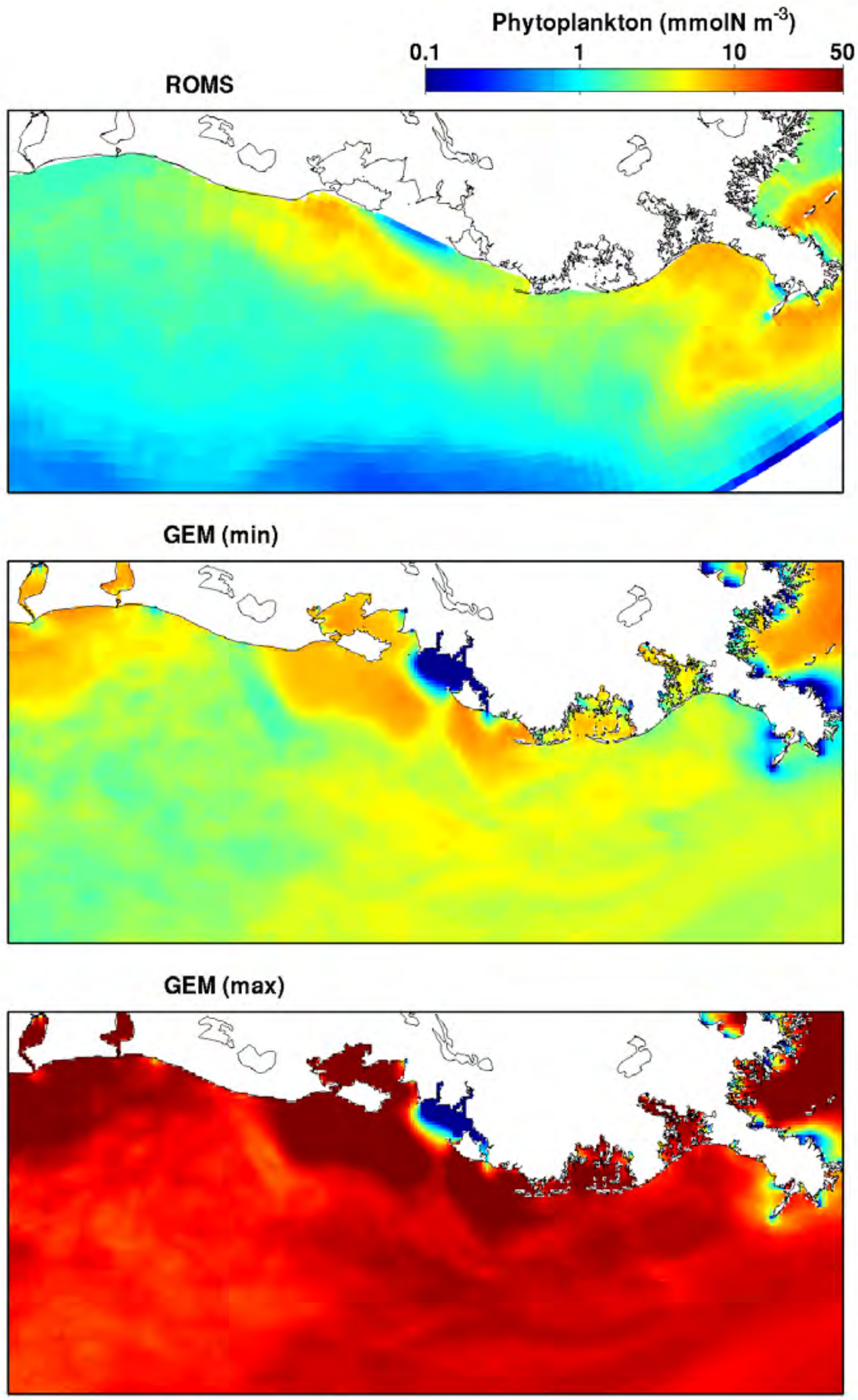

Figure G9: Like Figure G6 for July 2007.

Summary

ROMS simulations with realistic boundary conditions and instantaneous remineralization provide a more realistic inshore position of hypoxic area relative to EPA GEMS with comparable representation of hypoxic area size. The EPA GEMS hypoxic area and phytoplankton biomass are consistently too far offshore for each of the four years. ROMS with climatological boundary conditions and instantaneous remineralization gets the inshore location correct but appears to under-represent the size of hypoxic area relative to EPA GEMS.

Future hypoxic zone area and phytoplankton biomass comparisons of ROMS, using the Hetland and DiMarco sediment oxygen consumption formulation, with EPA GEMS would be of interest as these ROMS simulations better represented the size of the hypoxic area even with climatological boundary conditions but, as with the EPA GEMS, tended to be too far offshore relative to the instantaneous remineralization cases.

References:

Eldridge, P.M, and D.L. Roelke, 2010: Origins and scales of hypoxia on the Louisiana shelf: importance of seasonal plankton dynamics and river nutrients and discharge, Ecological Modeling, 221, 1028-1042.

Ko, D.S., R.H. Preller, and P.J. Martin, 2003: An experimental real-time Intra-Americas Sea Ocean Nowcast/Forecast System for coastal prediction, Proceedings, AMS 5th Conference on Coastal Atmospheric and Oceanic Prediction and Processes, 97-100.

Appendix H:

Summary Accomplishment(s): Supported transition of U.S. Navy operational Gulf of Mexico regional ocean nowcast/forecast capability. [Contacts: Jerry Wiggert (USM), Frank Bub (Naval Oceanographic Office), Pat Fitzpatrick(NGI) & John Harding]

Introduction

The Naval Research Laboratory and NAVOCEANO jointly created a capability, now routine at NAVOCEANO, to relatively easily (1-2 week effort) set up a regional ocean nowcast/forecast system. The time consuming effort comes with the rigorous evaluation of the resultant system to assure its utility for the expected applications and to better understand its limitations. Aware of NOAA's interest in the region, the availability of funding via the SURA testbed to support the technical operational evaluation, and the opportunity to have additional academic exposure to its regional products, the Naval Oceanographic Office originally planned to set up the pre-operational regional AMSEAS (Gulf of Mexico/ Caribbean) ocean nowcast/forecast system in summer of 2010. The Deepwater Horizon Incident accelerated this original time schedule with initial AMSEAS set up and output occurring even before the SURA testbed kickoff meeting in late June 2010. Given the national interest in the DHI, NAVOCEANO proceeded to instrument the northern Gulf with gliders, drifters, and profiling floats, and used this information along with available academic and NOAA measurements to provide an early evaluation of AMSEAS in the oil spill region. This observational focus around the spill site led to a concentrated accumulation of physical data during the summer months of 2010 that peaked at 21,257 profiles in June (Figure H1).

AMSEAS real-time fields were provided daily via the NGI/NCDDC EDAC/OceanNOMADS developmental server to the NOAA Oil Spill Response team providing daily forecasts of the oil distribution. Based on their accelerated, early summer evaluations, AMSEAS is now considered operational by the Navy. The SURA shelf hypoxia testbed funding supplemented the initial summer 2010 technical evaluation effort with its year-long follow-on evaluation.

Analysis of ocean forecasts

A pair of NAVO OPTEST evaluation toolkits MAVE (Model and Analysis Viewing Environment) and PAVE (Profile Analysis and Visualization Environment, since migrated to PAM) has been successfully transitioned from NAVO to academic partner (Univ. Southern Mississippi, USM). MAVE provides tools for visualizing AMSEAS model solutions, while PAM acts to aggregate model output and accumulations of in situ profiles so direct comparison to ocean state can be accomplished and quantifiable metrics obtained. NAVO has a number of in house metric assessments that can then use these co-located model/observation points to assess the 4-day AMSEAS forecasts, where assessment within PAM allows for effectively concentrating on specific time-space portions of the model domain where close scrutiny is of interest. For example, quantification of temperature difference at 50 m (model – observation, MO), 27°C isotherm depth, and sonic layer depth comparisons during the first week of October 2010 are easily extracted and visualized using PAM (Figure H2).

NAVO Profiles Database: Distributions by Month

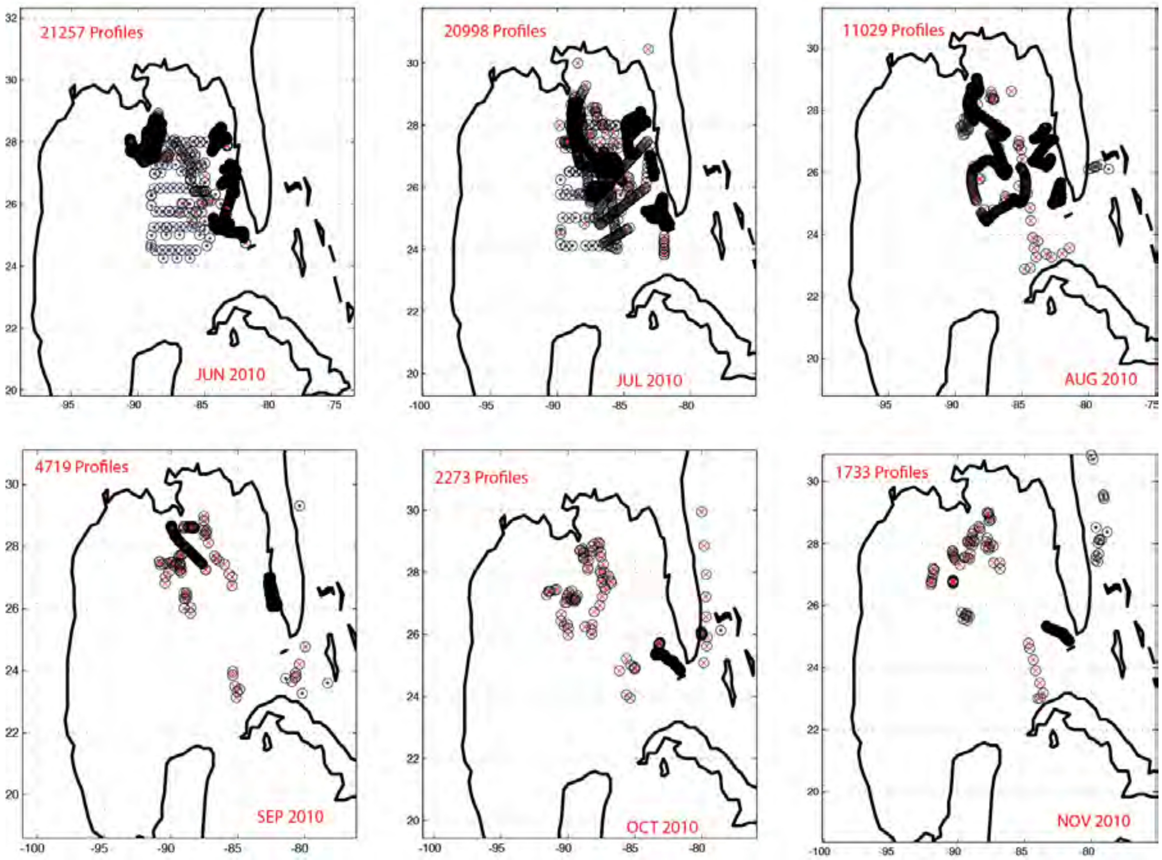

Figure H1: Distribution of profiles in the northern and eastern Gulf of Mexico obtained from sampling assets deployed in the months following the Deepwater Horizon incident.

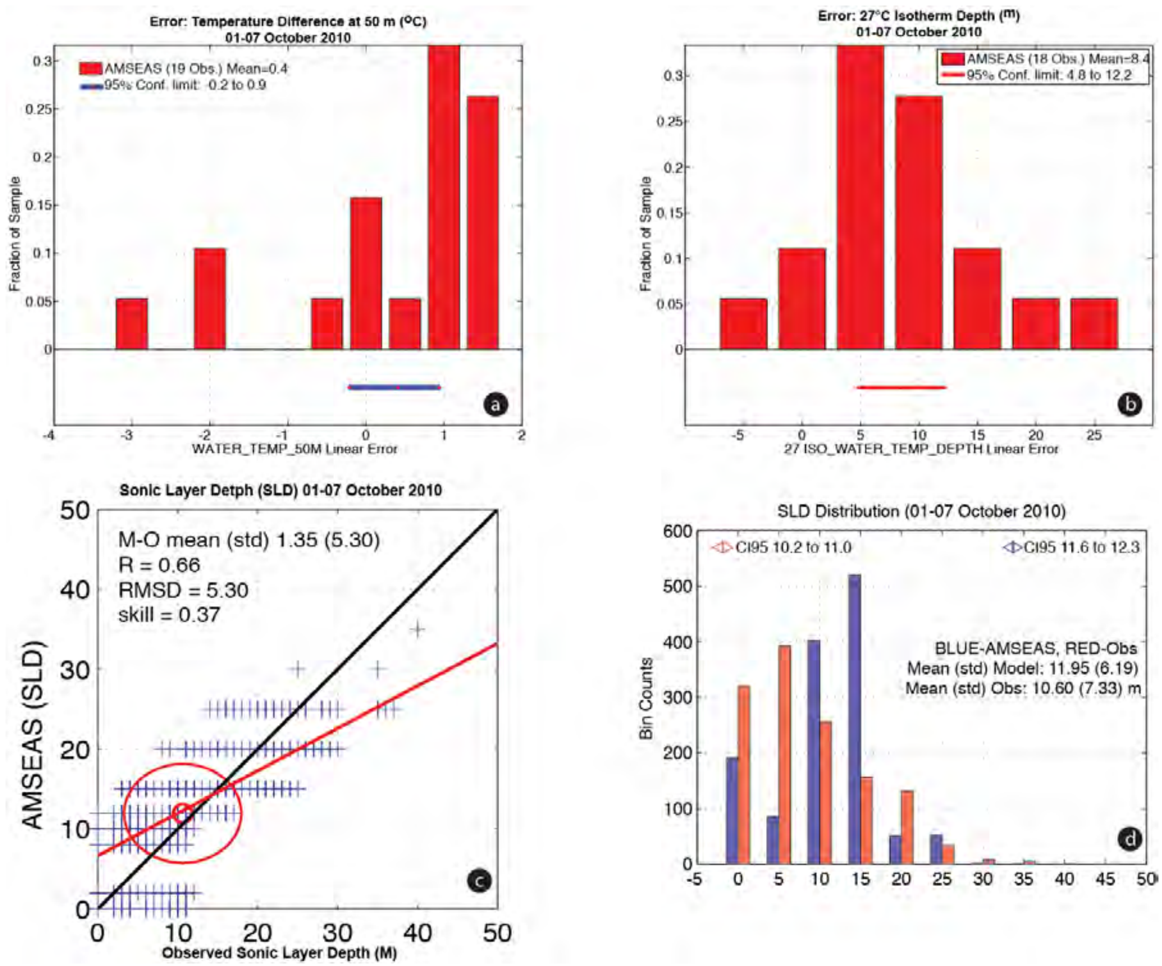

Figure H2: AMSEAS assessments produced by PAM for first week of October 2010. (a) Temperature error (model-observations) at 50 m. (b) Difference in 27 ° isotherm depth. (c) Scatter plot of sonic layer depth (SLD) based on observations vs. SLD from AMSEAS. (d) Histogram of SLD based on observations (red) and AMSEAS (blue).

Another example assessment features sonic layer depth (SLD). SLD is defined as the depth of the maximum sound speed between the surface and the deep sound channel axis (DSCZ, sound speed inflection point at depth). It is analogous to the mixed layer depth that is commonly reported in oceanographic context but has obvious significance to naval operations. The four-panel figure shows the magnitude of SLD MO difference for the four-day AMSEAS forecast from October 2010 (Figure H3). Profile location is graphically shown, with the magnitude of SLD MO indicated by the color of its location marker. The difference codes are defined along the right side of the graphic.

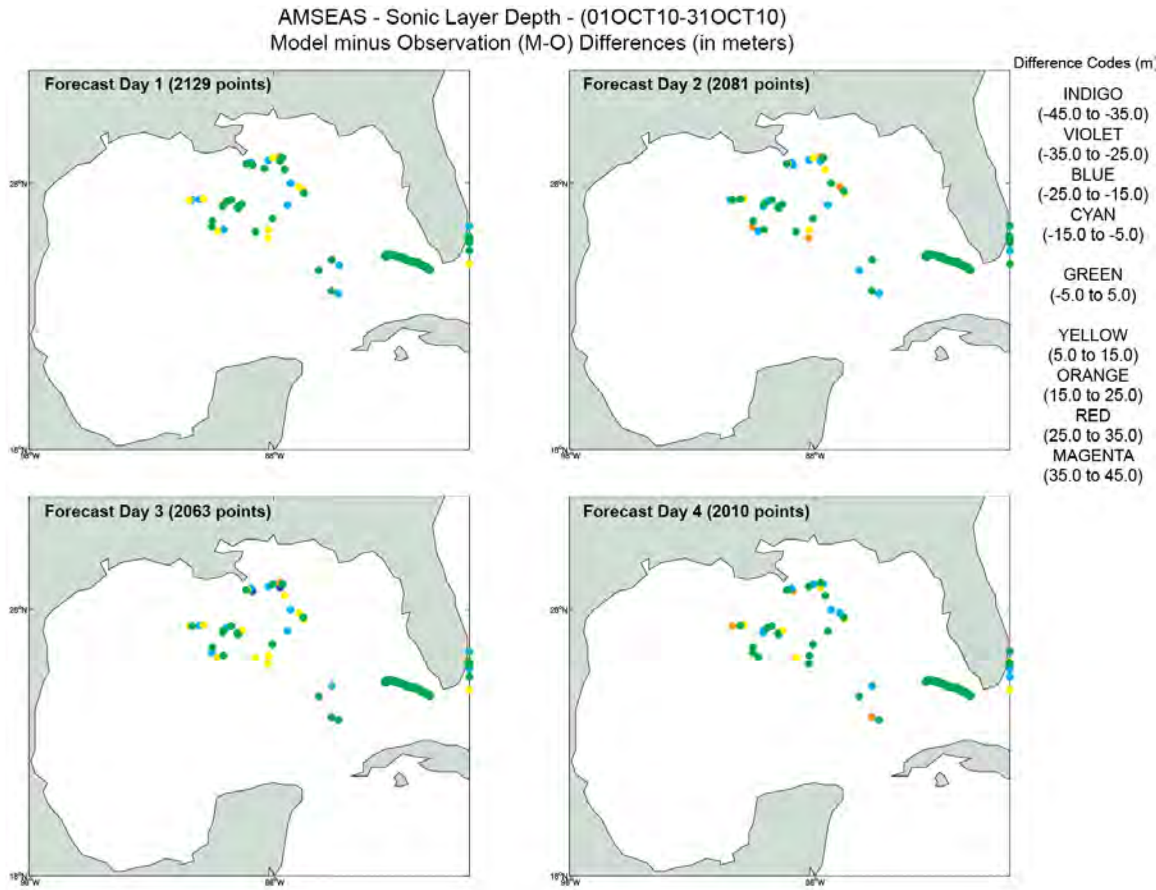

Figure H3: 4-Day Forecast Assessment. Profile location is graphically shown. The magnitude of SLD MO indicated by the color of its location marker. The green markers represent ± 5m difference. The difference codes for all error ranges are defined along the right side of the graphic.

To examine these data more closely, the spatial map for each difference code bin is generated. Along with these spatial distributions for each of the nine difference bins, basic metrics are extracted that reveal more quantitatively how well the model matches the in situ observations. The nine-panel figure below (Figure H4) shows these distributions for forecast day 1 of AMSEAS for October 2010, which corresponds to the upper left panel of Figure H3. By examining the three panels in second row of Figure H4, it can be seen that nearly 50% of the 2129 SLD MO points fall within the +/- 5 m bin and that 97% are within +/- 15 m.

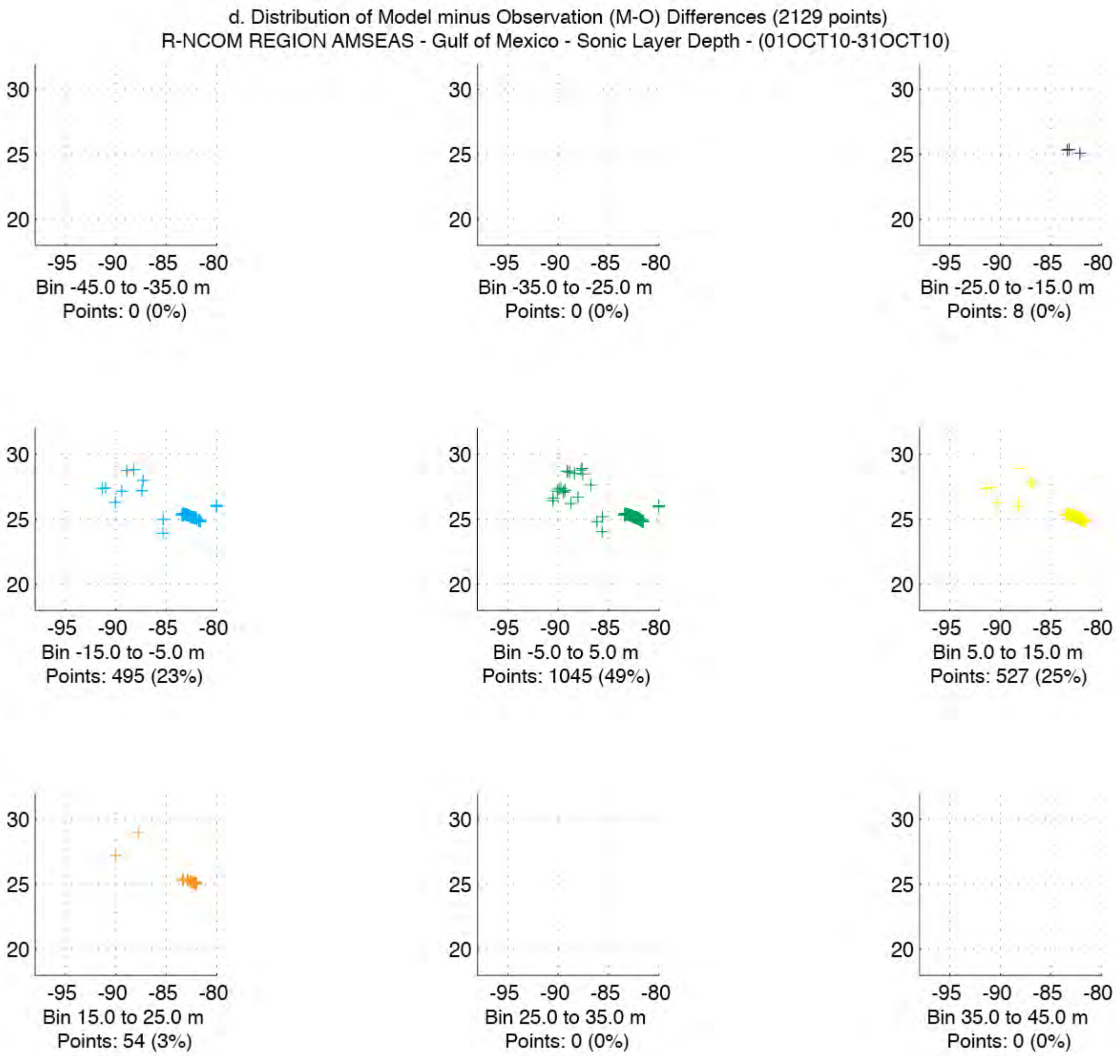

Figure: H4: Assessment of sonic layer depth (SLD) for day 1 forecasts from October 2010 where SLD is defined as the depth of the maximum sound speed between the surface and the deep sound channel axis (DSCZ, sound speed inflection point at depth).

In their current form the NAVO OPTEST toolkits (MAVE, PAM) are configured to assess model output hosted locally on the analyst's workstation. The compressed form of the 4-day model forecast for each day takes up 5.7 GB. With AMSEAS output being generated since inception on 25 May 2010, this represents a significant storage investment should there be an interest in retaining the files for ongoing analysis with NAVO's OPTEST toolkits, and/or as new metric concepts are revealed. An extremely useful feature of the OceanNOMADS portion of the NGI/NCDDC Ecosystem Data Assembly Center (EDAC) is its ability to serve AMSEAS data via OpenDAP protocols. This allows analysts that do not have direct access to NGI's AMSEAS holdings to extract only the output (i.e., model parameter, at a specified spatio-temporal location) that they require. There are a number of data and model analysis packages (e.g., Matlab, Ferret, DODS, etc.) that are capable of exploiting this capability.

Summary of Mooring Information

Station ID	SurfTemp	Salinity	Currents	Station Caretaker	Depth (m)	Instrument Depth (m)	Lon	Lat
41009				NDBC Buoy	44	1	-80.17	28.52
41010				NDBC Buoy	873	1	-78.47	28.91
41012				NDBC Buoy	37	1	-80.53	30.04
42001				NDBC Buoy	3365	1	-89.66	25.89
42003				NDBC Buoy	3283	1	-85.61	26.04
42021				COMPS Station	-	1	-83.31	28.31
42035				NDBC Buoy	14	1	-94.41	29.23
42036				NDBC Buoy	55	1	-84.52	28.50
42039				NDBC Buoy	307	1	-86.01	28.79
42040				NDBC Buoy	165	1	-88.21	29.21
42044				TABS Station	21	2	-97.05	26.19
42045				TABS Station	62	1 , 2	-96.50	26.22
42049				TABS Station	22	2	-96.01	28.35
42050				TABS Station	24	2	-94.24	28.84
42055				NDBC Buoy	3566	1	-94.00	22.20
42056				NDBC Buoy	4684	1	-84.86	19.80
42099				SCRIPPS Station	94	1	-84.25	27.34
42360				Petrobas Station	245	1	-90.46	26.70
LCIY2				ICON Station	7	2	-80.06	19.70

Table A: For each mooring, its NDBC ID and location are provided. The type of data obtained is indicated by the green highlighted cells. The caretaker, water depth and instrument depth are noted. Further information for each mooring site can be obtained at (where XXXXX is the Station ID):
http://www.ndbc.noaa.gov/station_page.php?station=XXXXX

Table H1: For each mooring, its NDBC ID and location are provided. The type of data obtained is indicated by the green highlighted cells. The caretaker, water depth and instrument depth are noted. Further information for each mooring site can be obtained at (where XXXXX is the Station ID):

This was leveraged in the AMSEAS model assessment to extract time series of temperature, currents and salinity at a number of sites within the AMSEAS domain that featured moored instrumentation. Identifying these sites was accomplished by exploring the locations that are catalogued on the National Data Buoy Center (NDBC) website. After a thorough exploration of the sites indicated within the Gulf of Mexico and the adjoining regions that are contained within the AMSEAS domain (i.e., Caribbean Seas, SW Atlantic), data from 19 sites was acquired (Table H.1). These represent the locations where the available moored time series were essentially complete over the course of the assessment time frame (JUN 2010 – OCT 2011).

To provide spatial context for these sites, the locations are superimposed on a map of bottom topography for a subset of the AMSEAS domain (Figure H5). Sites that feature temperature time series are by far the most numerous. These data also consistently exhibit more complete return and higher quality. With NDBC releasing quality controlled time series in monthly increments, the scripts used to retrieve these files and the subsequent extraction of the corresponding time series from the EDAC were set up to generate monthly comparison plots. These monthly AMSEAS/NDBC time series were then concatenated and refreshed as monthly segments became available. Examples of the full time series (JUN 2010 – OCT 2011) plotted for three variables (temperature, currents and salinity) for forecast day 1 are shown (Figure H6).

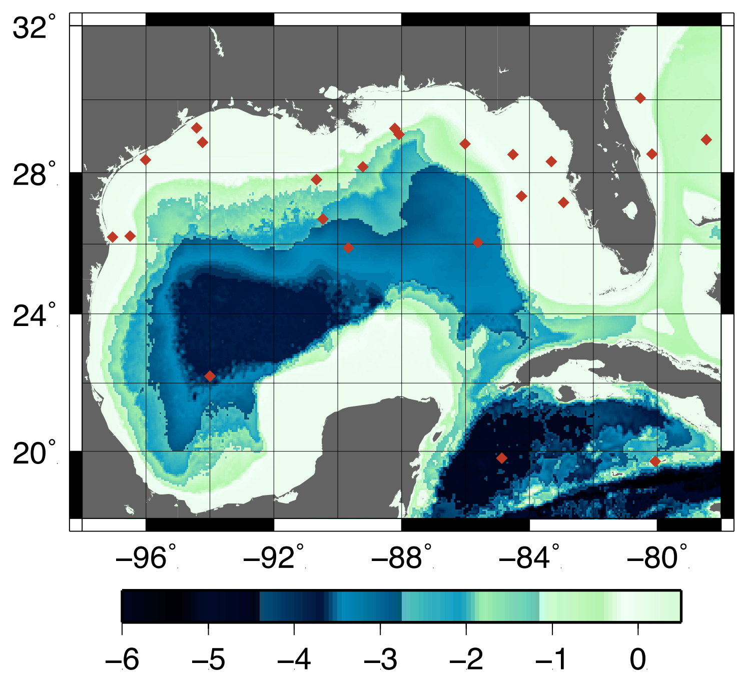

Figure H5: Location of mooring sites from which time series data were acquired from the NDBC website. The parameter(s) obtained from a given location are indicated in Table H1. All parameters are not available from all locations. Bathymetry obtained from the ETOPO1 product available from NOAA's National Geophysical Data Center.

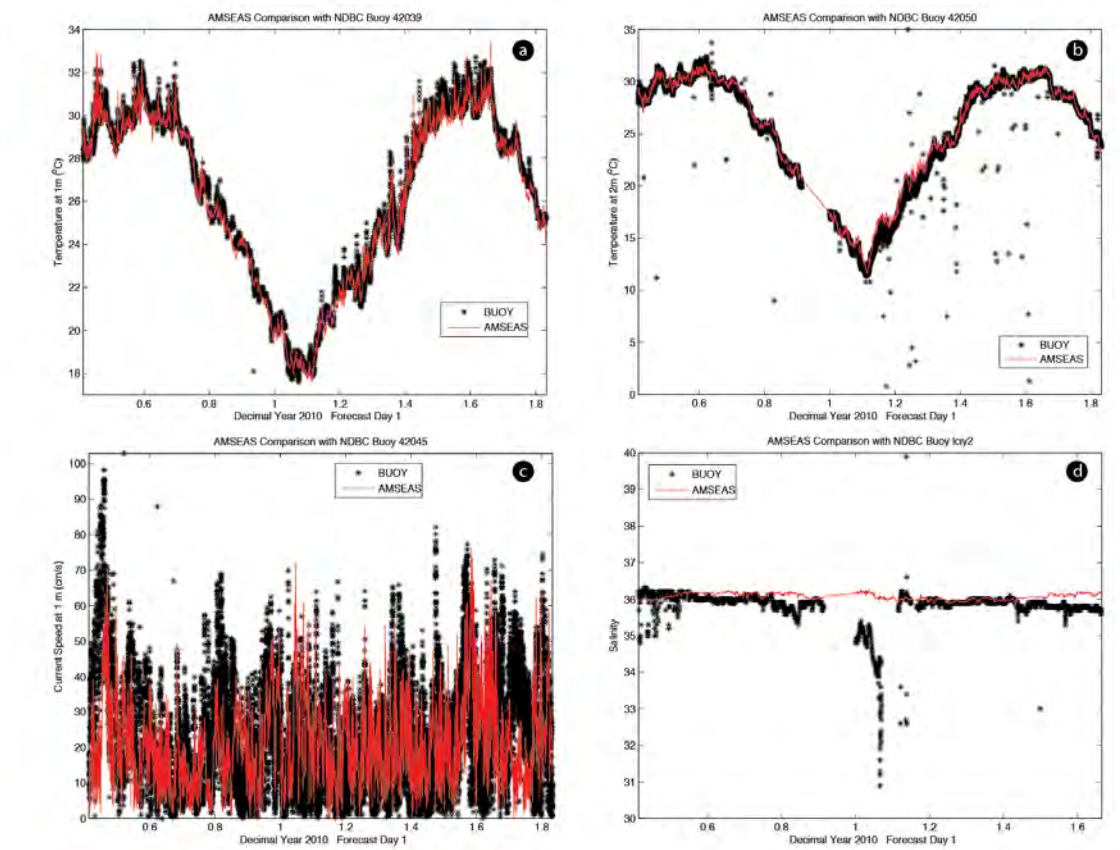

Figure H6: Time series for the full AMSEAS-NDBC comparison period (JUN 2010 – OCT 2011) from four separate sites. The parameter shown in each panel is: a) Temperature (1 m) at NDBC buoy site 42039; b) Temperature (2 m) at TABS buoy site 42050; c) Current speed (1 m) at TABS site 42045; d) Salinity (4.7 m) at Little Cayman Research Centre site LCIY2. NOTE: The LCIY2 salinity time series only extend through AUG 2011.

To gain a more quantitative perspective on the model – data comparison, scatter plots with a one-one line were generated that illustrate how far individual points match up. The AMSEAS output is saved on 3-hourly intervals. When mooring time series were of higher temporal resolution, those data were averaged within 3-hour bins. For the four locations shown in Figure H6, the model – data scatter plot is shown from MAR 2011 (Figure H7). The red ellipse on each plot represents the mean +/- one standard deviation around the mean value (center point of the ellipse) of the model (y axis) and observations (x axis). The ellipse boundary thus gives a clear visual representation of the variability for each, and the one-one line demarks whether the model is generally above or below (or well aligned with) the state of the natural system. A number of metrics are reported on these scatter plots. These include percentage of points that lie above or below (similar to SLD MO above, Figs. H3 and H4), within a prescribed tolerance.

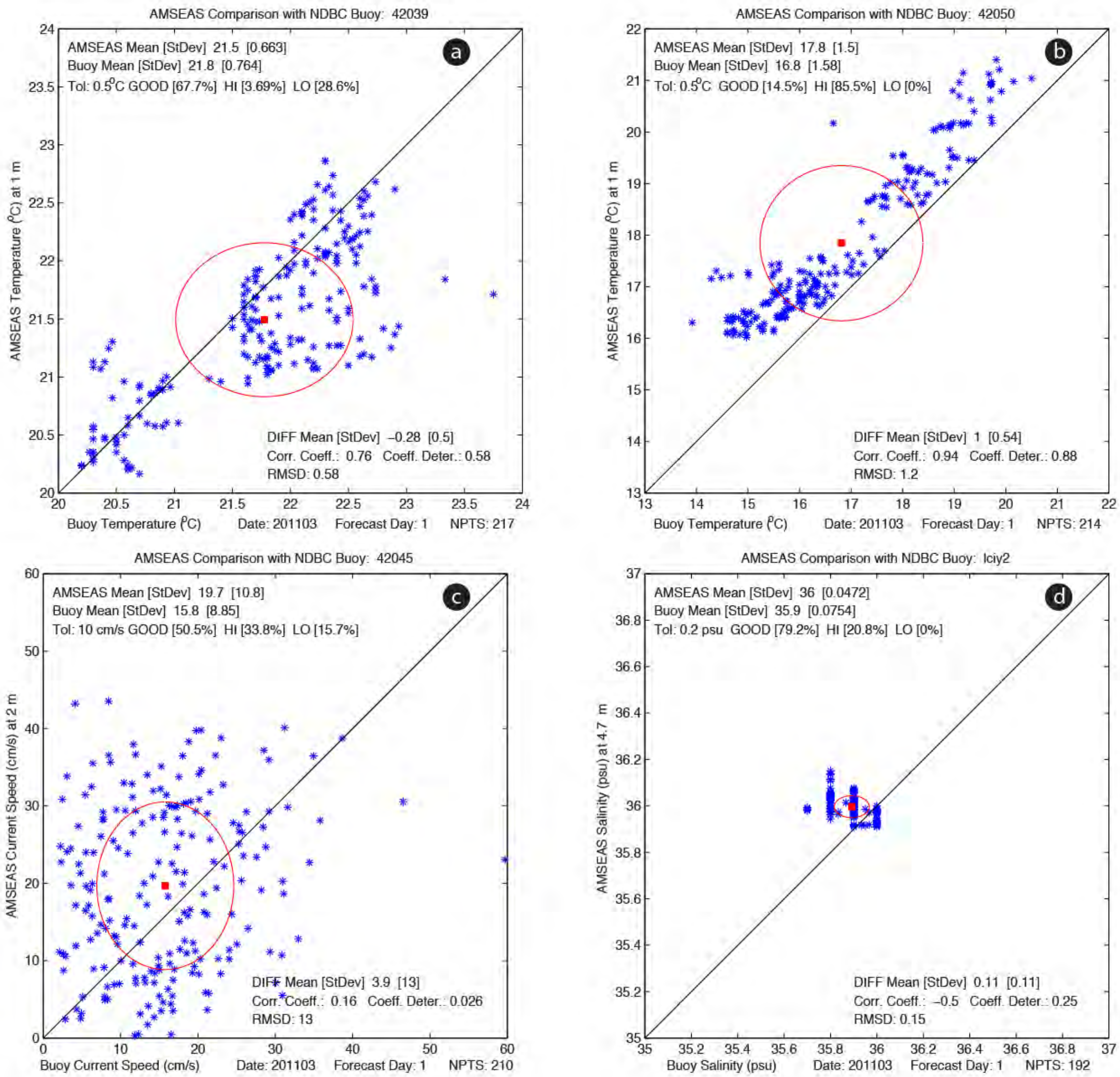

Figure H7: Scatter plots of model – data (AMSEAS – Mooring) comparisons. The mooring locations for these four panels coincide with those shown in Fig. H.6. The time frame for these comparisons is MAR 2011. The one-one lines reveal the degree to which the modeled environment captures the natural system. The red ellipse on each plot represents the mean +/- one standard deviation around the mean value (center point of the ellipse) of the model (y-axis) and observations (x-axis). The tolerance values, used to determine the percentage of values above/below an acceptable linear error, are defined as 0.5 °C, 10 cm/s and 0.2 psu for temperature, current speed and salinity, respectively. Mean, standard deviation of the model and data separately, and the mean and standard deviation of the model-obs difference are listed. The correlation coefficient, coefficient of determination and RMSD are also noted on

Scatter plots for each month and forecast day have been generated for every good data location listed in Table H1. To visualize the percentage of low, high and good points, as determined by applying the specified tolerances, time series bar graphs have been generated. For the four sites and data types in Figure H6, the bar graph time series of low/good/high percentage are shown for forecast day 1 (Figure H8).

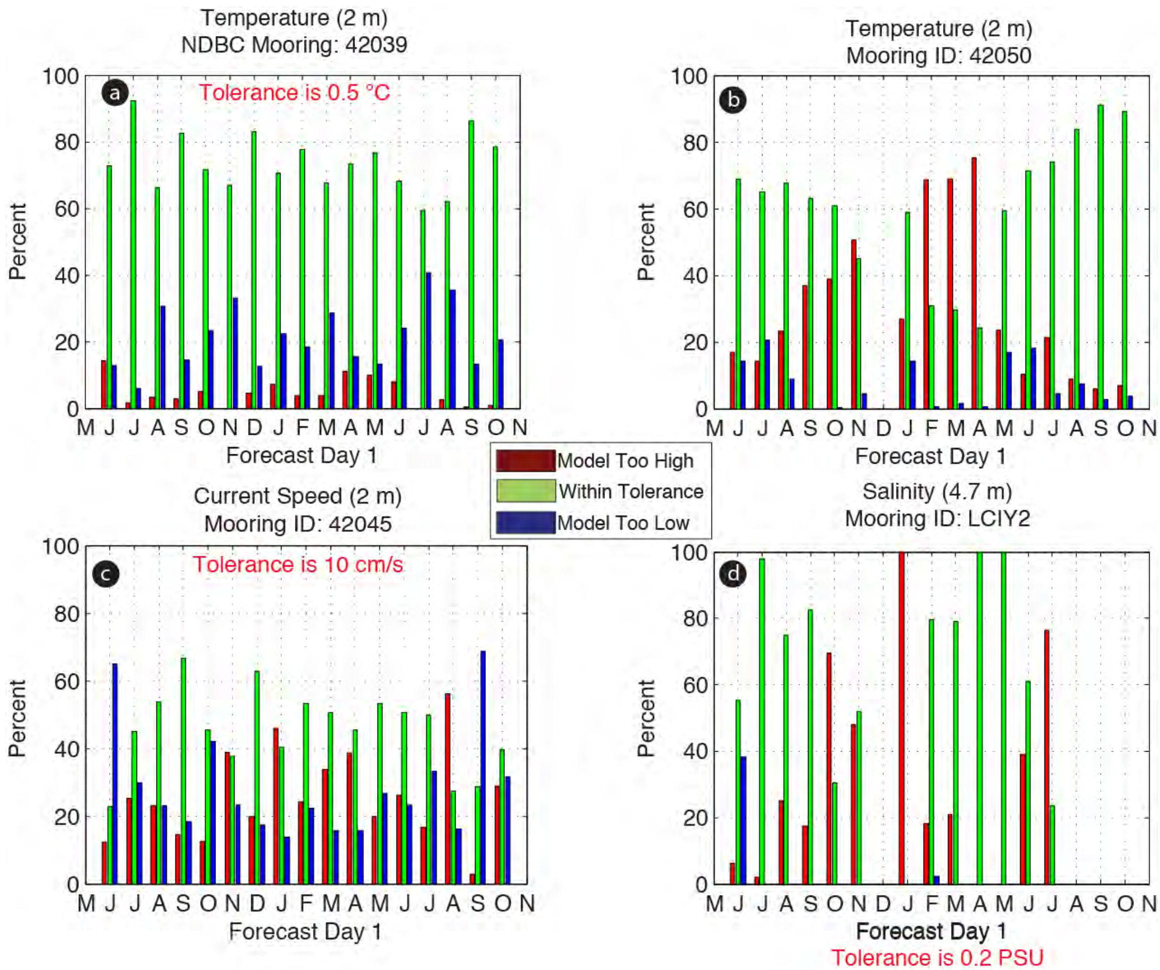

Figure H8: Bar plot time series showing the percentage of AMSEAS solution that is in the high/good/low bin for each month of forecast day 1 over the full AMSEAS-NDBC comparison period (JUN 2010 – OCT 2011) from four separate sites. The four panels coincide with the location/variable shown in Figures H6 and H7: a) temperature (1m) at NDBC buoy site 42039; b) temperature (2 m) at TABS buoy site 42050; c) Surface current speed (1 m) at TABS site 42045; d) Salinity (4.7 m) at Little Cayman Research Centre site LCIY2. NOTE: The LCIY2 salinity time series only extend through AUG 2011. When data return for a given month is less than 45 points (20% data return), no bar graph is shown. Green bars are within tolerance. Red bars are too high (model too warm/energetic/salty). Blue bars are too low (model too cold/fresh).

For a given forecast day, as shown in Figure H8, the bar graph time series are useful ways of revealing seasonality in AMSEAS skill. For a more complete picture of any consistent seasonality, it would be useful to consult all available locations. Given the data availability from the NDBC repository, surface temperature is clearly the most viable possibility for identifying any such seasonality in AMSEAS skill. Another useful comparison to make is to explore how the bar graph percentages evolve over the course of the AMSEAS forecasts (nominally these are 4-day forecasts, except for JUN/JUL 2010). The complete set of bar graph time series for NDBC station 42039, located on the Florida Shelf southeast of Pensacola, is shown in Figure H9.

These metrics suggest that the model, at least in that region, trends toward being too cool beginning in February 2011 on the third and fourth day of the model forecasts. In the day 4 forecast, these too low surface temperatures persist from February through September, with the model only reestablishing within tolerance results (> 50% of the time) in October 2011.

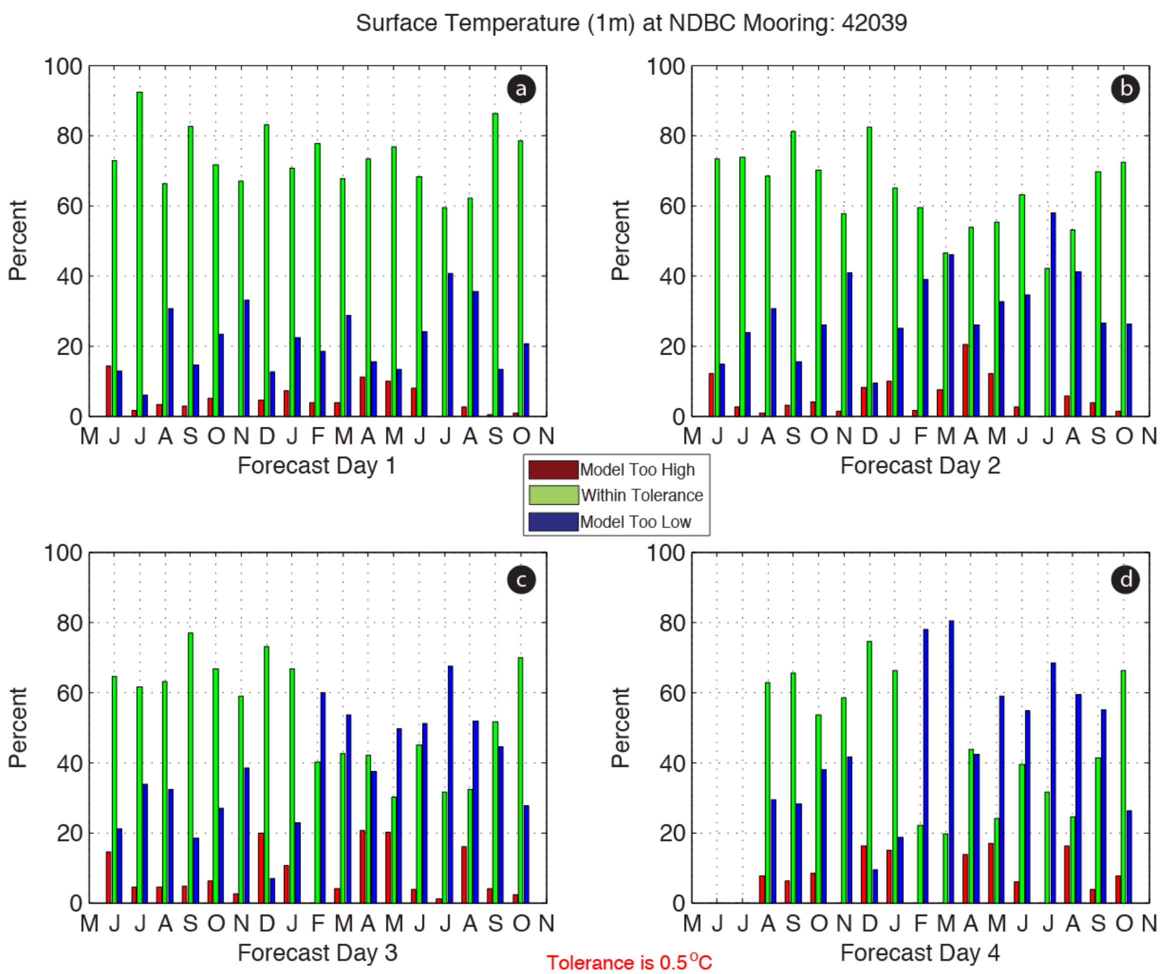

Figure H9: Bar plot time series showing the percentage of AMSEAS solution that is in the high/good/low bin for each month of all four forecast days over the full AMSEAS-NDBC comparison period (JUN 2010 – OCT 2011) of surface temperature (1 m) at NDBC buoy site 42039. For forecast day 4, there is no JUN or JUL 2010 result since 4-day AMSEAS forecasts were not implemented until mid-July 2010.

Summary - AMSEAS Assessment

The assessment of the Navy's Gulf of Mexico regional NCOM operational model (AMSEAS) has relied on skill metrics that are included in the OPTEST toolkits (MAVE and PAM) developed by NAVOCEANO and set of tools developed in house as part of USM's contribution to the SURA Super-Regional Modeling Testbed's Shelf Team efforts.

The Navy's toolkits rely on having the AMSEAS output locally accessible on the workstation on which they are executed. The USM-developed tools rely on the NGI-EDAC server that acts as a data portal for OpenDAP access to the AMSEAS output. The opportunity to implement this latter method of remotely accessing AMSEAS solution files, rather than accumulating a locally stored archive, proved to be highly effective and efficient since each of the daily AMSEAS 4-day forecast files is 5.7 GB. Having a web-accessible archive maintained by a dedicated support staff is a great asset for multi-institutional collaborative efforts such as the SURA Testbed activity.

The summary results shown here indicate that the model in general performs well. The one-week assessment from October (Fig. H2) suggests that at that time the model temperature in the upper water column is slightly elevated. However for the full month of October, the distribution of SLD above and below the +/- 5 m range has no bias and no systematic spatial pattern (Figs. H3 and H4).

Examination of the time series comparisons of surface temperature from moored thermistors shows that AMSEAS very accurately captures the seasonal evolution (Fig. H6a,b). This result is consistent for all temperature time series obtained in the AMSEAS domain (see Table. H1). The skill in capturing the seasonal evolution and matching the surface temperature value is so well-captured that in the one case where there is a consistent offset from OCT 2010 onward (Station ID 42045, not shown) one must consider that there may be a problem with the instrumentation. The velocity comparison is more of a challenge, with some major events not captured by AMSEAS (e.g., AUG-SEP 2011, Fig. H6c). Reinforcing the relative skill at capturing temperature vs. currents variability can be seen in the scatter plots (Fig. H7). The model-data comparison for temperature reveals a more pronounced tendency to track the one-one line, with correlation coefficients of 0.76 and 0.94 (Fig. H7a, b). For currents, the model-data comparison reveals a rather random distribution, which is confirmed by the correlation coefficient of 0.16 (Fig. H7c). It is likely that the currents from the site represented here (TABS mooring on Texas Shelf) are strongly impacted by lateral advection and therefore more of a challenge to simulate precisely. The salinity comparison shows a basic ability to capture the magnitude; deeper interpretation is problematic without clear understanding of the veracity of the time series measurements.

The model's relative skill at capturing temperature and current velocity for the stations shown here is reinforced by the bar graph time series for forecast day 1 (Fig. H8). The temperature time series are consistently within the prescribed tolerance (0.5 °C) more than 60% of the time whereas the current time series exceeds that threshold only twice.

The bar graph time series are an excellent means of assessing the full four-day forecast. These reveal a general reduction in forecast skill of surface temperature over the four days at station 42039 (Figure H9), with the model becoming cooler than the mooring-observed conditions. At this location, the forecasts appear to decay most rapidly during the FEB – SEP 2011 time frame. However, further investigation is needed to understand why August/September 2010 should outperform August/ September 2011 and why the degradation of the model skill in the February-September 2011 time frame is so pronounced for Day 3 and Day 4 of the forecast.

Examination of all the surface temperature sites reveals that this day 4 skill reduction in early spring to fall of 2011 is relatively consistent, manifesting at ~ 50% of the examined mooring sites. These results are not shown here, but can be examined by acquiring the complete set of assessment figures that are included in the technical report that is available on the SURA website at: http://testbed.sura.org/node/580. Such a consistent cooling of surface waters in the model suggests that some examination of the surface heat fluxes used to force AMSEAS is warranted.

For a more complete characterization and understanding, synoptic distributions, particularly at the surface but at depth as well, should be examined to assess the degree to which lateral advection contributes to model-data mismatch. Such an examination of synoptic distributions could also benefit from a skill assessment that featured remotely sensed data, particularly a strategically designed exploration of the day 3 and day 4 portions of the forecast.

Summary - AMSEAS wind forcing

An additional task analyzing the quality of the wind forcing, not typically undertaken during routine ocean model transitions, was performed as part of the SURA AMSEAS evaluation effort. Results of this study, comparing the COAMPS atmospheric forcing to available buoy winds during provide confidence in the general quality of the wind forcing used to drive the AMSEAS system.

COAMPS winds were validated using standard error metrics and vector correlation. Three different vector correlation schemes were also performed. An examination of bias and absolute errors during the summer study period (0000 UTC 20 June 2010 to 0000 UTC 10 July 2010) show very small wind direction or speed bias, computed as buoys minus COAMPS. However, COAMPS consistently underpredicted wind speed. An examination of COAMPS during a windy winter period containing several frontal passages (0000 UTC 1 December 2010 to 0000 UTC 15 January 2011) show similar error statistics except the wind direction absolute error is reduced by approximately 10 deg. Validation metrics include: 1) daily speed and direction biases with color shading to emphasize large errors; 2) daily speed and direction absolute errors with color shading to emphasize large errors; 3) scatterplots of all errors including standard deviation metrics of model and observation errors (for comparison whether the same error ranges are captured by both); 4) vector correlation including scaling factors and rotation angle; and 5) tables of average errors for both study periods. A COAMPS validation example for a difficult December cold front passage in the Gulf is shown in Figure H10. A detailed report along with all daily graphics is available at http://testbed.sura.org/node/403.

Useful future studies would include continuation of the initial assessments of the advantages of vector correlations versus standard error metrics for wind fields as well as closer examination of the forecast heat flux fields as alluded to earlier.

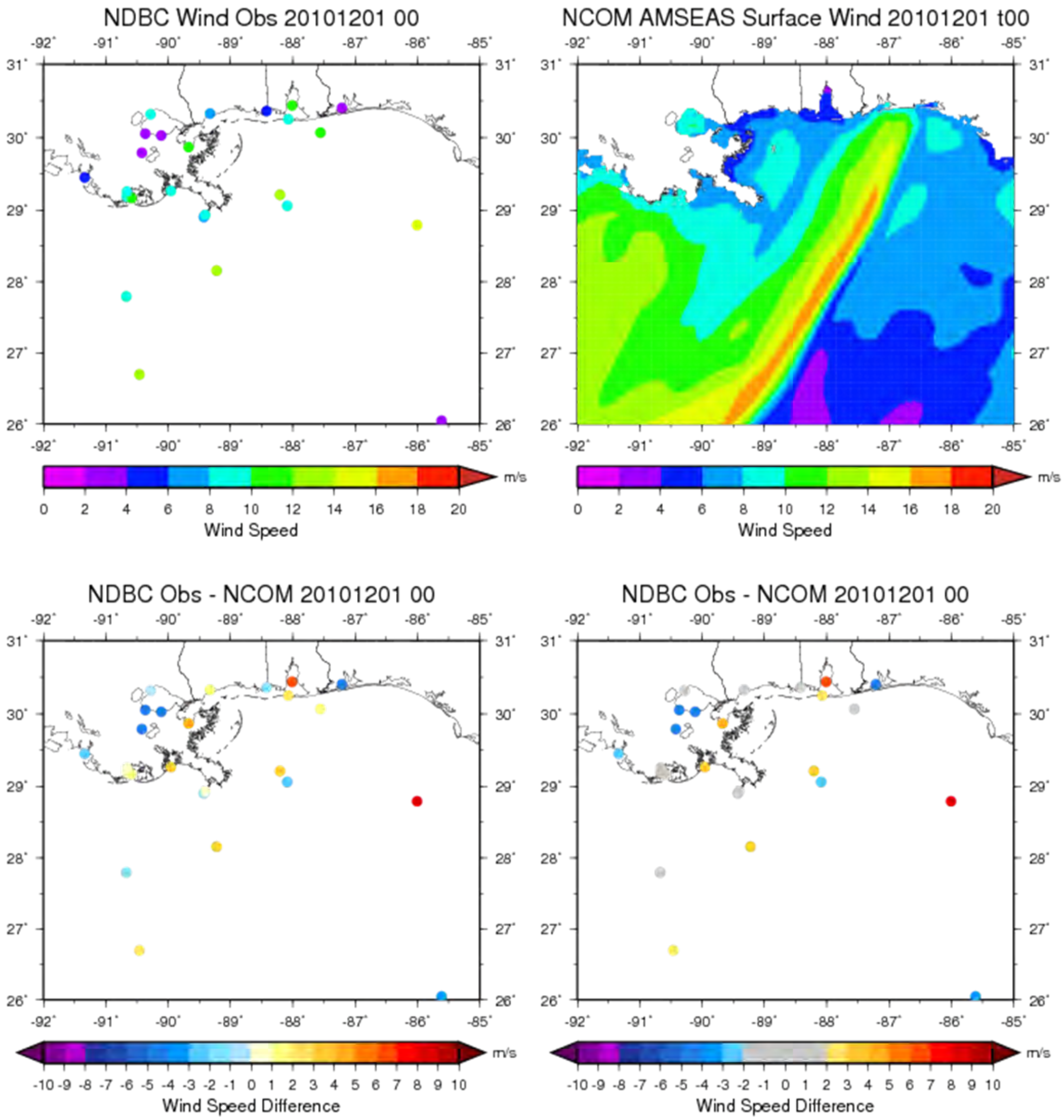

Figure H10: Wind speed comparison between NOAA Data Buoy Center measured winds for 1 December 2010 and the corresponding COAMPS winds used to force the NAVOCEANO AMSEAS ocean forecasts

Final Comments

It is worthwhile to reiterate the utility of the SURA Testbed capability that provides ready access to coastal products and tools (e.g., sites such as the NGI/ NCDDC OceanNOMADS), that are accessible to the research community. This affords marine scientists and resource managers ready access to model-predicted environmental fields via software applications that can be developed/provided with relative ease. The tools developed in house by NAVOCEANO, MSU and USM for assessing the AMSEAS solutions and the COAMPS forcing fields are well-positioned for further refinement and integration into a comprehensive operational model assessment toolkit, and would represent a notable contribution to the SURA Super-Regional Testbed's legacy.

Knowledge transfer of needed programming techniques is worth focusing on, and is being integrated into USM curriculum delivery. Further, access to the AMSEAS and other regional forecasts (e.g., USEast via OceanNOMADS) has numerous potential linkages to marine studies looking to examine transport pathways of fish larvae and nuisance species (e.g., jellyfish). Furthermore, techniques for basing ecological forecasts of noxious and potentially toxic HAB species such as dinoflagellates (*Karlodinium veneficum*) or cyanobacteria (*Microcystis aeruginosa*) on operational model output, particularly temperature and salinity, are currently an active area of research (cf., Appendix K). As operational models with coupled biogeochemical modules become available, these ecological forecasts will be expanded to exploit forecast distributions of nutrients, dissolved oxygen and phytoplankton.

Appendix I:

Summary Accomplishment(s): Provided insight relevant to NOAA CSDL operational Gulf of Mexico coastal nowcast/forecast system developers. [Contacts: Rich Patchen (NOAA CSDL), Jerry Wiggert (USM) & John Harding (NGI)]

As noted earlier, the NOAA CSDL transition plan for real-time hypoxia forecasts for Gulf of Mexico include transition of hydrodynamic only FVCOM coastal model as part of Northern Gulf Operational Forecast System (NGOFS) with planned transition in early 2012. Boundary conditions for this model are currently planned to come from the Navy Global ocean nowcast/forecast system available in real-time from the NCEP Ocean Prediction Center. As part of the transition process CSDL also plans to evaluate the use of higher resolution boundary conditions using the developmental Gulf of Mexico NGOM POM regional model. The hindcast model coupling experiments of the SURA Hypoxia Testbed (including the NGOM POM) is providing initial insights into the importance of the regional boundary conditions on the coastal hypoxia models. Given these expected insights as well as the availability of real-time Navy AMSEAS at NCEP may provide a future operational alternative to the currently planned global boundary conditions.

As an initial step toward assessing NAVO's AMSEAS model for usage as operational provision of lateral boundary conditions for the CSDL implementation of FVCOM as a component of NOAA's NGOFS, a water level analysis has been initiated. At the request of Patchen, Wiggert (USM) extracted water level time series from the AMSEAS forecasts hosted on the NGI-EDAC. Per NOAA's request a group of seven sites from the National Water Level Observation Network (NWLON) were targeted as AMSEAS extraction locations from the AMSEAS forecasts. The location of these extraction sites/water-level stations, along with station ID and descriptor are given in Table I1. Time series from OCT 2010 at six sites are shown in Figure I1. Water level data were extracted and provided to NOAA over the period JUN 2010 – SEP 2011.

Station ID	NWS ID	Lon	Lat	Location
[illegible]	[illegible]	[illegible]	[illegible]	[illegible]
[illegible]	[illegible]	[illegible]	[illegible]	[illegible]
[illegible]	[illegible]	[illegible]	[illegible]	[illegible]
[illegible]	[illegible]	[illegible]	[illegible]	[illegible]
[illegible]	[illegible]	[illegible]	[illegible]	[illegible]
[illegible]	[illegible]	[illegible]	[illegible]	[illegible]
[illegible]	[illegible]	[illegible]	[illegible]	[illegible]

Table I1: Table of NWLON site locations at which water level from AMSEAS forecasts was extracted.

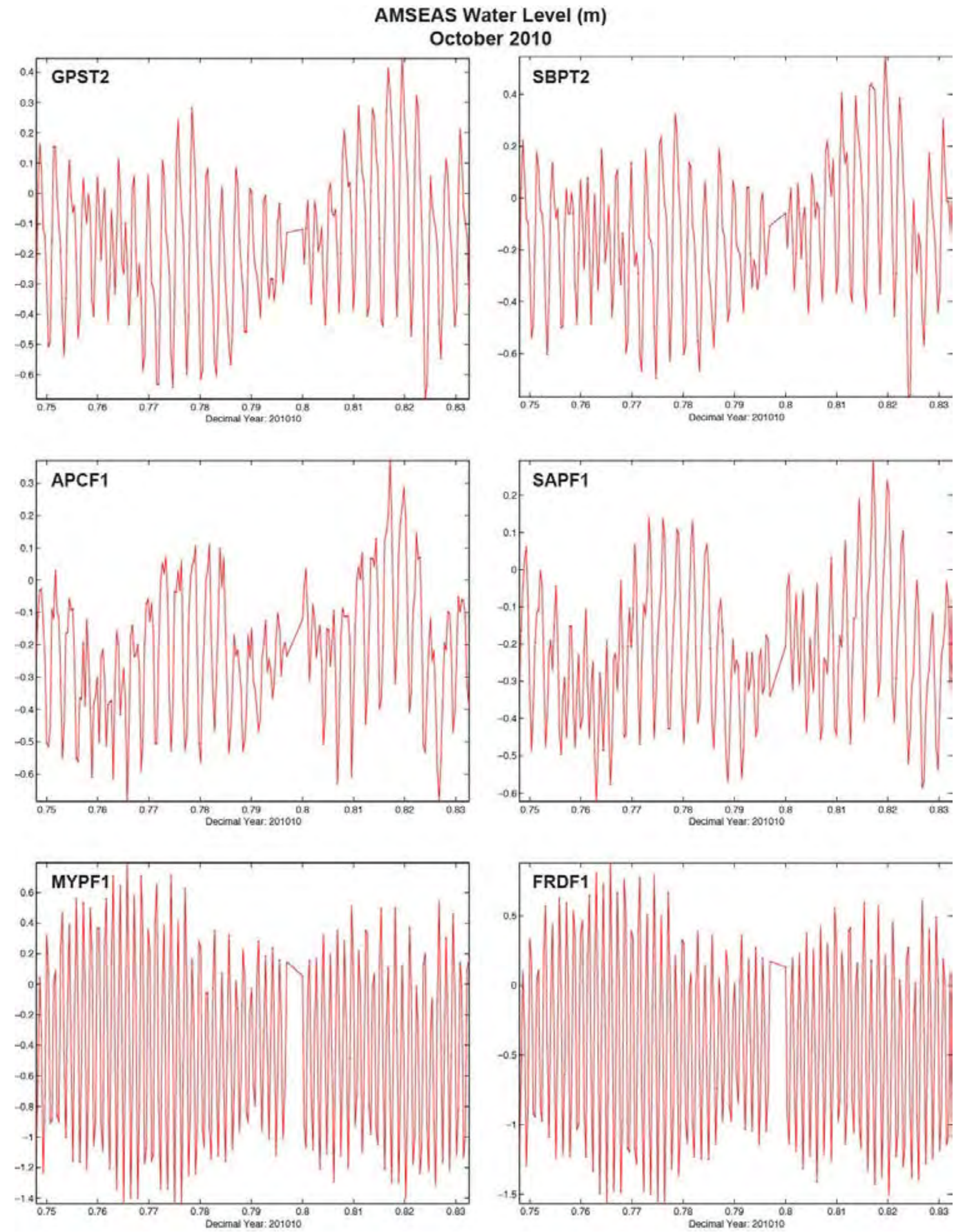

Figure I1: Time series of water level from AMSEAS day 1 forecasts for October 2010 extracted at six NWLON locations.

Appendix J:

Summary Accomplishment(s): Restructured NCDDC/NGI developmental EDAC facilitated transition of top NOAA NODC FY 11 external milestone for retrospective OceanNOMADS capability as Navy "White Front Door" for operational ocean nowcast/forecast products.
[Contacts: Scott Cross (NOAA NCDDC) & John Harding (NGI)]

The NOAA Operational Model Archive and Distribution System (NOMADS) provides both real-time and archived atmospheric model output from servers at NCEP and NCDC respectively (http://nomads.ncep.noaa.gov/txt_descriptions/marRutledge-1.pdf). NOAA NODC/NCCDC with NCEP is planning an ocean forecast system analogue called OceanNOMADS with the real-time ocean forecast output provided via servers at the NCEP Ocean Prediction Center and archival by NODC/NCDDC. Creation of the NOAA archival production version of OceanNOMADS is one of the top ten NODC FY 11 external milestones. A joint Northern Gulf Institute/ NOAA NCDDC effort initially created the developmental version of the archival OceanNOMADS capability under the NGI Ecosystem Data Assembly Center (EDAC) project. Without the complementary Year 1, IOOS SURA Testbed support NODC would not have attained this FY 11 milestone. Access tool development and storage of initial data sets occur on the NGI/ NCDDC developmental servers with planned transition to NODC/NCCDC production servers as the model archives mature and operational space and distribution capability grow. Initial operational NODC/NCDDC archive server capability occurred in 4th quarter 2011. Navy global ocean forecast subsets for U.S waters are mature and are the first fields currently resident on the operational server. Year 1 testbed activities in coordination with the SURA CI team provided for an expansion and acceleration of the developmental EDAC/OceanNOMADS capability for archived Navy regional ocean nowcast/forecast delivery to both academic and NOAA interests (Figure J1). The NGI/NCDDC developmental server now includes the Naval Research Laboratory developmental Inter-America Seas Nowcast/Forecast System over the Gulf of Mexico from 2004- Mar 2011, the operational Naval Oceanographic Office regional USEast ocean nowcast/forecast system from 2009 to present, and the operational regional AMSEAS (Gulf of Mexico/Caribbean) ocean nowcast/forecast system from its inception 25 June 2010 to present (Figure J2). See http://www.northerngulfinstitute.org/edac/ocean_nomads.php for the developmental server and http://www.ncddc.noaa.gov/ocean-nomads/ for the production server (Figure J3).

NGI & NCDDC EDAC/ OceanNOMADS Improve Access to Gulf Data & Predictions

http://www.northerngulfinstitute.org/edac

Figure J: NGI/ NOAA Ecosystem Data Assembly Center (EDAC) link to developmental OceanNOMADS. Data and ocean forecast archival data accessible via menu at right.

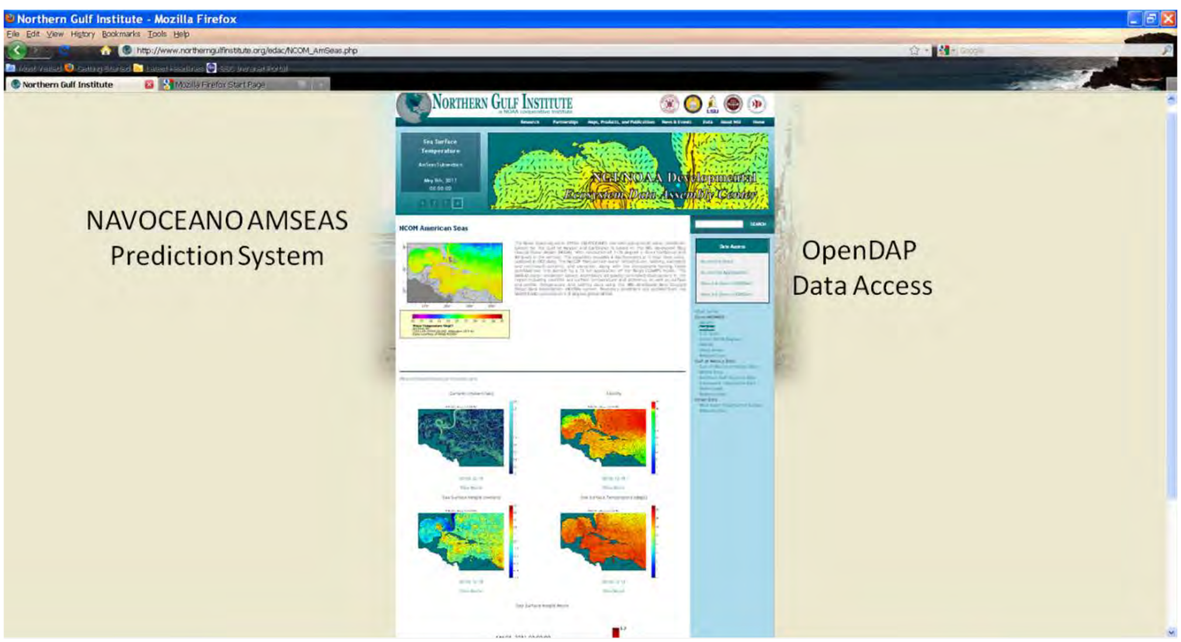

http://www.northerngulfinstitute.org/edac/NCOM_AmSeas.php

Figure J2: OceanNOMADS access page for NAVOCEANO operational AMSEAS

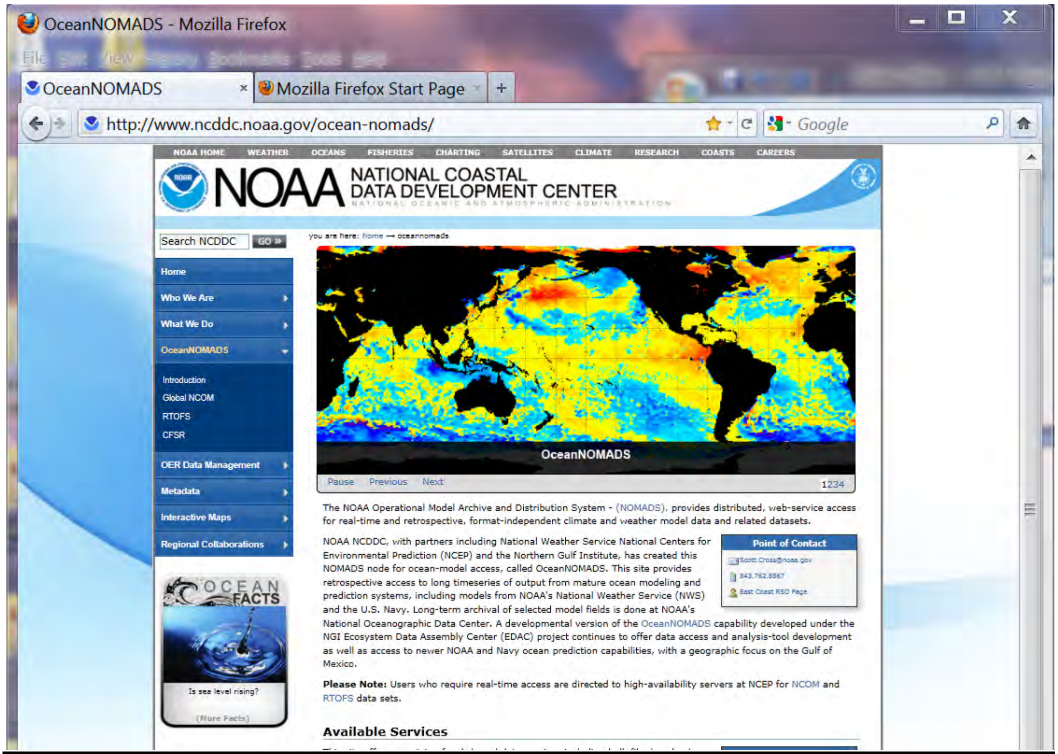

Figure J3: NOAA NODC site for production version of OceanNOMADS presently serving regional extracts from Navy global ocean prediction system, Global NCOM.

<u>Appendix K:</u>

Summary Accomplishment(s): Provided collaborative linkage between the SURA Super-Regional Testbed's Shelf and Estuarine Hypoxia teams through Wiggert's Role as a principal architect in development of the ChesROMS Biogeochemical Model. [Contacts: Jerry Wiggert (USM), Raleigh Hood (UMCES)]

A ROMS-based physical model of Chesapeake Bay (Xu et al., 2011), termed ChesROMS, has been used as the basis for a coupled physical-biogeochemical model. The biogeochemical version of ChesROMS features a mechanistic dissolved oxygen formulation that allows for realizing a dynamic dissolved oxygen field that responds to seasonal and interannual variation in nitrogen loading from rivers, diffuse sources and atmospheric deposition. This biogeochemical model development effort, which originated with a MERHAB-funded project, has been led by Raleigh Hood (UMCES) and Wiggert (USM), both of whom are participants in the SURA Super-Regional Testbed Project. Hood is a member of the Estuarine Hypoxia Team, while Wiggert is a member of the Shelf Hypoxia Team. Through his active connection to the ChesROMS modeling group led by Hood, Wiggert has liaised extensively with the Estuarine Team.

The ChesROMS biogeochemical model was one of several model applications employed in the assessment activity of the Estuarine Team. The assessment of these models' skill in simulating the seasonal evolution of the dissolved oxygen, in particular the regular establishment of hypoxia along the main stem of the middle and upper Bay, was a primary aspect of the Estuarine Team's efforts. Marjy Friedrichs (VIMS) led this skill assessment effort. One result of interest is the comparison of the seasonal evolution of the Bay's hypoxic volume (Fig. K1).

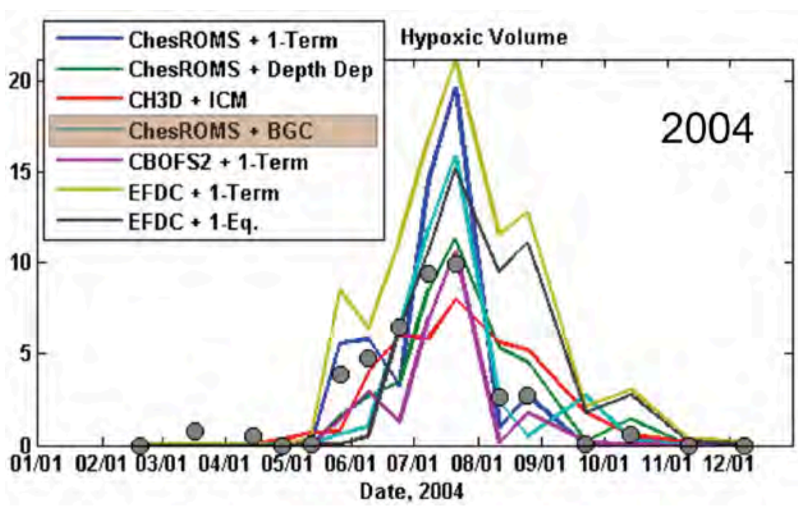

Figure K1. Time series of hypoxic volume in Chesapeake Bay in 2004. The grey circles are hypoxic volume estimates based on the in situ measurements obtained by the Chesapeake Bay Program. Figure courtesy of M. Friedrichs and A. Bever (VIMS), members of the SURA Estuarine Hypoxia Team.

An originating motivation for the development of the ChesROMS biogeochemical model was for generation of near real-time water quality forecasts that could provide critical physical and biogeochemical property inputs to ecological models used to generate nowcasts and forecasts of harmful algal blooms (HABs) and other nuisance species. A prototype operational version of ChesROMS is now providing the needed short-term, near real-time water quality forecasts.